2013-01-11

Physical Properties of Athabasca Bitumen and Liquid Solvent Mixtures

Guan, Jianguo

UNIVERSITY OF CALGARY

Physical Properties of Athabasca Bitumen and Liquid Solvent Mixtures

by

Jianguo (James) Guan

A THESIS

SUBMITTED TO THE FACULTY OF GRADUATE STUDIES

IN PARTIAL FULFILMENT OF THE REQUIREMENTS FOR THE

DEGREE OF MASTER OF SCIENCE

Chemical and Petroleum Engineering

CALGARY, ALBERTA

January, 2013

UNIVERSITY OF CALGARY

FACULTY OF GRADUATE STUDIES

The undersigned certify that they have read, and recommend to the Faculty of Graduate Studies for acceptance, a thesis entitled " Physical Properties of Athabasca Bitumen and Liquid Solvent Mixtures" submitted by Jian Guo Guan in partial fulfilment of the requirements of the degree of Master of Science.

Supervisor, Dr. Jalal Abedi,
Department of Chemical and Petroleum Engineering

Dr. Zhangxing Chen
Department of Chemical and Petroleum Engineering

Dr. Shengnan (Nancy) Chen
Department of Chemical and Petroleum Engineering

Dr. Edwin Peter Nowicki
Department of Electrical Engineering

December 24, 2012
Date

ABSTRACT

Heavy oil and bitumen are composed of high molecular weight compounds, resulting in more viscous fluids than most conventional crude oils. For the production and transportation of such heavy fluids, it is necessary to reduce their viscosity. The dilution of such heavy fluids with liquid solvent is one of the practical methods to reduce the oil viscosity to the desired level.

In this study, a designed experimental apparatus has been set up to accurately measure the variations of viscosity and density for raw bitumen, aromatic solvents and bitumen/solvent mixtures under conditions applicable for both in situ recovery methods and pipeline transportation. The bitumen samples were taken from an Athabasca oil field, and the aromatic solvents were highly purified toluene and xylenes.

On the basis of the experimental results, the influences of pressure, temperature and solvent concentration on the density and viscosity of the raw bitumen and its pseudo-binary mixtures with aromatic solvents were considered. The experimental density and viscosity data for the solvents and for raw bitumen were then correlated using different correlations from the literature. The experimental density and viscosity data for the mixtures of Athabasca bitumen with toluene and xylenes were also evaluated with models representing certain mixing rules proposed in the literature.

The density data were well predicted with an equation that assumed no volume change occurs upon mixing. In contrast, the viscosity data of the studied conditions were well correlated with Lederer's model and the power law model, both of which include one adjustable parameter. The comparison of the experimental and modeling results

demonstrates that the calculated values of mixture density and viscosity showed slight deviations from the measured values at the highest temperature and highest solvent concentrations.

ACKNOWLEDGEMENTS

I would like to express my sincere gratitude to my supervisor Dr. Jalal Abedi for his outstanding support, encouragement, insight, and invaluable guidance throughout the entire course of this project. I would also like to thank him for providing me with several opportunities to present my studies to industry experts.

I also wish to express my gratitude to Mr. Hossein Nourozieh and Mr. Mohammad Kariznovi for their generous help.

The financial support from the Natural Science and Engineering Research Council of Canada (NSERC) and the Department of Chemical and Petroleum Engineering, the University of Calgary is greatly appreciated.

Especially, I would like to thank my parents and my brother and sisters for their years of support, care and guidance.

I remain indebted to my wife and my children for their patience and understanding throughout the entire span of this work.

To My Parents

and

My Family

TABLE OF CONTENTS

LIST OF TABLES

LIST OF FIGURES

Nomenclature

ΔF	viscous free energy to activation, *cal/gmol*
T	temperature, *K*
P_g	gauge pressure, *MPa*
P	period of oscillation
t	temperature in *°C*
p	absolute pressure, *bar,* in Eq. [3-1]
a	apparatus constants in Eq. [3-1]
a, b	adjustable parameters in Eq. [5-1]
a_1, a_2, a_3, a_4	adjustable characteristic parameters in Eq. [5-2]
b_1, b_2, b_3	adjustable parameterinEq. [5-3] and [5-4]
P	pressure, *kPa,* in Eq. [5-2]
x	fraction
n	adjustable coefficient in Eq. [5-8]

Greek symbols

μ	viscosity, *mPa.s*
ρ	density, kg/m^3
α	adjustable parameter in Eq. [5-9]
υ	volume fractions

Subscripts

i, j, k	components
solv, s	solvent
m	mixture
B	bitumen
corr	correlation
exp	experimental

Chapter 1 Introduction

1.1 General Introduction

With the decline of conventional petroleum sources, the demand for the non-conventional crude oil is significantly increasing. In 1995, an unprecedented and complex report, *The Oil Sands – a New Energy Vision for Canada*, was compiled by the National Task Force on Oils Sands Strategies. In this report, the prediction of crude oil production will be 1.2 million barrels daily by 2020. This forecast "has already been achieved by an increasingly dynamic industry" (Industry Canada: Technology Roadmap). Industry Canada has predicted that the daily oil sands bitumen production will reach five million barrels by 2030.

Oil sands bitumen is a major source of non-conventional petroleum deposits. Canadian oil sands, including the Athabasca, Peace River, Cold Lake and Wabasca deposits, are increasingly recognized as an extremely important part in the global energy source supply chain, covering over 140,000 square kilometres (Wikipedia: Oil sands) with proven reserves of 1.75 trillion barrels (Wikipedia: Oil sands) of bitumen in place.

The viscosity of bitumen is, however, extremely high, up to 5×10^5 mPa.s at 20°C and local atmospheric pressure, making it the main obstacle in the economic recovery of the bitumen. Therefore, some special extraction methods, such as the cyclic steam stimulation (CSS), steam-assisted gravity drainage (SAGD) and vapour recovery extraction (VAPEX) methods have been developed.

A new approach has been emerging – the solvent/bitumen process. In contrast with the above thermal extraction techniques, this process is highly energy efficient; however, there is a scarcity of property data for solvent/bitumen mixtures and the lack of a suitable empirical viscosity model for specific mixtures. It is, therefore, absolute necessary that the variation of bitumen and bitumen/solvent mixtures viscosity with temperature, pressure and composition be thoroughly studied, so that suitable modelling methods can be developed.

Viscosity is one of the critical transport properties of hydrocarbon fluids. In the design of any efficient chemical process or pipeline transportation, the accurate viscosity of the chemical fluid of interest under real conditions needs to be calculated to decide the capability of the process or facility. In the reduction of bitumen viscosity for enhanced recovery through steam, hot water injection and in situ combustion, reservoir engineering practices need the accurate viscosity value of the bitumen (heavy oil) to estimate the hydrocarbon fluid in place, the potential future of reservoir, and the production scheme.

The simulation and optimization of crude oil production and processing require a proper understanding of reservoir fluid phase behaviour and various physical properties. Among these properties, crude oil viscosity is considered as one of the most important parameter that can characterize reservoir hydrocarbons and affect the efficiency of down-hole and surface facilities and transportation systems.

To obtain bitumen viscosity data, the most reliable and routine practice in industry takes fluid samples from the reservoir and measure the viscosity values in a laboratory for different industrial purposes. However, there are cases where such direct measurements

are not always available. Considering the time-consuming and capital-intensive nature of sample collection, viscosity data are extremely difficult to measure directly for all of complex mixtures in all relevant conditions. The main reasons are as follows:

- Full-scope samples that truly represent conditions of a reservoir are not available;
- Reliable samples are not enough to understand the behaviour of the reservoir for economic purposes; and,
- Pressure, volume, temperature (PVT) analyses cannot be completed due to the lack of necessary data.

In order to predict crude oil properties, a common approach is the application of PVT correlations. Unfortunately, due to the nature of chemical fluid molecule movement complexity, there is not a single integrated theory description for viscosity prediction.

1.2 Research Objective

The primary objectives of this research are, therefore: (1) the accurate measurement of the physical properties of solvent, bitumen and their mixtures in different proportions; (2) a detailed understanding of the integrated relationships for Athabasca bitumen and solvents in terms of pressures, temperatures and compositions. In order to fulfil this project's aims, the research activities have been split into the following two steps.

1. Experimental measurements:
   - Raw bitumen viscosity and density measurements as functions of temperatures and pressures;

- Physical property measurements of solvent/bitumen mixtures at a wide range of condition;
- Evaluation of the influence of three important variables, i.e. pressures, temperatures and compositions on mixture properties; and,
- Investigation of the effect of different solvents on the reduction of mixture viscosity.

2. Modelling prediction:
    - Suitable correlations for raw bitumen and pure solvents; and,
    - Investigation of the different mixing rules.

The content of this thesis is primarily divided into five sections. The main function of the first chapter is a general introduction to the topic of the thesis. In this chapter, the study area is briefly depicted; and, the motivation for this research activity is presented. The research objectives are stated; and, the methodology used to fulfil the research aim is summarized. In Chapter 2, the recent literature is reviewed, and the related research works on this area are presented. Through this process, the different methods in this area can be understood fully; moreover, an appropriate way to fulfil the present research goal can be found. In Chapter 3, the details of the experimental setup and procedure are described, including the apparatus, instrument function, viscometer and densimeter calibration, and operational conditions and processes. In Chapter 4, the suitable models are evaluated, and correlations are determined with the experimental measurement data to find out the best fit parameters. Finally, in Chapter 5, the graphic charts and data tables are utilized to state the research results and analyze these data. In addition, the reliability of this research is determined.

Chapter 2 Literature Review

The study on the bitumen characteristic and physical properties has a long history. Numerous research activities had been conducted extensively and tremendous literatures had been proposed and scattered in different journals around global. This review focuses on experimental measurement and modeling prediction methods for bitumen and bitumen/ solvents' viscosity and density with respective of pressure, temperature and constitutions.

2.1 Viscosity and density modeling and experimental study on raw bitumen or heavy oil

In 1984, Khan et al. [1] developed two empirical correlation based on double-logarithmic viscosity function which can be described as:

Model I: $\ln\ln(\mu) = [1.0 + b_1 T + b_2 (b_1 T)^2] e^{b_1 T}$ 2-1

Model II: $\ln\ln(\mu) = C_2 \ln T + C_2$ 2-2

To compare with four bitumen sample data, the average deviation of both model ranged from 3.6% to 10.7% respectively. In addition, the Eyring's and Hildebrand's equations have been investigated. In this work, the Eyring's equation was given as

$$\frac{\mu}{d} = 6.466126 \times 10^{-4} exp \frac{\Delta F}{1.987T} \quad 2\text{-}3$$

Where,

$$d = 0.120(616.62 - T)^{1/3} \quad 2\text{-}4$$

$$\ln \Delta F = \frac{b_1}{T^{b_2}} \quad 2\text{-}5$$

b_1, b_2 are adjustable parameters.

And, Hildebrand's equation was given as

$$\ln(\frac{1}{\mu}) = B_0 + B_0 sinh\beta + B_2 sinh^2\beta + B_3 sinh^3\beta \quad 2\text{-}6$$

The average deviations for Eyring's and Hildebrand's equations are 13% and 7.5% respectively.

In 1986, Mehrotra and Svrcek [2] measured the viscosity of Athabasca bitumen over the temperature range of 30-120oC and pressures up to 10 MPa. The authors developed two correlations for bitumen viscosity versus temperature and pressure using the model developed by Khan et al. The correlation was in the form of following equations,

Model 1: $\ln(\mu) = \exp[a_1 + a_2 \ln T] + a_3 P_g$ 2-7

Model 2: $\ln\ln(\mu) = [a_1 + a_2 \ln T] + a_3 P_g$ 2-8

Where,

The pressure is Gauge Pressure in MPa, and the viscosity in cp and temperature in K.

The authors used the developed correlations to model the viscosity of Athabasca bitumen over studied pressure and temperature ranges. The models fit the data within 2.8% and 1.8% accuracy respectively.

In 1987, Mehrotra et al. [3] applied the principle of Corresponding State Theory to calculate the viscosity of Alberta bitumen, including Athabasca, Peace River, Marguerite Lake and Wabasca. The correlation based on Corresponding State Theory can be described as follow:

$$f_{\alpha,o} = (Tc_\alpha / Tc_o)\theta_{\alpha,o} \quad \text{2-9}$$

$$h_{\alpha,o} = (\rho c_o / \rho c_\alpha)\phi_{\alpha,o} \quad \text{2-10}$$

2-

$$\dot{\Phi}_{\alpha,o}(Tr_\alpha, Vr_\alpha, \omega) = [1 + (\omega_\alpha - \omega_o)\left(a_2 Ap(V_\alpha^+ + b_2 Ap) + c_2 Ap(V_\alpha^+ + d_2 Ap)\right) lnT_\alpha^+]Z_{co}/Z_{c\alpha}$$

2-12

$$T_\alpha^+ = min[2, max(Tr_\alpha, 0.5)] \quad \text{2-13}$$

$$V_\alpha^+ = min[2, max(Vr_\alpha, 0.5)] \quad \text{2-14}$$

$$\eta_x(\rho, T) = \eta_o \left[\rho h_{x,o}, \frac{T}{f_{x,o}}\right] \left(\frac{M_x}{M_o}\right)^{1/2} h_{X,o}^{-2/3} f_{x,o}^{-1/3} \quad \text{2-15}$$

$$h_{x,o} = \sum_\alpha \sum_\beta X_\alpha X_\beta \, h_{\alpha\beta,o} \quad \text{2-16}$$

$$\Gamma_{x,o} h_{x,o} = \sum_\alpha \sum_\beta X_\alpha X_\beta \, h_{\alpha\beta,o} \Gamma_{\alpha\beta,o} \quad \text{2-17}$$

$$f_{\alpha\beta,o} = \left(1 - k_{\alpha\beta}\right)(f_{\alpha,o} f_{\beta,o})^{1/l} \quad \text{2-18}$$

$$h_{\alpha\beta,o} = \left(1 - l_{\alpha\beta}\right)\left(\frac{1}{2} h_{\alpha,o}^{\frac{1}{l}} + \frac{1}{2} h_{\beta,o}^{\frac{1}{l}}\right)^3 \quad \text{2-19}$$

$$f_{x,o}^{1/2} M_x^{1/2} = h_{x,o} = \sum_\alpha \sum_\beta X_\alpha X_\beta \, h_{\alpha\beta,o}^{3/4} f_{\alpha\beta,o}^{3/4} M_{\alpha\beta}^{1/2} \quad \text{2-20}$$

In this work, PSU No. 625 (1,2,3,4,5,6,7,8 octahrydrophenanthrene) has been taken as reference fluid instead of Methane. The bitumen samples from Athabasca, Peace River, Marguerite Lake and *W*abasca have been characterized as the mixtures of two, three, and four pseudo components to incorporate with Corresponding State method. The overall deviation is less than 10% at wide viscosity range.

In 1987, Mehrotra and Svrcek [4] conducted an experiment to measure the viscosity of Cold Lake bitumen over temperature range of 37-115°C and pressure range of 0-10MPa. Moreover, the two correlations which have been adopted in the preliminary study for

Athabasca oil deposit correlated to suit for Cold Lake bitumen. The two correlations can be expressed as:

Model 1: $\ln(\mu) = \exp[a_1 + a_2 \ln T] + a_3 P_g$ 2-21

Model 2: $\ln\ln(\mu) = [a_1 + a_2 \ln T] + a_3 P_g$ 2-22

Where,

The pressure is Gauge Pressure in MPa, and the viscosity in cp and temperature in K.

To compare with 30 experimental data point, these two models gave 2.2% and 2.1% average deviation respectively. This study also concluded the impact of pressure associated strongly with the bitumen constitutions.

In 1987, Johnson et al. [5] investigated different forms of Corresponding States modeling to predict the viscosity of gas-free and gas saturated Athabasca bitumen. To optimise the predicting results, bitumen had been characterized into four pseudo components according to the specific gravity and normal boiling point or molecular weight of each pseudo component. For gas-free bitumen, they found the modified extended Corresponding States modeling is successful, in which, the parameter A_p is function of critical pressure instead of the function of acentric factor ω. In addition, an Aromatic-Naphthenic compound fluid which is PSU625 replaced methane as reference fluid. The accuracy of prediction can achieved in highly agreement and the deviation is less than 6%. For gas saturated bitumen, Teja-Rice Corresponding States mixing rule gave the best prediction results in comparing with Wong et al. mixing rule. The mixing rule of Teja-Rice can be described as follows:

$$T_{cm}V_{cm} = \sum_i \sum_j x_i x_j T_{cij} V_{cij} \quad (2\text{-}23)$$

$$V_{cm} = \sum_i \sum_j x_i x_j V_{cj} \quad (2\text{-}24)$$

$$\omega_m = \sum_i x_i \omega_i \quad (2\text{-}25)$$

$$M_m = \sum_i x_i M_i \quad (2\text{-}26)$$

$$T_{cij}V_{cij} = \Psi_{ij}(T_{ci}V_{ci}T_{cj}V_{cj})^{1/2} \quad (2\text{-}27)$$

$$V_{cij} = \frac{1}{8}(V_{ci}^{\frac{1}{3}} + V_{cj}^{\frac{1}{3}})^3 \quad (2\text{-}28)$$

According to the author, the predicting results for the CO_2-, CH_4-, and N_2-saturated bitumen viscosity, average absolute deviations of 19%, 29%, and 7%, can be observed respectively.

In 1989, Mehrotra et al. [6] investigated the temperature effect on viscosity of Cold Lake bitumen fractions. In this work, the experimental measurement had been performed via RV8 viscometer and Cannon-Fenske viscometer at atmospheric pressure, and the bitumen was characterized five "cuts" whose viscosity value varied from 4.3mPa.s at 30^{o}C to 800,000mPa.s at 120^{o}C. To correlate the viscosity-temperature relationship for each fraction, the double-log correlation was found satisfactory and can be expressed as:

$$\log\log(\mu + 0.7) = b_1 + b_2 \log T \quad (2\text{-}29)$$

Where, b_1, b_2 are the characterized coefficients and varied with different fractions. For Cold Lake bitumen fractions, b_1 was taken the value of 11.6244, 11.2120, 10.4535, 10.1941 and 8.9592 in correspond to Cut1 to Cut5 fractions as well as b_2 was taken -4.7535, -4.4068,-3.9527, -3.8016, -3.1573 respectively. To compare with experimental data, the AAD was less than 3.1%.

To predict the whole bitumen viscosity, the correlation was generalized via modified Reid correlation and can be described as:

$$\log(\mu_m + 0.7) = \sum_{i=1}^{n} \left[x_i \left(\frac{M_i}{\bar{M}}\right)^{0.5} \right] \log(\mu_i + 0.7) \qquad 2\text{-}30$$

Where, x_i is mole fraction and the term $x_i\left(\frac{M_i}{\bar{M}}\right)^{0.5}$ is the geometric mean of mass and mole fractions. The prediction error was report as 38%.

In 1992, Mehrotra et al. [7] present a one parameter viscosity-temperature equation to predict the effect of temperature on viscosity of liquid hydrocarbons and their mixtures. The correlation can be described as: $\text{Log}\,(\mu + 0.8) = \Theta\,(\Phi T)^b$, where μ is in mPa.s, T in Kelvin, and Θ=100, Φ=0.01 for pure hydrocarbons. According to this work, this correlation has been validated by all of 273 pure hydrocarbon fluids or bitumen fractions. In addition, in this study, they introduced two mixing rules approach to calculate the viscosity of CO_2-saturated or toluene-diluted bitumen.

Mixing Rule I: $\text{Log}\,(\mu + 0.8) = \Sigma \nu_i\, \Theta\, (\Phi T)^{bi}$ 2-31

Mixing Rule II: $\text{Log}\,(\mu + 0.8) = \Sigma \nu_i\, \Theta\, (\Phi T)^{bi} + \Sigma_i \Sigma_j\, \nu_i\, \nu_j B_{ij}$ 2-32

Of the two mixing rules, the mixing rule I demonstrated well-fitting with experimental data within one order of magnitude of data.

Puttagunta et al., in 1993, [8] presented a viscosity correlation as function of pressure and temperature by correlated 570 data points of various Alberta heavy oils and bitumens at temperatures ranging from 20 to120^{o}C and gauge pressures up to 18MPa. The model can be expressed as:

$$\ln \mu = 2.30259[b/(1 + (T - 30)/303.15) + C] + B_0 P exp(dT) \quad 2\text{-}33$$

Where b is the characterization coefficient and can be calculated by:

$$b = \log_{10} \mu_{30°C} - C \quad 2\text{-}34$$

$$C = -3.0020 \quad 2\text{-}35$$

$$S = 0.0066940b + 3.53641 \quad 2\text{-}36$$

$$B_0 = 0.0047424b + 0.0081709 \quad 2\text{-}37$$

$$d = -0.0015646b + 0.0061814 \quad 2\text{-}38$$

To compare with experimental values of compressed Cold Lake bitumen, Athabasca bitumen and dried cold-bailed Cold Lake bitumen at wide range conditions, the predicted results had shown good agreement with AAD of 2.32%, 4.43% and 3.85% respectively.

Miadonye, Singh and Puttagunta (1994) [9] presented a viscosity modelling dependence on temperature. This study was based on the concept of a curvilinear relationship between the viscosity and the temperature for crude oil, in order to derive the viscosity characterization parameter and develop a suitable single-parameter viscosity model through a modified Roeland equation.

The following correlation was modified by Briggs et al.:

$$ln\mu_{P,T,x} = ln\mu_{T(P=0,x=0)} + B_T P - C_T X \quad 2\text{-}39$$

Where, for Alberta bitumen:

$$ln\mu_{(P=0,x=0)} = 2.303[b/(1 + \frac{T}{135})^s - 1.2] \quad 2\text{-}40$$

$$B_T = B_0 \exp[-DT] \quad 2\text{-}41$$

$$C_T = C_0 exp[-ET] \quad 2\text{-}42$$

In which

x is the mole fraction of the additive (mole %);

b and s are constants in Roeland's equation;

B_T and $B_0$and are the pressure coefficients of the viscosity at temperatures T°C and 0°C $(MPa)^{-1}$ for dead oil, respectively;

C_T and C_0 are concentration coefficients at temperatures T°C and 0°C $(mole\ \%)^{-1}$.

By modifying Equation [2-40], a generalized one-parameter correlation can be obtained:

$$\log_{10}\mu = b/(1+\frac{T-30}{303.15})^s + C \qquad 2\text{-}43$$

Where, μ is the dynamic viscosity in Pa.s, at temperature T°C.

Adjustable characterization coefficient b is obtained by measuring a single viscosity value of the particular bitumen or heavy oil at 30°C and one atmosphere pressure can be calculated as:

$$b = \log_{10}\mu_{30°C} - C \qquad 2\text{-}44$$

$$C=-3.0020 \qquad 2\text{-}45$$

$$S=0.0066940*b + 3.5364 \qquad 2\text{-}46$$

In this study, the prediction method can provide overall absolute average deviation 4.9%, The prediction results turned out the average deviation for three Cold Lake samples are 5.12%, 6.30%, and 4.41% respectively; the average deviation for two Peace River bitumen samples are 6.24% and 6.28% respectively; the average deviation for Wabasca sample is 5.08%; and 6.95%, 4.13% for two Marguerite Lake samples. Meanwhile, the authors pointed out the selection of temperature can affect the prediction accuracy.

Miadonye, Singh and Puttagunta (1995) [10] addressed bitumen viscosity modelling after studying the application of a generalized viscosity-temperature relationship based on 300 experimental data points. This correlation was the mixing rule between bitumen and diluents that obeys the power-law principle. The Einstein-type relationship, which is analogous to the observations in suspension rheology, had been applied. The prediction AAD was 8.7%. However, it was found that the correlation gave a high percentage of errors for mixtures with high disparity between the bitumen and diluents' viscosities.

Recently, in 2007, Zhang et al. [11] present a correlation prediction method for the viscosity of Heavy oil from Liaohe Basin, NE of China. In this work, a set of viscosity data have been measured at different temperature (40, 50, 60, 70, 80 and 90°C). They found a certain function between the viscosity of heavy oil at 50°C and the viscosity at 60, 70, 80 and 90°C. A closely investigation has been carried out for the correlation: $\mu_T = a\mu_{50}^b$. Where, μ_T is viscosity (mPa.s) at temperature T (°C), μ_{50} is viscosity at 50°C, a and b are viscosity parameters. To compare with measured data, the most error is less than 10% for the viscosity prediction of Liaohe basin.

2.2 Viscosity and density modeling and experimental study on pure solvents

In 1991, Allan and Teja [12] introduced a new methodology based on effective carbon number to estimate the viscosity for pure hydrocarbon. In this work, total sixty-nine hydrocarbon liquid had been studied to correlate Vogel equation which can be described as:

$$\ln \mu = A\left[-\frac{1}{B}+\frac{1}{T+C}\right] \quad 2\text{-}47$$

Where, constant A, B and C can be obtained by correlated with effective number of carbon atoms.

$$A = 145.73 + 99.01n + 0.83n^2 - 0.125n^3 \quad 2\text{-}48$$

$$B = 30.48 + 34.01n - 1.23n^2 + 0.017n^3 \quad 2\text{-}49$$

$$C = -3.01 - 1.99n \quad 2\text{-}50$$

According the authors, the average deviation in estimation of normal alkanes viscosity was less than 10%. The smaller the number of carbon atom in this family, the less of accuracy of prediction. For largest members, such as pentadecane and hexadecane, the error was less than 1.0%.

Also in 1991, Mehrotra [13] proposed a generalized viscosity equation to calculate pure solvents, such as toluene, via modified Walther correlation. The single parameter correlation can be shown as:

$$\log(\mu + 0.8) = 100(0.01T)^b \quad 2\text{-}51$$

And parameter b is the function of boiling temperature and can be obtained by fitted the results to the below equation:

$$b = Bt_0 + Bt_1/T_b^{10} \quad 2\text{-}52$$

According to author, this correlation can provide 2-3%AAD for branched paraffins and olefins, but slightly more than 10% for fused-ring aromatic and naphthenic compound.

In 2003, Barrufet and Setiadarma [14] conducted a study on experimental measurement for heavy oil-solvent viscosity and investigated some populate viscosity mixing rules. In this work, heavy oil was taken from Canada's heavy oil reserves and solvent was n-decane. The experiment conducted at temperatures ranging from ambient to 450K and the oil-solvent viscosity ratios up to 400,000. The main equipment is the mercury capillary viscometer and DB Robinson PVT apparatus. Moreover, several mixing rules had been correlated and evaluated by experimental measurements. The results can be stated as bellowing:

1. Beggs and Robinson correlation

$$\mu_{OD} = 10^{yT^{-1.163}} \quad \text{2-53}$$

$$y = 10^{(3.0324-0.02023\gamma_0)} \quad \text{2-54}$$

In which, γ_0 is specific gravity in ^{o}API.

The AAD for decane viscosity prediction is 21%.

2. Miadonye correlation

$$\ln \mu = 2.30259\left(\frac{\log(\mu_{30^{\circ}C}) - b_1}{[1+(T-30)/303.15]^s} + b_1\right) \quad \text{2-55}$$

$$s = b_2 \times (\log \mu_{30^{\circ}C} - b_1) + b_3 \quad \text{2-56}$$

Where, T is temperature in ℃, μ in Pa.s.

After recalibrated the coefficientsb_1, b_2, and b_3, the error of 11% for global fit can be observed.

3. Orbey and Sandler correlation

$$\ln\frac{\mu}{\mu_{ref}} = k\left[-1.6866 + \frac{1.4010}{T/T_B} + \frac{0.2406}{(T/T_B)^2}\right] \quad 2\text{-}57$$

In which, μ_{ref} and k are viables that vary with different categories of hydrocarbon families, and k can be described as:

$$k = 0.143 + 0.00463 \times T_B - 0.00000405 \times T_B^2 \quad 2\text{-}58$$

Where,

T_B is the normal boiling point.

The authors evaluated this correlation for n-decane, and showed an average absolute error was 1.14%.

More recently, Badamchi-Zadeh et al. (2009) [15] conducted a study on physical property measurements for propane and Athabasca bitumen. In this work, the experiments were performed in DB Robinson Jefri PVT cell which can operate pressure up to 69MPag and temperature from -15°C to 200°C. In addition, they proposed two correlations to calculate the density and viscosity for pure liquid propane as following:

$$\log\rho_{c3} = \log(221.51) - \log(0.27744)\left(1 - \frac{T}{369.82}\right)^{0.287} \quad 2\text{-}59$$

$$\log\mu_{c3} = -3.1759 + \frac{297.12}{T} + 0.0095452T - 0.000018781T^2 \quad 2\text{-}60$$

The authors also mentioned that the density correlation is valid at 369.62K which is the critical temperature of propane.

2.3 Bitumen/solvents binary mixtures viscosity and density experimental investigation and modeling study

Early in 1980, Jacobs et al. [16] conducted an experiment to measure viscosity of diluted Athabasca bitumen by carbon dioxide, methane and nitrogen. In this work, a Contraves Model DC 44 viscometer coupled to the measuring bob inside the flow-through cup was employed to measure viscosity data. The measurement accuracy was varying between 0.8% and 4%. To compare the effect of viscosity reducing, this study indicted carbon dioxide is the most prominent dilute gas, methane is the next and nitrogen has less influence. In addition, the authors mentioned the effect of dissolved gas is the function of pressure and temperature.

In 1984, a critical viscosity correlation review for mixtures of heavy oil, bitumen and petroleum fractions had been done by W. R. Shu. [17] In this work, Shu evaluated and considered some correlations including Arrhenius, Bingham, and Monroe were not proper to predict mixtures viscosity. Neither ASTM D341 nor Cragoe method can be valid for wide range condition. Instead of above correlation, Lederer equation is promising to be improved and can be expressed as:

$$\ln \mu = x_A \ln \mu_A + x_B \ln \mu_B \quad (2\text{-}61)$$

$$x_A = \frac{\alpha V_A}{\alpha V_A + V_B} \quad (2\text{-}62)$$

$$x_B = 1 - x_A \quad (2\text{-}63)$$

Where

α is an adjustable parameter and varying with different interest fluids. Through

transformed Einstein Equation and regression analysis, α can be calculated by following equation:

$$\alpha = \frac{17.04\Delta\rho^{0.5237}\rho_A^{3.2745}\rho_B^{1.6816}}{\ln(\mu_A/\mu_B)} \quad \text{2-64}$$

According to the author, the generalized equation can provide good fit for high viscosity region but limited to low viscosity ratio system.

In 1990, Eastick et al. [18] invested the two-parameter viscosity correlation to predict the binary mixtures viscosity of Cold Lake fractions. First of all, they correlated the Viscosity-Temperature correlation for bitumen fraction by model I with average deviation below 10%.

Model I: Log [Log (μ +0.7)] =b_1 +b_2 Log (T) 2-65

Then, they prepared twelve binary mixtures of Cold Lake bitumen fractions by mixing different proportions of the individual constituents. The following mixing formula has been proposed:

$$\log(\bar{\mu} + 0.7) = \sum_{i=1}^{n} x_i \sqrt{M_i/\bar{M}} \log(\mu_i + 0.7) \quad \text{2-66}$$

Where, x_i is the mole concentration for component i, M_i is the molar mass of component i, and $\bar{M}$ is the average mixture molar mass. The average of deviation of the mixtures viscosity prediction is within 17% with this mixing rule and generalized parameters.

In 1992, Mehrotra [19] presented a method to predict the viscosity of oil-sand bitumens diluted with gases or light liquids by extended the one parameter equation which is:

$$\log(\mu + 0.8) = \Theta(\Phi T)^b \quad \text{2-67}$$

Into two mixing rule

I: $$\log(\bar{\mu} + 0.8) = \sum v_i \, \Theta(\Phi T)^{b_i} \quad \text{2-68}$$

II: $$\log(\bar{\mu} + 0.8) = \sum v_i \, \Theta(\Phi T)^{b_i} + \sum\sum v_i v_j B_{ij} \quad \text{2-69}$$

By valid with experimental data, the one parameter correlation can predict gas viscosity within 1.9% errors and the AAD for mixing rule I can approach to 23.6% in the prediction of CO_2 saturated bitumen viscosity; in contrast with mixing rule I, mixing rule II gave an significant error up to 61.8% .

Miadonye et al. (2000) [20] developed a correlation for viscosity and solvent mass fraction of bitumen-diluents mixture. In this paper, a viscosity reduction parameter was introduced to account for the large curvilinear relationship between the mixture viscosity and the solvent concentrations.

The concepts of the new correlation can be described as following:

$$v_m = \exp\{exp[a(1 - X_D^n)] + lnv_D - 1\} \quad \text{2-70}$$

Where, *a* is the viscosity interaction parameter, and *n* is the viscosity reduction parameter of the diluents:

$$a = \ln(lnv_B - lnv_D + 1) \quad \text{2-71}$$

$$n = \frac{v_D}{0.1351 + 0.9029 v_D} \quad \text{2-72}$$

By regression of 102 experimental data points, the values of equation [2-72] can be obtained.

Equation [2-70] can also be rearranged to express the solvent mass fraction as a function of the mixture viscosity:

$$X_D = \exp\left\{\frac{\ln\left[\frac{a-ln(lnv_m-lnv_D+1)}{a}\right]}{n}\right\} \quad 2\text{-}73$$

According to the authors, the prediction from the above correlation can give an overall average absolute deviation of 13.5%.

In 2004, Lindeloff et al. [21] developed the Corresponding State method to predict the viscosity of hydrocarbon fluid. In this study, three pseudo critical properties have been introduced. The modeling form can be described as follow:

$$\eta_r = f(P_r, T_r) \quad 2\text{-}74$$

$$\eta_c = T_c^{-1/6} P_c^{2/3} M^{1/2} \quad 2\text{-}75$$

$$\eta_r = \frac{\eta}{T_c^{-1/6} P_c^{2/3} M^{1/2}} \quad 2\text{-}76$$

$$\eta_x(P_r, T_r) = \left[\frac{T_{cx}}{T_{co}}\right]^{-\frac{1}{6}} \left[\frac{P_{cx}}{P_{co}}\right]^{\frac{2}{3}} \left[\frac{M_x}{M_o}\right]^{\frac{1}{2}} \eta_o \left[\frac{PP_{co}}{P_{cx}}, \frac{TT_{co}}{T_{cx}}\right] \quad 2\text{-}77$$

$$\eta_{mix}(P,T) = \left[\frac{T_{c,mix}}{T_{co}}\right]^{-\frac{1}{6}} \left[\frac{P_{c,mix}}{P_{co}}\right]^{\frac{2}{3}} \left[\frac{M_{mix}}{M_o}\right]^{\frac{1}{2}} \left(\frac{\alpha_{mix}}{\alpha_o}\right) \eta_0[P_o, T_o \quad 2\text{-}78$$

Where

$$P = \frac{PP_{co}\alpha_o}{P_{c,mix}\alpha_{mix}} \quad 2\text{-}79$$

$$T = \frac{TT_{co}\alpha_o}{T_{c,mix}\alpha_{mix}} \quad 2\text{-}80$$

$$T_{c,mix} = \frac{\sum_{i=1}^{n}\sum_{j=1}^{n} z_i z_j [\left(\frac{T_{ci}}{T_{ci}}\right)^{\frac{1}{8}} + \left(\frac{T_{cj}}{T_{cj}}\right)^{\frac{1}{8}}]^8 \sqrt{T_{ci}T_{cj}}}{\sum_{i=1}^{n}\sum_{j=1}^{n} z_i z_j [\left(\frac{T_{ci}}{T_{ci}}\right)^{\frac{1}{8}} + \left(\frac{T_{cj}}{T_{cj}}\right)^{\frac{1}{8}}]^8} \quad 2\text{-}81$$

$$P_{c,mix} = \frac{8\sum_{i=1}^{n}\sum_{j=1}^{n} z_i z_j [\left(\frac{T_{ci}}{T_{ci}}\right)^{\frac{1}{8}} + \left(\frac{T_{cj}}{T_{cj}}\right)^{\frac{1}{8}}]^8 \sqrt{T_{ci}T_{cj}}^2}{\{\sum_{i=1}^{n}\sum_{j=1}^{n} z_i z_j [\left(\frac{T_{ci}}{T_{ci}}\right)^{\frac{1}{8}} + \left(\frac{T_{cj}}{T_{cj}}\right)^{\frac{1}{8}}]^{1/8}\}} \quad 2\text{-}82$$

$$M_{mix} = 1.304 \times 10^{-4}(\overline{M_{\varpi}^{2.303}} - \overline{M_n^{2.303}}) + \overline{M_n} \quad 2\text{-}83$$

$$\overline{M_{\varpi}} = \frac{\sum_{i=1}^{n} z_i M_i^2}{\sum_{i=1}^{n} z_i M_i} \quad 2\text{-}84$$

$$\overline{M_n} = \sum_{i=1}^{n} Z_i \quad 2\text{-}85$$

$$\alpha_{mix} = 1.000 + 7.378 \times 10 - 3\rho_{\gamma}^{1.847} M_{mix}^{0.5173} \quad 2\text{-}86$$

$$\rho_{\gamma} = \frac{\rho_o\left(\frac{PP_{co}}{P_{c,mix}}, \frac{TT_{co}}{T_{c,mix}}\right)}{\rho_{co}} \quad 2\text{-}87$$

In this work, the performance of the Corresponding State model has been discussed in its classic form, and the feasibility of the extrapolating was also investigated.

In 2005, Hossain et al. [22] investigated empirical correlations for dead, saturated and under-saturated oils. In this study, Bennison's equation which described as $\mu_{od} = AT^B$ has developed into

$$\mu_{od} = 10^{(-0.71523API + 22.13766)} T^{(0.269024API - 8.268047)}$$

for the calculation of dead oil viscosity and 3-50% improvement to compare the existed correlation. For the prediction of saturated oil viscosity, the correlation in form

$$\mu_{ob} = (1 - 0.001718831R_s + 1.58081 \times 10^{-6} R_s^2)\mu_{od}^{(1-0.002052461R_s + 3.\times 10^{-6} R_s^2)}$$

has been adopted and given a 5-13% better results in bubble point viscosity calculation. For under-saturated oil viscosity prediction, the correlation

$$\mu_o = \mu_{ob} + 0.004481(P - P_b)(0.555955\mu_{ob}^{1.068099} - 0.527737\mu_{ob}^{1.063547})$$

demonstrated 2% improvement to compare with Beal's equation.

More recently, Wang and Lv (2009) [23] presented a volume translation equation of state (EOS). This work was based on the Peng-Robinson (PR) cubic equation and expressed the relationship between PVT and *T*μ*P*. This research also studied the similarity of the PVT and *T*μ*P* functions and modified the temperature-dependent volume translation for the PR EOS.

Volume Translation for the PR EOS

$$P = \frac{RT}{v-b} - \frac{a}{v^2+2bv-b^2} \qquad 2\text{-}88$$

In which

a and *b* are energy and size parameters, respectively. For pure component, parameters *a* and *b* are the function of critical properties *Tc* and *Pc*, and can be calculated by following eqautions:

$$a = \left(\frac{0.45724R^2T_c^2}{P_c}\right)\alpha(T_c) \qquad 2\text{-}89$$

$$b = 0.0778RT_c/P_c \qquad 2\text{-}90$$

$$\alpha(T_\gamma) = T_\gamma^{N(M-1)}exp[L(1 - T_r^{NM})] \qquad 2\text{-}91$$

$$v = v^{PR} + c - \Delta v_c(t) \qquad 2\text{-}92$$

$$\Delta v_c = v_c^{PR} - v_c^{EXP} \qquad 2\text{-}93$$

Where

υ^{PR} refers to the molar volume.

Constant *c* can be obtained from following generalized correlation:

$$c = 0.252(\frac{RT_c}{P_c})(1.5448Z_c - 0.4024) \quad \text{2-94}$$

in which

Zc is the critical compressibility.

The following β function is proposed:

$$\beta(T) = \frac{0.35}{0.35+0.5|d_r\alpha(T_r)-T_r|} \quad \text{2-95}$$

$$\alpha(T_r) = T_r^{N(M-1)} exp[c_1(1 - T_r^{NM})] \quad \text{2-96}$$

$$d_r = d_{sat}^{PR}/d_c^{PR} \quad \text{2-97}$$

Where, $d_r$is the reduced density along the saturated liquid line, $d_{sat}^{PR}$is the calculated saturated liquid density in mol/L and $d_c^{PR}$is the calculated critical density.

$$\upsilon = \upsilon^{PR} + c(T) \qquad (T < T_c) \quad \text{2-98}$$

In the supercritical region:

$$d_r = d^{PR}(T_c, P)/d_c^{PR} \quad \text{2-99}$$

$$\upsilon = \upsilon^{PR} + c(T) \qquad (T > T_c) \quad \text{2-100}$$

$$\upsilon = \upsilon^{PR} + c - \Delta\upsilon_c \frac{0.35}{0.35+0.5(d_r-1)} \quad \text{2-101}$$

Viscosity Model Based on the PR EOS

$$T = \frac{rp}{\mu-b} - \frac{a}{\mu^2+2b\mu-b^2} \quad \text{2-102}$$

$$a = 0.45724r_c^2P_c^2/T_c \quad \text{2-103}$$

$$b = 0.0778 r_c P_c / T_c \quad (2\text{-}104)$$

$$R = \frac{P_c v_c}{Z_c T_c} \quad (2\text{-}105)$$

$$r_c = \frac{T_c \mu_c}{Z_c P_c} \quad (2\text{-}106)$$

$$\mu_c = 7.7 T_c^{-1/6} M_\omega^{1/2} P_c^{2/3} \quad (2\text{-}107)$$

To express the relationship of the saturated liquid density with temperature, the regression calculation form can be described:

$$log\mu = -A + B/T(\frac{T}{K}) \quad (2\text{-}108)$$

$$r = r_c[1 + m(T_r - 1)]^2 \quad (2\text{-}109)$$

$$m = 1.538\omega + 1.40\omega - 0.554\omega^2 \quad (2\text{-}110)$$

Viscosity model in supercritical Region

$$\mu = \mu^{PRl} - \Delta\mu_c(Q + s(l + Q)P_r) \quad (2\text{-}111)$$

Where

$$\Delta\mu = \mu_c^{PRl} - \mu_c^{exp} \quad (2\text{-}112)$$

The reference state is selected to avoid an overlap mistake in the supercritical region by following equation:

$$s = \delta exp(\sum_{i=1}^{3} Q_i (\mu_r^{-1} - 1)^i) \quad (2\text{-}111)$$

Where

The reduced viscosity $\mu_r$can be defined as:

$$\mu_r = \mu^{PRl}(T, P_c)/\mu_c^{PRl} \quad (2\text{-}112)$$

PR Viscosity Equation

$$T = \frac{RP}{\mu - b_1} - \frac{a}{\mu(\mu+b)+b(\mu-b)} \quad (2\text{-}113)$$

in which,

a and *b* are calculated from Equations [2-103] and [2-104], respectively, and

$$r = r_c[1 + k_1(\sqrt{T_r P_r - 1})]^{-2} \quad \text{2-114}$$

$$b_1 = b(\exp[k_2(\sqrt{T_r - 1})] + [k_3(\sqrt{P_r - 1})]^2 \quad \text{2-115}$$

In which

parameters *k1*, *k2* and *k3* are calculated from the following generalized expressions:

ω < 0.3

$$k1 = 0.829599 + 0.350857w - 0.747680w^2 \quad \text{2-116}$$

$$k2 = 1.94546 - 3.19777w + 2.80193w^2 \quad \text{2-117}$$

$$k3 = 0.299757 + 2.20855w - 6.64959w^2 \quad \text{2-118}$$

ω ≥0.3

$$k1 = 0.956763 + 0.192829w - 0.303189w^2 \quad \text{2-119}$$

$$k2 = -0.258789 - 37.1071w + 20.5510w^2 \quad \text{2-120}$$

$$k3 = 5.16307 - 12.8207w + 11.0109w^2 \quad \text{2-121}$$

In 2012, Kariznovi et al. [24] conducted an experiment to measure the viscosity of heavy oil with methane and ethane at temperature range from 50-190°C and pressure up to 8MPa. In this study, Anton Paar density measuring cell DMA HPM was applied to measure the density of interesting fluid under different condition and the Cambridge Viscometer measured the viscosity at wide range with ±1.0% accuracy. The experimental results shown that the viscosity of saturated bitumen/methane and bitumen/ethane system exist the linear relationship with temperatures. Meanwhile, one phenomenon has been observed that the solubility of ethane at 50°C is much higher than those at other temperature set-points and cause the density of bitumen/ethane system at 50°C dramatically reduction

2.4 Summary of mixing rules for Bitumen/solvents binary mixtures

More recently, in 2011, Guillermo et al. summarized 26 mixing rule that are popular in the literatures. These mixing rules can be described as 5 major categories:

1: Pure mixing rules including equations of Arrehnius, Bingham, Kendall and Monroe, Linear, Cragoe, Reid and Chirinos;

2: Mixing rules with viscosity blending index including correlation of Refutas index method and Chevron;

3: Mixing rules with additional parameter including equations of Walther, Latore, Lederer, Shu, Ishikawa, Lobe, Power Law, Barrufet & Setiadarma, Twu & Bulls, Panchenkov, Reik and Lima;

4: Mixing rules with a binary interaction parameter including equations of Van der Wyk, Grunberg & Nissan, and Tamura & Kurata; and

5: Mixing rules with excess function including Ratckiff & Khan, and Wedlake & Ratckiff.

In this study, the authors only investigated total of 18 correlations including three categories of Mixing Rules that were pure mixing rules, mixing rules with viscosity blending index and mixing rules with additional parameters by both of their own experimental data and literatures' data. As usual, the test results demonstrated no single mixing rule can predict viscosity properly for all of mixtures under wide range conditions. In general terms, the pure mixing rule is the simplest correlation required least computational procedure and experimental information with lowest accuracy. Generally, the mixing rule involved with viscosity blending index provided positive prediction error

to compare with existing data point. To predict the heavy oil viscosity, the mixing rules with additional parameter had shown their advantage and capability in relative high accurate magnitude.

Chapter 3 Experimental Procedure and Evaluation

3.1. Experimental Apparatus

Figure 1 provides a schematic diagram of the experimental apparatus that was used to measure the density and viscosity of bitumen/solvent mixtures. This apparatus consists of a feeding cell, cleaning cell, syringe 500d reciprocating ISCO pump, vacuum pump, viscometer, density measuring cell, pressure transducer, and temperature-controlled air bath oven. The density measuring cell, viscometer and pressure transducer are placed in the temperature-controlled air circulation oven.

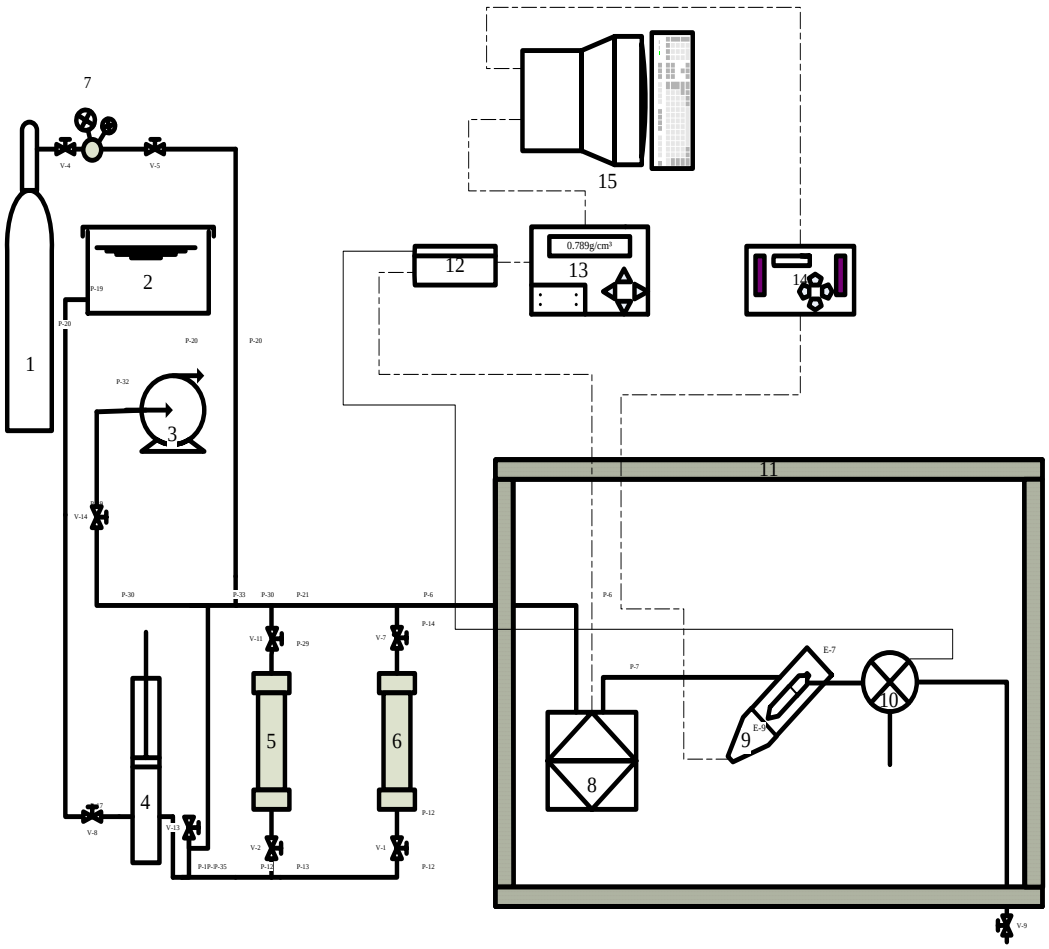

Figure 1 Schematic diagram of apparatus: (1) nitrogen cylinder, (2) water tank, (3) vacuum pump, (4) reciprocating pump, (5) cleaning cell, (6) process sample cell, (7) pressure regulator, (8) density measuring cell, (9) viscometer, (10) pressure transducer, (11) temperature-controlled oven, (12) interface module, (13) density evaluation unit, (14) viscopro 2000 unit, and (15) personal computer.

The fluid is injected into the system by the syringe 500d reciprocating ISCO pump, which also controls the system pressure. The exact fluid pressure in the viscometer and density meter is measured with an in-line pressure transducer, a Rosemount 3051CG5A capable of measuring the pressure in the range of -0.1 to 13.8 MPa (-14.2 to 2000 psi) with an accuracy of 0.04%. The value recorded by the in-line pressure transducer is

reported as the system pressure. The temperature within the system is controlled with a custom made oven.

3.1.1 Densitometer and DMA HPM Measuring Cell

Table 1 DMA HPM Density Measuring Cell General Features

Density Resolution:	approx. 1x 10^{-5} g/cm^3
Density Repeatability: (At optimum conditions)	1x 10^{-5} g/cm^3
Density Error: (At optimum conditions)	±1x 10^{-3} g/cm^3 up to ±1x 10^{-4} g/cm^3
Density Range:	0 to 3g/cm^3
Temperature Range:	263.15K to 473.15K (-10°C to +200°C)
Pressure Range:	0 to 140000kPa (0 to 1400 bar)

The density measuring cell DMA HPM is designed to measure the density of liquids and gases under high pressures (up to 140000kPa) and high temperatures (up to 473.15K). Combined with an additional evaluation unit mPDS2000V3, this system can determine the density of process fluids as a function of temperature and pressure, and display the measuring parameters as well.

The basic principle of measuring the density of the process fluids with DMA HPM and mPDS2000V3 is that the external cells measure the period of harmonic oscillation of the sample, which is excited to vibrate in the built-in U-shape Hastelloy® tube at its characteristic frequency electronically. The characteristic frequency is corresponding to the density of sample. By determining the characteristic frequency of sample precisely, the period of oscillation is converted into the density of the filled-in sample through an evaluation unit.

To calculate the density of the studied sample at wide ranges of temperature and pressure via the measured oscillation period, the following working equation can be used:

$$\rho = \sum_{i,j,k} a_{ijk} * P^i * t^j * p^k \qquad 3\text{-}1$$

Where ρ is unknown density; P is period of oscillation; t is temperature (°C); p is absolute pressure (bar); 'a' is apparatus constants.

Usually terms of i=0 and i=2 are taken. For j, terms of j=0 up to 3 may be necessary. For k, Terms of k=0 up to 3 may be necessary. In that case, the computation is carried out with the following polynomial equation:

$$\rho = a_{000} + a_{010} * t + a_{020} * t^2 + a_{001} * p + a_{002} * p^2 + a_{011} * t * p + (a_{200} + a_{210} * t + a_{220} * t^2 + a_{201} * p + a_{202} * p^2 + a_{211} * t * p) * P^2 \qquad 3\text{-}2$$

To determine the value of apparatus constants $'a_{ijk}'$, it is necessary to perform a number of measurements with different samples at different temperatures and pressures. For above equation, at least 12 measuring points would be needed. The more data points are measured, the more accurate the coefficients are. One measuring point consists of 4 values: density, period, temperature, pressure.

3.1.2 Cambridge Viscometer System

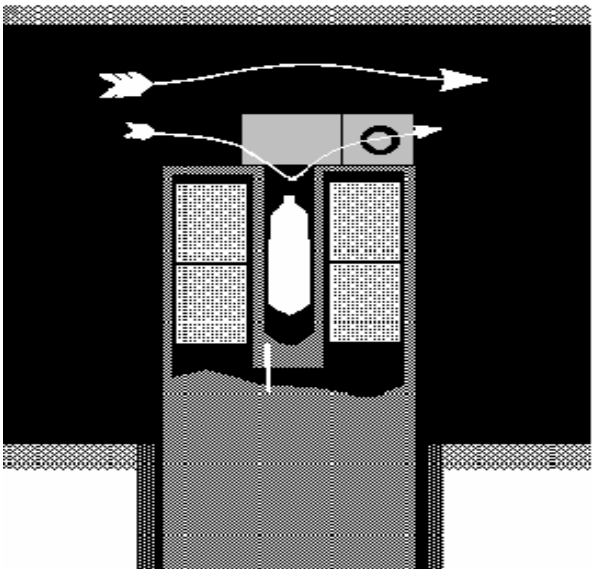

Figure 2 Sensor SPC-372 of VISCOpro2000 (From Cambridge operation manual)

Table 2 VISCOpro2000 General Specification

Model of Sensor:	spc-372
Model of Electronics:	BCC-323
Maximum Temperature:	463.15K (190°C), Process Sensors Only
Maximum Recommended Pressure:	6894.75kPa (1000psi)Tested for 2000psi
Viscosity Accuracy:	±1.0% Full Scale

The principle of the Cambridge Viscosity piston-style viscometer is that a solid piston travels through the process fluid in a chamber. The related traveling time of the fluid through a solid surface is accurately measured and converted into th*e* viscosity of interesting fluid. The Cambridge Viscosity piston-style viscometer contains two electronic coils, one magnetic piston and platinum Resistance Temperature Detector (RTD). When it is been put into working, the sample fluid is deflected into the measurement chamber by

the deflector fence and surround the low mass stainless steel (316) piston. By alternatively powering, the two magnetic coils therefore generate electromagnetic force field which interact with the magnetic piston and drive the piston travel a preset distance (0.508cm or so) back and forth. The build-in computer is enabling to measure the trip time. The viscosity of sample fluid is increasing, the traveling time also increasing over same distances. The computer measures the time of piston completed two-way cycle and convert it into fluid viscosity.

When the piston is driven toward the bottom of the measurement chamber, the fluid at the bottom of chamber is forced to flow around the piston toward the sensor opening where it interchanges with the mainstream flow of the fluid. In that way, fresh fluid keeps flowing into the bottom of measurement chamber when piston moves upward. The deflector continuously diverts fluid from the process stream into the outer portion of the measurement chamber, thereby refreshing the measured fluid.

To measure different fluids with specific range viscosity, the corresponding specific size of piston is required. In order to maximum the accuracy of measurement, the following chart can be used as a guide.

Table 3 reference of piston size for viscometer sensor corresponding with different viscosity range

Viscosity Range (cp)	Piston Size (cm)
0.02---0.2	0.792
0.2---2	0.787
1---20	0.776
10---200	0.752
50---1000	0.721
500---20000	0.572

The heats produce continuously by the movement of piston and drive the temperature of fluid rising. Temperature is measured continuously with the use of platinum Resistance Temperature Detector (RTD) mounted at the base of the measurement chamber. To compensate the effect of increasing temperature for the process fluid viscosity at specific temperature point, the Cambridge Viscosity piston-style viscosmeter embeds a function which is Temperature Compensated Coefficient (TCC). The parameter TCC describes the relationship between the viscosity and temperature for every process fluid and is obtained by the following working equation:

$$TCC = \frac{\ln(\ln(\mu_1+0.8))-ln(\ln(\mu_2+0.8))}{\ln(\theta_2+273.15)-ln(\theta_1+273.15)} \quad 3\text{-}3$$

Where μ_1 (cp) is the viscosity of process fluid at temperature θ_1 (°C); μ_2 (cp) is the viscosity at temperature θ_2 (°C).

To maximum the accuracy of measurement, it is recommended that these two temperatures be taken 5 to 10 °C apart.

3.2. Instruments Calibration

3.2.1. Densitometer Calibration

For work in large ranges of pressures and temperature, a set of apparatus constants has to be determined. In order to fulfill so, two samples of known density at the required pressure and temperature are necessary. In this work, Nitrogen and distilled Water had been taken to carry out the experiment. The operation procedure is described below:

Set up temperature and pressure point. Temperatures vary from Room temperature up to 333.15K in 10K stepwise. Pressures vary from Atmosphere pressure up to 10MPa in 1MPa stepwise. Once set up the measurement point, wait until the period of oscillation is absolutely stable. The second digit after the comma should be constant. Note down 15-20 data point of temperature, pressure, period, and density for each setup, in addition of average value for each measurement. Change temperature and pressure setup, repeat above operation. Find the target density under each average set point (Temperature, Pressure) from NIST Chemistry Web Book for both of Nitrogen and Water. Input the value of each average Temperature, Pressure and the corresponding target density into the Excel file “DMA HPM Excel Tool for Wide Range Adjustment” and calculate out the coefficients that are AA,AB,AC,AD,AE,AF,AG,AH,AI,AJ in respect. According to the calculated coefficients under particulate Temperature and Pressure range, adjust the control parameter and store into the mPDS 2000V3 evaluation unit.

From 110x2x3 data point of Nitrogen and Water, including Temperature, Pressure and target density, the adjustable density measuring cell coefficients for this experiment can be figured out and present below.

Table 4 Value of Coefficients

AA	-1.638859E+01
AB	3.726857E-04
AC	-1.056057E-06
AD	-1.348395E-06
AE	2.531434E-09
AF	2.444293E-06
AG	-6.988187E-10
AH	9.985195E-14
AI	2.054809E-13
AJ	-3.696243E-16

3.2.2. Viscometer Calibration

The Cambridge viscometer equipped with an SPC-372 sensor is factory calibrated.

3.3. Process Materials

The toluene and xylene were supplied by VWR International LLC. The toluene had a minimum purity of 0.995, and the xylene had a minimum assay of 0.985. All the chemicals were used without any further purification. The bitumen was obtained from an Athabasca field, and the density and viscosity of the bitumen was measured over a wide range of temperatures by an Anton Paar density measuring cell and a Cambridge viscometer, respectively. The measured densities and viscosities are reported in Section 4.

3.4. Experimental Procedure

At the beginning of each experiment, the entire system should be cleaned thoroughly. The procedure can be described as follow:

Firstly, close all of valves except the valve on the outlet side of reciprocating pump, two valves on the bottom and top of cleaning cell and the disposal valve; then inject 200cc ~ 400cc toluene from cleaning cell into system via the syringe 500d reciprocating ISCO pump. After that, close above mentioned valves and open the valves on the nitrogen line and surge nitrogen into system to swipe out the residual toluene from system. If the residual fluid is bitumen, a good attempt to clean the system is that warm up the air-bath oven first to reduce the viscosity of bitumen and make it mobilization before inject toluene, then execute the rest operation step.

Repeat above operation for several times. Turn on the vacuum pump and close all of valves except the valve in vacuum pump line. The system was then evacuated using the vacuum pump about 10 ~ 20 minutes to make sure no toluene vapors remain in the system.

Once the system is cleaning, close all of valves, set up target temperature point, and turn on the air-bath oven. The setup temperature then is controlled by the air-bath oven and keeps the temperature stable.

The binary bitumen/solvent mixtures then were prepared in compositions of 0.05, 0.1, 0.2, 0.2, 0.4, 0.5 and 0.6 weight fractions of solvent. For the preparation of the samples, a Sartorius balance (Model: LP4200S) with the measurement uncertainty of ± 0.01 g was used. The prepared mixtures had a weight of 300 to 400 g; therefore, the uncertainty introduced by sample preparation was less than ± 0.0001 for all mixtures.

After the desired mixture was prepared, setup the target pressure point via reciprocating pump, open the valve on the outlet side of pump and the two valves on bottom and top of the process sample cell, the sample then is injected into the system using the syringe pump. The ISCO pump controller has the capability of setting the required pressure precisely and discharging the sample fluid from the top of the sample cell to the measuring chambers. The pressure during the measurements was controlled and kept constant with the pump at the constant pressure mode. The in-line pressure transducer reported the exact system pressure.

The desired temperature was set with the temperature-controlled oven. After the desired temperature and pressure were fixed, the density and viscosity of the mixture were recorded. At a constant temperature, the system pressure was increased, covering the entire pressure range. Once finish the recording for one temperature setup, another temperature point is set via the air-bath oven and repeats the above operation steps until the viscosity and density data in whole temperatures range are recoded.

3.5 Calibration Evaluation

3.5.1 Density measurement evaluation through n-Decane

Finally, the density measuring cell is ready to be evaluated. The first evaluation has been carried out by n-Decane and compared with NIST data. The comparison result is showed by table 5 and figure 3. For 303.15K temperature setup, measurements have been taken once at different pressure. For 323.15K temperature setup, measurements have been taken twice to compare with NIST data. When present these data, the Absolute experimental pressures have been taken instead of gauge pressure because the data from NIST WEBBOOK are under absolute pressure.

Table 5 measured density for n-Decane and NIST data at 303.15K and 323.15K. Absolute experimental pressure vary from 0.12MPa to 10MPa at 1MPa stepwise

Temp. (K)	Abs. Pres (MPa)	Measured Density (kg/m^3)	NIST Density (kg/m^3)	Error, %
303.2	0.122	721.5	722.6	0.1522
302.8	0.998	723.3	723.6	0.0414
302.9	2.000	724.2	724.4	0.0276
302.9	2.997	724.8	725.2	0.0551
302.9	3.997	725.6	726.0	0.0550
02.9	4.998	726.4	726.8	0.0550
303.2	5.994	726.0	727.4	0.1924
303.0	6.992	726.9	728.3	0.1922
303.1	7.994	727.7	729.1	0.1920
303.2	8.994	728.3	729.7	0.1918
303.2	9.992	729.6	730.5	0.1232

First density measurement				
323.0	0.119	706.4	707.2	0.1131
323.2	0.998	707.3	707.8	0.0706
323.3	1.996	708.3	708.7	0.0564
323.3	2.999	709.3	709.6	0.0423
323.3	3.996	710.3	710.5	0.0281
323.3	4.994	711.1	711.4	0.0422
323.0	5.992	712.0	712.3	0.0421
323.2	6.993	712.8	713.2	0.0561
323.3	7.992	713.6	714.0	0.0560
323.3	8.992	714.5	714.9	0.0560
323.3	9.994	715.3	715.7	0.0559
Second density measurement				
323.8	0.121	706.4	706.7	0.0424
323.3	0.997	707.3	707.8	0.0706
323.3	1.999	708.4	708.7	0.0423
323.3	2.994	709.3	709.6	0.0422
323.3	3.996	710.2	710.5	0.0422
323.3	4.997	711.2	711.4	0.0281
323.3	5.995	712.0	712.3	0.0421
323.3	6.995	712.9	713.2	0.0421
323.4	7.994	713.7	714.0	0.0420
323.4	8.992	714.5	714.9	0.0560
323.4	9.990	715.4	715.7	0.0419

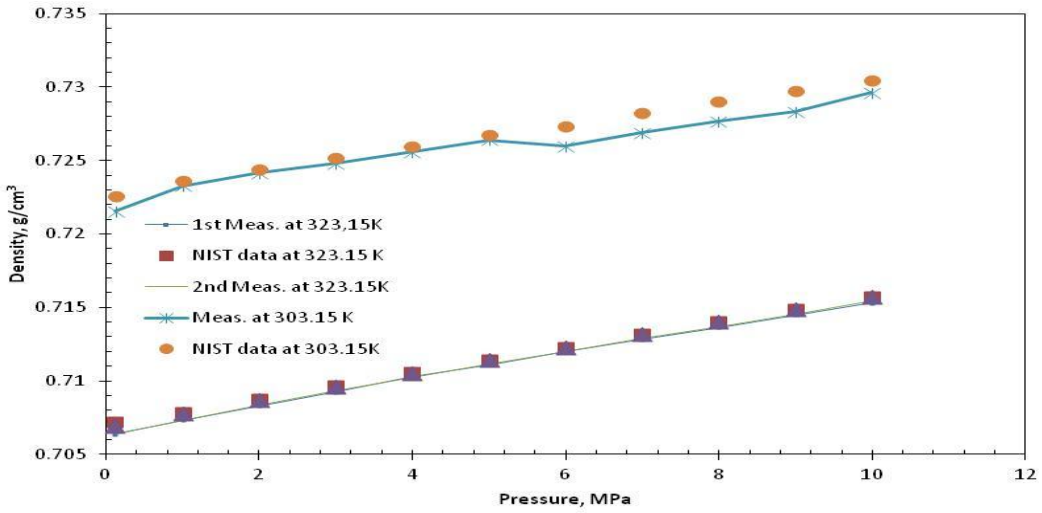

Figure 3 Comparison of measured density versus pressure at temperature 303K and 323K respectively between measurement and NIST data for pure n-Decane

3.5.2 Density measurement evaluation through binary mixture contains 50%C_{10} and 50%C_{16}

After the evaluation of n-Decane density, the measurement for mixture of 50%C10 and 50%C16 can be carried out. The following table 6 and figure 4 are the summary of data point at different condition.

Table 6 the density measurements of process mixture 50% C10 and 50%C16 at Room Temperature (295.7K or so), 321K, and 332K or so, gauge pressure vary from atmosphere pressure to 10MPa

Temperature, K	Absolute Pressure, Mpa	Density, kg/m^3
295.8	0.119	755.0
295.6	0.997	756.0
295.7	1.995	756.0
295.6	2.993	757.0
295.7	4.000	758.0
295.7	4.999	758.0
295.7	5.993	759.0
295.7	6.996	760.0
295.7	7.994	760.0
295.9	8.992	761.0
296.1	9.988	761.0
321.4	0.034	735.7
321.4	0.915	736.5
321.4	1.911	737.4
321.0	2.911	738.5
321.0	3.909	739.4
321.0	4.912	740.2
320.9	5.909	741.0
320.9	6.909	741.8
320.9	7.909	742.6
320.8	8.906	743.3
320.8	9.907	744.1
332.7	0.031	727.7

332.7	0.914	728.4
332.7	1.911	729.3
332.7	2.913	730.3
332.7	3.911	731.2
332.7	4.908	732.0
332.7	5.908	732.8
332.7	6.907	733.6
332.7	8.904	735.2
332.7	9.908	735.9

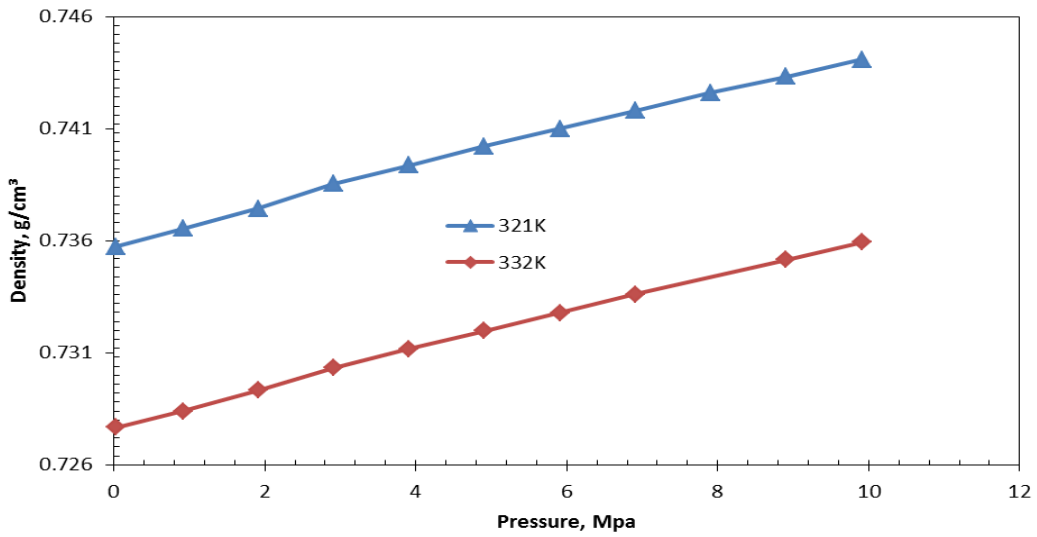

Figure 4 Density versus pressure at temperature 321K and 332K respectively for binary mixture contains 50%C_{10} +50%C_{16}

3.5.3 Density measurement evaluation through 50%C_{10} and 50%C_{18}

Then, the density for another mixture, 50% C_{10} and 50%C_{18}, can be measured at room temperature, and the pressures vary from atmosphere pressure or 0.13MPa to 10MPa.

Table 7 present the data point. Figure 5 shows the density versus pressures at room temperature around 296.5K.

Table 7 the density measurement of process mixture 50% C10 and 50%C18 at 296k, pressure vary from atmosphere pressure to 10MPa

Temperature(K)	Pressure(MPa)	Density(kg/m^3)
296.3	0.041	760.5
296.7	0.909	761.2
296.7	1.912	762.0
296.5	2.912	762.8
296.5	3.908	763.5
296.5	4.910	764.2
296.5	5.910	764.9
296.5	6.904	765.6
296.5	7.910	766.2
296.5	8.909	766.9
296.5	9.907	767.5

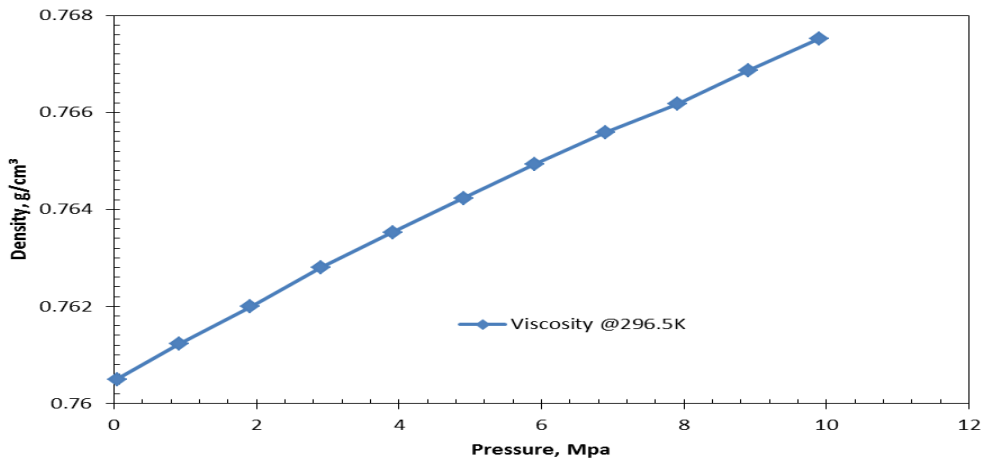

Figure 5 Density versus pressure at temperature 296.5K for binary mixture contains 50%C_{10} +50%C_{18}

3.5.4 Viscosity measurement evaluation by n-Decane

To evaluate the measurement of n-Decane viscosity, it is necessary to find out the TCC for different temperature range. According to equation [3-3], for TCC at 303.15K (30°C), the viscosity of n-decane@298.15K (25°C) and308.15K (35°C) need be known, and for TCC at 323.15K (50°C), the viscosity of n-decane@213.15K (45°C) and323.15K (55°C) need be known. Since n-decane properties are well defined, the viscosity at different condition can be found from NIST Web Book. The calculated TCC present below.

Table 8 Calculated Temperature Compensated Coefficient (TCC) at 303.15K and 323.15K respectively for n-Decane experiment

Temperature(K)	NIST Viscosity(cp)	Target Temperature(K)	TCC (Eq. 3-3)
298.15	0.854	303.15K	4.5164
308.15	0.743		
318.15	0.653	323.15K	4.8666
328.15	0.579		

Thereafter, the value of TCC at different temperature can be input into Cambridge viscometer and the control parameter of temperature can be adjusted to target temperature that are 303.15K and 323.15K respectively. The measurement data are compared with NIST data and present by Table 9.

Table 9 Measured Viscosity for n-Decane and Corresponding NIST data at 303.15K and 323.15K

Temp.(K)	Pres.(MPa)	Visc.(cp)	NIST Visc.(cp)	Error (%)
303.15	0.034	0.779	0.789	1.2674
	0.913	0.783	0.798	1.8796
	1.912	0.783	0.807	2.9739
	2.911	0.785	0.817	3.9167
	3.910	0.802	0.826	2.9055
	4.909	0.790	0.836	5.5023
	5.908	0.799	0.846	5.5555
	6.907	0.802	0.856	6.3084
	7.906	0.803	0.865	7.1676
	8.905	0.829	0.875	5.2240
	9.904	0.816	0.885	7.7490
323.15	0.034	0.569	0.609	6.5681
	0.913	0.578	0.616	6.1688
	1.912	0.576	0.623	7.5441
	2.911	0.581	0.631	7.9239
	3.910	0.578	0.638	9.4043
	4.909	0.582	0.646	9.9071
	5.908	0.583	0.653	10.7197
	6.907	0.599	0.661	9.3797
	7.906	0.596	0.668	10.7784
	8.905	0.598	0.675	11.4074
	9.904	0.601	0.683	12.0058

Before carrying out the viscosity measurement experiment of some interest sample fluid whose properties data are unknown, the TCC value at target temperature need to be

figured out firstly. Since the viscosity data do not exist, the way that uses on n-Decane is invalid. In this case, one of function of viscometer can be taken advantage. For example, to measure the viscosity for mixture of 50%C_{10}+50%C_{16} at target temperature 333.15K, the sensor temperature can be set up 3-10K up and low apart from 333.15K, and the temperature corresponding viscosity can be read from the viscometer directly. Therefore Temperature Compensation Coefficients (TCC) at target temperature 333.15K is able to be calculated out by equation [3-3]. Then this calculated value can be input the viscometer control parameter and carry out the viscosity measurement at 333.15K. Table 10 shows the results of calculation and measurement data.

Table 10 Measured and calculated Viscosity at Target Temperature 333.15K for 50%C10 and 50%C16 mixture through TCC procedure (Eq. 3-3)

50%C10 +50%C16	Pressure, MPa								
	0.034			0.913			1.912		
	Measurement		**Calculated**	**Measurement**		**Calculated**	**Measurement**		**Calculated**
Temp.,K	328.7	343.3	333.15	330.2	343.8	333.15	328.7	343.3	333.15
Visc., cp	1.061	0.792	0.954	1.064	0.800	0.976	1.048	0.796	0.972

50%C10 +50%C16	Pressure, MPa								
	2.911			3.910			4.909		
	Measurement		**Calculated**	**Measurement**		**Calculated**	**Measurement**		**Calculated**
Temp., K	330.5	343.9	333.15	330.3	344.0	333.15	330.4	344.0	333.15
Visc., cp	1.01833	0.796	0.973	1.0235	0.7958	0.9733	1.021	0.803	0.9835

50%C10 +50%C16	Pressure, MPa								
	5.908			6.907			7.906		
	Measurement		**Calculated**	**Measurement**		**Calculated**	**Measurement**		**Calculated**
Temp., K	330.5	344.0	333.15	330.5	344.1	333.15	330.5	344.1	333.15
Visc., cp	1.02825	0.802	0.983	1.0288	0.809	0.9923	1.034	0.809	0.9923

50%C10 +50%C16	Pressure, MPa					
	8.905325			9.284275		
	Measurement		**Calculated**	**Measurement**		**Calculated**
Temp., K	330.5	344.1	333.15	330.5	344.1	333.15
Visc., cp	1.037	0.809	0.994	1.0426	0.8145	1.0014

For the viscosity measurement at room temperature, which is 299K-300K or so, the value can be read from viscometer at sensor temperature directly, but make sure the circulate fans should be powerful enough to keep the sensor temperature stable at room temperature.

Table 11 The Measurement Viscosity at Sensor Temperature 299.6K and Temperature Compensation Viscosity at 295.65K for 50%C10 and 50%C16 mixture

Pressure, MPa	Temperature, K	Viscosity, cp	TCV@295.65K
0.034	299.7	1.737	1.958
0.913	299.7	1.745	1.967
1.912	299.5	1.757	1.969
2.911	299.5	1.750	1.962
3.910	299.5	1.751	1.967
4.909	299.6	1.752	1.970
5.908	299.6	1.744	1.959
6.907	299.6	1.750	1.970
7.906	299.7	1.748	1.974
8.905	299.9	1.754	1.988
9.904	301.1	1.725	2.029

Table 12 The Measurement Viscosity at Sensor Temperature 300K for 50%C10 and 50%C16 mixture

Pressure, MPa	Temperature, K	Viscosity, cp
0.034	300.9	1.027
0.091	300.3	1.379
1.912	300.2	1.407
2.911	300.2	1.416
3.910	300.2	1.427
4.909	300.2	1.431
5.908	300.3	1.443
6.907	300.4	1.449
7.906	300.5	1.461
8.905	300.5	1.476
9.904	300.4	1.490

Chapter 4 Experimental Results

4.1. Measured Density and Viscosity Values of Pure Solvents

Experimental measured density values for pure aromatic solvents (toluene and xylene) summarized in table 13. The measurement was conducted under pressure varied from atmospheric pressure (~0.124MPa) up to 10MPa or so at 1MPa stepwise increasing at each temperature setup that started from ambient temperature (~296.4K) up to 333.2K at 10K stepwise increasing. For each temperature point, the setup fluctuation can be controlled under 0.8K and pressure fluctuation can be controlled under 0.006MPa.

Table 13 experimental measured densities value of toluene and xylene as function of temperatures, T, and pressures, P.

Toluene			***Xylene***		
***T*/K**	***P*/MPa**	ρ_{exp}/(kg/m^3)	***T*/K**	***P*/MPa**	ρ_{exp}/(kg/m^3)
296.4	0.123	863.1	295.8	0.122	861.8
296.4	1.004	863.8	295.9	1.002	862.4
296.4	2.004	864.6	295.9	2.004	863.1
296.4	3.003	865.4	296.0	3.006	863.9
296.4	4.005	866.2	296.0	4.003	864.6
296.5	5.002	866.9	296.1	5.002	865.3
296.5	6.005	867.7	296.1	6.004	866.0
296.5	7.000	868.4	296.1	7.003	866.7
296.5	7.999	869.1	296.1	8.002	867.4
296.5	9.004	869.8	296.2	9.000	868.1
296.5	10.000	870.6	296.2	9.999	868.8
303.1	0.125	856.7	302.9	0.128	855.0

303.0	1.003	857.5	302.9	1.005	855.7
303.0	2.001	858.3	302.9	2.006	856.6
303.0	2.936	859.1	302.9	3.003	857.3
303.1	4.004	859.9	302.9	4.004	858.1
303.1	5.002	860.7	302.9	5.001	858.9
303.1	6.003	861.5	302.9	6.000	859.6
303.1	7.004	862.3	302.9	7.000	860.4
303.1	8.000	863.0	302.9	7.999	861.1
303.1	9.002	863.8	302.9	9.001	861.8
303.1	10.003	864.5	303.0	10.001	862.5
313.1	0.123	847.3	312.9	0.129	846.2
313.1	1.001	848.1	312.9	1.003	847.0
313.1	2.001	849.0	312.9	2.004	847.8
313.1	3.002	849.9	312.9	3.003	848.7
313.1	4.001	850.7	312.9	4.001	849.5
313.2	5.001	851.5	312.8	5.004	850.3
313.2	6.003	852.3	312.8	6.005	851.1
313.2	7.003	853.1	312.8	7.003	851.9
313.3	8.001	853.9	312.8	8.003	852.7
313.3	9.001	854.6	312.8	8.999	853.4
313.4	10.003	855.4	312.8	10.001	854.2
322.9	0.124	838.0	323.4	0.121	837.3
323.0	1.002	838.9	323.4	1.006	838.1
323.1	2.003	839.8	323.4	2.005	839.1
323.1	3.002	840.7	323.4	3.002	839.9
323.1	4.003	841.7	323.4	4.000	840.8
323.1	5.002	842.6	323.4	5.001	841.6
323.1	6.002	843.4	323.4	6.002	842.5

323.1	7.002	844.3	323.4	7.004	843.3
323.1	8.002	845.1	323.4	8.004	844.1
323.2	9.003	845.9	323.4	8.998	844.9
323.2	10.004	846.7	323.4	9.997	845.7
332.9	0.124	828.8	333.4	0.123	828.8
332.9	1.001	829.6	333.4	1.006	829.6
333.1	1.991	830.4	333.4	2.000	830.7
333.1	3.005	831.5	333.4	3.001	831.6
333.2	4.005	832.4	333.4	4.003	832.5
333.2	5.004	833.3	333.4	5.006	833.4
333.2	6.005	834.2	333.4	6.002	834.3
333.2	7.003	835.2	333.4	7.003	835.2
333.2	8.004	836.1	333.3	8.005	836.0
333.2	9.003	837.0	333.3	9.001	836.9
333.2	10.000	837.9	333.3	10.001	837.7

Table 14 summarized the measured viscosity values for two aromatic solvents that are toluene and xylene for different temperature and pressure conditions. Similarly as the density measurement setup, for each fixed pressure point that varied from atmospheric pressure up to 10MPa at 1MPa stepwise, the measurement took at five temperature settings that were 300.5K, 300.8K, 320K, 331K, and 342K within 0.6 K fluctuations.

Table 14 experimental measured viscosity values of toluene and xylene as functions of temperatures, T, and pressures, P.

Pressure (MPa)	Toluene		Xylene	
	Temperature (K)	Viscosity (cp)	Temperature (K)	Viscosity (cp)
0.124	341.6	0.343	342.7	0.356
	330.2	0.384	330.9	0.412
	319.8	0.433	317.5	0.482
	308.3	0.498	306.2	0.551
	300.5	0.53	299.1	0.605
1.003	342	0.34	342.7	0.359
	331	0.384	331.1	0.412
	319.9	0.43	318.5	0.481
	308.4	0.495	307.1	0.543
	300.5	0.529	299.5	0.603
2.002	342	0.334	342.8	0.361
	331.2	0.381	331.2	0.412
	319.8	0.431	319.1	0.47
	308.5	0.493	307.6	0.544
	300.6	0.525	300	0.594
3.001	342.2	0.332	342.8	0.36
	331.1	0.38	331.3	0.405
	319.8	0.428	319.2	0.467
	308.5	0.49	307.9	0.536
	300.6	0.524	300.2	0.594
4	342.1	0.335	342.8	0.36
	331.1	0.375	331.3	0.409
	320.1	0.426	319.3	0.466
	308.5	0.489	308	0.536
	300.6	0.528	300.3	0.599
4.999	342	0.334	342.8	0.359
	331.2	0.377	331.3	0.405
	320.2	0.425	319.3	0.465
	308.6	0.488	308.2	0.537
	300.7	0.546	300.3	0.593
5.998	341.9	0.333	342.8	0.36

	331.3	0.374	331.3	0.408
	320.3	0.424	319.3	0.464
	308.6	0.487	308.2	0.535
	300.7	0.549	300.3	0.59
	341.9	0.331	342.8	0.359
	331.3	0.374	331.3	0.407
6.997	320.3	0.424	319.3	0.464
	308.6	0.487	308.2	0.531
	300.7	0.544	300.4	0.59
	341.9	0.333	342.5	0.363
	331.4	0.373	331.4	0.405
7.996	320.4	0.421	319.3	0.464
	308.5	0.488	308.3	0.531
	300.8	0.542	300.4	0.59
	341.9	0.334	342.6	0.361
	331.4	0.373	331.4	0.405
8.995	320.4	0.422	319.3	0.465
	308.5	0.489	308.2	0.534
	300.8	0.526	300.4	0.592
	341.9	0.333	342.6	0.361
	331.4	0.372	331.4	0.406
9.994	320.5	0.422	319.3	0.464
	308.5	0.491	308.3	0.539
	300.8	0.542	300.4	0.592

4.2. Measured Density and Viscosity Values of Raw Athabasca Bitumen

Table 15 shows the summary of measured density values for raw Athabasca bitumen. The measurement conditions are similar with pure solvent measurement setup. When present the pressure point in below table, the average values have been taken instead of each instrument recording.

Table 15 experimental measured density values of Athabasca bitumen as function of temperatures, T, and pressures, P.

***T*/K**	***P*/MPa**	ρ_{exp}/(kg/m^3)	***T*/K**	***P*/MPa**	ρ_{exp}/(kg/m^3)
	0.127	1006.1		0.123	988.7
	1.003	1006.5		1.001	989.2
	2.001	1006.8		2.000	989.8
	3.003	1007.3		2.998	990.3
	4.004	1007.8		4.003	990.9
296.3	4.996	1008.4	323.3	4.999	991.4
	5.997	1008.9		6.000	992.0
	6.998	1009.4		6.996	992.5
	7.995	1009.9		7.995	993.0
	8.995	1010.3		8.993	993.5
	9.992	1010.7		9.997	994.1
	0.123	1001.5		0.121	982.7
	1.005	1001.7		1.004	983.2
	2.003	1002.2		-------	-------
	2.998	1002.7		3.002	984.4
	4.002	1003.2		4.003	985.0
303.4	5.000	1003.7	333.0	4.995	985.6
	5.999	1004.2		6.001	986.2
	6.999	1004.7		6.994	986.7
	7.996	1005.2		8.001	987.3
	8.999	1005.7		8.995	987.8
	9.995	1006.1		9.996	988.4
	0.129	994.9		-------	-------
313.2			-------		
	1.003	995.4		-------	-------

2.000	996.0	-------	-------
3.000	996.6	-------	-------
4.000	997.2	-------	-------
5.002	997.7	-------	-------
5.997	998.2	-------	-------
6.998	998.7	-------	-------
7.998	999.2	-------	-------
8.996	999.8	-------	-------
9.997	1000.2	-------	-------

According to the table 15, Figure 6 descript the trend of density varied with pressure as temperature dependence that are 296.3K, 303.4K, 313.2K, 323.3K, and 333K in average value. From Figure 6, the linear relationship between density and pressure can be observed. Moreover, as expected, density value versus temperature in inverse ratio.

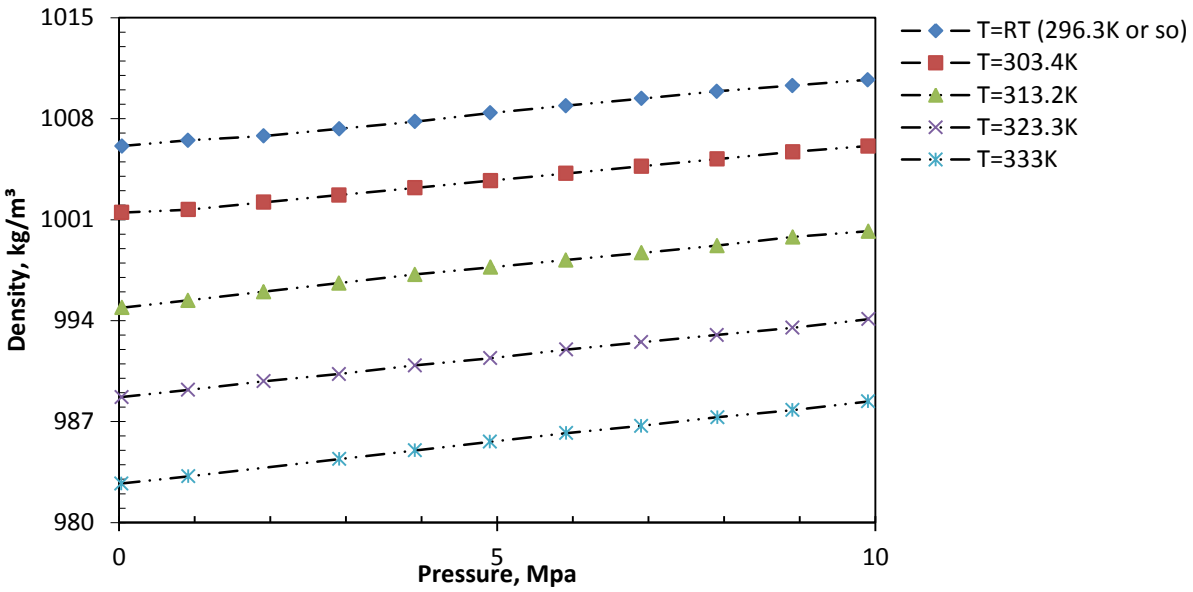

Figure 6 comparison of Athabasca bitumen density versus pressure up to 333.0K temperature

The experimental measured viscosity values of Athabasca bitumen as the function of temperature and pressure can be stated in table16. The measurement conditions were setting in similar way with mentioned way. However, due to the capacity limitation of Viscopro2000, when pressure up to 3.001MPa and temperature low to 309K, the measurement record were out of range, lost the accuracy reliability.

Table 16 experimental measured viscosity of Athabasca bitumen as function of temperatures, T, and pressures, P.

***P*/MPa**	***T*/K**	μ_{exp}**/(mPa.s)**	***P*/MPa**	***T*/K**	μ_{exp}**/(mPa.s)**
0.124	342.2	1236	7.996	331.7	4621
1.002	341.1	1465	8.995	331.7	4848
2.002	342.0	1499	9.994	331.7	5061
4.000	342.2	1561	0.124	319.5	10499
4.999	341.8	1708	1.002	319.8	11135
5.998	342.6	1643	2.002	319.9	11882
6.997	342.3	1765	3.001	319.9	12446
7.996	342.6	1789	4.000	319.9	12869
8.995	342.7	1859	4.999	319.9	13342
9.994	342.8	1944	5.998	319.9	13843
0.124	330.0	3619	6.997	319.8	14590
1.002	331.3	3519	7.996	319.9	15184
2.002	330.3	3945	8.995	319.9	16119
3.001	331.5	3728	9.994	319.9	17048
4.000	331.6	3876	0.124	308.7	36164
4.999	331.6	4053	1.002	308.8	38371

5.998	331.6	4246	2.002	308.9	40237
6.997	331.6	4433	3.001	309.0	41420

4.3. Physical Properties of bitumen/toluene Binary System

4.3.1 Measured Viscosity Values of bitumen/toluene Mixtures

Similarly as viscosity of pure solvent and raw bitumen, viscosity of binary mixtures is the function of temperature, pressure. In addition, the viscosity of mixtures has certain relationship with solvent concentration.

Through table 17 to 23, a systemic measured viscosity values for Athabasca bitumen and toluene mixtures are summarized at different conditions. From table 17 to 23, the toluene weight fractions are 5%, 10%, 20%, 30%, 40%, 50%, and 60% respectively. For each toluene concentration, the experiment measuring values were gained under pressure up to ~10MPa, temperature up to ~333.1K

Table 17 experimental measured viscosities of bitumen/toluene mixtures as function of temperatures, T, and pressures, P for constant weight fraction of toluene (w_s=0.05) in the mixture.

w_s = 0.05

P/MPa	*T*/K	μ_m/(mPa.s)	*P*/MPa	*T*/K	μ_m/(mPa.	*P*/MPa	*T*/K	μ_m/(mPa.s)
0.124	342.6	330.4	3.001	301.4	11804	6.997	309.6	5316
0.124	332.3	622.6	4.000	344.4	341	6.997	301.4	13804
0.124	319.8	1371	4.000	333.2	669.3	7.996	344.5	393.9
0.124	309.6	3839	4.000	320.9	1630	7.996	333.1	791.9
0.124	301.6	8865	4.000	309.6	5048	7.996	320.5	2026
1.002	344.4	308.9	4.000	301.4	12204	7.996	309.5	5595
1.002	333.0	613.7	4.999	344.2	358	7.996	301.5	14352
1.002	320.6	1448	4.999	333.1	696.8	8.995	344.5	407.5
1.002	309.6	4349	4.999	320.7	1653	8.995	333.0	828.3
1.002	301.6	10243	4.999	309.6	5162	8.995	320.5	2106
2.002	344.5	317.4	4.999	301.4	12610	8.995	309.5	5971
2.002	333.1	628.8	5.998	344.3	369.2	8.995	301.5	15049
2.002	320.8	1478	5.998	333.1	721.6	9.994	344.6	422.8
2.002	309.6	4658	5.998	320.5	1831	9.994	333.0	869.2
2.002	301.5	10980	5.998	309.6	5336	9.994	320.4	2199
3.001	344.6	326.1	5.998	301.4	13163	9.994	309.5	6258
3.001	333.1	646.2	6.997	344.4	381	9.994	301.5	15628
3.001	321.0	1539	6.997	333.1	752.3	-------	-------	-------
3.001	309.6	4802	6.997	320.5	1916	-------	-------	-------

Table 18 experimental measured viscosities of bitumen/toluene mixtures as function of temperatures, T, and pressures, P in constant weight fraction of toluene (w_s=0.1) in the mixture.

w_s = 0.1

P/MPa	*T*/K	μ_m/(mPa.s)	*P*/MPa	*T*/K	μ_m/(mPa.s)	*P*/MPa	*T*/K	μ_m/(mPa.s)
0.124	342.0	121.3	3.001	302.6	1810	6.997	310.6	1104
0.124	331.0	216.6	4.000	344.7	118.1	6.997	302.8	2086
0.124	321.0	410.9	4.000	332.9	226.4	7.996	344.2	140.1
0.124	310.2	881.5	4.000	321.6	448	7.996	333.2	254
0.124	302.4	1666	4.000	310.6	981.3	7.996	321.6	517.4
1.002	344.3	110.2	4.000	302.6	1868	7.996	310.6	1156
1.002	332.4	212.8	4.999	344.6	122.8	7.996	302.8	2175
1.002	321.3	416.4	4.999	332.8	234.2	8.995	344.3	144.5
1.002	310.5	891.2	4.999	321.6	463.6	8.995	333.4	262
1.002	302.6	1698	4.999	310.4	1034	8.995	321.6	537.8
2.002	344.5	112.3	4.999	302.8	1926	8.995	310.7	1197
2.002	332.8	213.1	5.998	344.5	128.6	8.995	302.8	2271
2.002	321.5	422.1	5.998	332.9	242	9.994	344.5	148.7
2.002	310.6	913.3	5.998	321.6	480.6	9.994	333.4	272
2.002	302.5	1759	5.998	310.5	1070	9.994	321.6	560.5
3.001	344.6	115.4	5.998	302.8	1996	9.994	310.4	1288
3.001	333.0	217.5	6.997	344.3	134.2	9.994	302.8	2395
3.001	321.5	437.2	6.997	333.0	247.6	-------	--------	-------
3.001	310.4	956.9	6.997	321.6	499.2	-------	--------	-------

Table 19 experimental measured viscosities of bitumen/toluene mixtures as function of temperatures, T, and pressures, P in constant weight fraction of toluene (w_s=0.2) in the mixture.

w_s = 0.2

P/MPa	*T*/K	μ_m/(mPa.s)	*P*/MPa	*T*/K	μ_m/(mPa.s)	*P*/MPa	*T*/K	μ_m/(mPa.s)
0.124	343.8	25.34	3.001	301.8	191.3	6.997	310.6	135
0.124	330.5	42.06	4.000	344.0	26.34	6.997	302.2	210.8
0.124	320.1	67.13	4.000	332.3	41.42	7.996	344.1	28.64
0.124	309.1	121.1	4.000	320.6	70.56	7.996	332.4	44.98
0.124	299.5	205.3	4.000	310.6	123.7	7.996	321.2	74.67
1.002	343.8	25.44	4.000	302.0	195.1	7.996	309.7	145.3
1.002	331.4	40.51	4.999	344.1	26.99	7.996	302.2	217.8
1.002	320.6	66.66	4.999	332.4	42.01	8.995	344.1	29.2
1.002	310.0	117.6	4.999	320.4	72.49	8.995	332.3	46.04
1.002	300.8	193.9	4.999	310.5	127.1	8.995	321.5	75.08
2.002	344.0	25.6	4.999	302.1	200.7	8.995	310.3	145.6
2.002	332.2	40.09	5.998	344.1	27.47	8.995	302.3	225
2.002	321.1	66	5.998	332.5	42.75	9.994	344.1	29.84
2.002	310.3	117.7	5.998	320.5	73.57	9.994	332.3	47.48
2.002	301.4	191.2	5.998	310.5	131.1	9.994	321.5	77.34
3.001	344.0	26	5.998	302.2	204.5	9.994	310.6	148.2
3.001	332.3	40.73	6.997	344.1	27.97	9.994	302.3	232.9
3.001	321.2	66.89	6.997	332.4	43.85	-------	--------	-------
3.001	310.5	119.6	6.997	320.7	73.68	-------	--------	-------

Table 20 experimental measured viscosities of bitumen/toluene mixtures as function of temperatures, T, and pressures, P in constant weight fraction of toluene (w_s=0.3) in the mixture.

w_s = 0.3

P/MPa	*T*/K	μ_m/(mPa.s)	*P*/MPa	*T*/K	μ_m/(mPa.s)	*P*/MPa	*T*/K	μ_m/(mPa.s)
0.124	343.3	8.851	3.001	301.7	38.37	6.997	309.8	29.67
0.124	329.9	13.16	4.000	343.9	9.139	6.997	302.1	40.87
0.124	320.9	17.78	4.000	332.3	12.88	7.996	343.7	9.814
0.124	309.5	26.98	4.000	320.9	18.72	7.996	332.2	13.83
0.124	300.5	38.77	4.000	309.9	27.86	7.996	320.9	20.13
1.002	343.6	8.861	4.000	301.8	38.85	7.996	309.9	30.03
1.002	331.0	12.79	4.999	343.6	9.322	7.996	302.1	41.69
1.002	320.9	18.01	4.999	332.3	13.04	8.995	344.0	9.914
1.002	309.6	27.11	4.999	320.9	19.03	8.995	332.2	14.09
1.002	300.9	38.35	4.999	310.0	28.4	8.995	320.9	20.57
2.002	343.9	8.903	4.999	302	39.31	8.995	310.0	30.52
2.002	331.6	12.76	5.998	343.6	9.482	8.995	302.1	42.78
2.002	320.9	18.19	5.998	332.3	13.25	9.994	344.1	10.1
2.002	309.7	27.34	5.998	320.9	19.41	9.994	332.5	14.23
2.002	301.4	38.17	5.998	309.7	29.19	9.994	320.9	20.92
3.001	343.9	8.997	5.998	302.0	40.09	9.994	310.1	31.07
3.001	332.1	12.72	6.997	343.6	9.658	9.994	302.1	43.8
3.001	320.9	18.49	6.997	332.2	13.54	-------	--------	-------
3.001	309.9	27.54	6.997	320.9	19.77	-------	--------	-------

Table 21 experimental measured viscosities of bitumen/toluene mixtures as function of temperatures, T, and pressures, P in constant weight fraction of toluene (w_s=0.4) in the mixture.

w_s = 0.4

P/MPa	*T*/K	μ_m/(mPa.s)	*P*/MPa	*T*/K	μ_m/(mPa.s)	*P*/MPa	*T*/K	μ_m/(mPa.s)
0.124	342.6	4.366	3.001	301.7	12.88	6.997	309.2	10.67
0.124	330.8	5.243	4.000	342.9	4.375	6.997	301.9	13.56
0.124	321.0	6.862	4.000	332.3	5.272	7.996	343.2	4.365
0.124	309.2	9.749	4.000	321.0	7.117	7.996	332.2	5.611
0.124	300.3	13.02	4.000	309.0	10.26	7.996	321.1	7.575
1.002	342.6	4.396	4.000	301.8	12.98	7.996	309.3	10.84
1.002	332.0	5.116	4.999	343.0	4.355	7.996	302.0	13.84
1.002	321.0	6.884	4.999	332.3	5.31	8.995	343.1	4.362
1.002	309.6	9.748	4.999	321.0	7.229	8.995	332.4	5.669
1.002	301.1	12.86	4.999	309.0	10.47	8.995	321.1	7.705
2.002	342.7	4.379	4.999	301.9	13.2	8.995	309.4	11.01
2.002	332.2	5.161	5.998	343.1	4.348	8.995	302.0	14.07
2.002	321.0	6.963	5.998	332.2	5.413	9.994	343.1	4.382
2.002	309.7	9.789	5.998	321.0	7.354	9.994	332.4	5.771
2.002	301.6	12.78	5.998	309.1	10.54	9.994	321.1	7.844
3.001	342.8	4.364	5.998	301.9	13.36	9.994	309.5	11.19
3.001	332.3	5.206	6.997	343.1	4.341	9.994	302.0	14.41
3.001	321.0	7.031	6.997	332.0	5.522	-------	--------	-------
3.001	309.0	10.14	6.997	321.0	7.453	-------	--------	-------

Table 22 experimental measured viscosities of bitumen/toluene mixtures as function of temperatures, T, and pressures, P in constant weight fraction of toluene (w_s=0.5) in the mixture.

w_s = 0.5

P/MPa	*T*/K	μ_m/(mPa.s)	*P*/MPa	*T*/K	μ_m/(mPa.s)	*P*/MPa	*T*/K	μ_m/(mPa.s)
0.124	343.6	2.307	3.001	301.2	5.396	6.997	308.6	4.956
0.124	331.1	2.954	4.000	342.6	2.357	6.997	301.5	5.671
0.124	319.9	3.736	4.000	331.3	2.952	7.996	342.9	2.38
0.124	308.3	4.928	4.000	320.0	3.768	7.996	331.3	2.983
0.124	300.2	5.465	4.000	308.5	4.925	7.996	320.1	3.816
1.002	343.0	2.33	4.000	301.4	5.449	7.996	308.6	4.968
1.002	331.1	2.958	4.999	342.7	2.369	7.996	301.5	5.767
1.002	319.8	3.762	4.999	331.3	2.96	8.995	343.0	2.388
1.002	308.4	4.915	4.999	320.1	3.775	8.995	331.3	2.988
1.002	300.6	5.413	4.999	308.6	4.934	8.995	320.1	3.822
2.002	342.7	2.336	4.999	301.4	5.51	8.995	308.6	4.971
2.002	331.2	2.973	5.998	342.8	2.376	8.995	301.5	5.842
2.002	320.0	3.762	5.998	331.3	2.965	9.994	343.0	2.402
2.002	308.5	4.906	5.998	320.1	3.782	9.994	331.3	3.01
2.002	300.9	5.424	5.998	308.5	4.945	9.994	320.1	3.833
3.001	342.6	2.354	5.998	301.5	5.607	9.994	308.6	5.016
3.001	331.3	2.951	6.997	342.9	2.379	9.994	301.6	5.998
3.001	320.1	3.762	6.997	331.3	2.968	-------	--------	-------
3.001	308.5	4.911	6.997	320.1	3.809	-------	--------	-------

Table 23 experimental measured viscosities of bitumen/toluene mixtures as function of temperatures, T, and pressures, P in constant weight fraction of toluene (w_s=0.6) in the mixture.

w_s = 0.6

P/MPa	*T*/K	μ_m/(mPa.s)	*P*/MPa	*T*/K	μ_m/(mPa.	*P*/MPa	*T*/K	μ_m/(mPa.s)
0.124	342.6	1.463	3.001	300.3	3.088	6.997	308.5	2.578
0.124	330.1	1.979	4.000	343.2	1.452	6.997	300.4	3.086
0.124	320	2.046	4.000	331.3	1.889	7.996	343.3	1.448
0.124	308.2	2.6	4.000	319.9	2.057	7.996	331.4	1.888
0.124	299.9	3.113	4.000	308.5	2.573	7.996	320.3	2.042
1.002	343	1.454	4.000	300.3	3.078	7.996	308.5	2.583
1.002	330.5	1.943	4.999	343.2	1.449	7.996	300.4	3.098
1.002	320	2.048	4.999	331.4	1.886	8.995	343.2	1.453
1.002	308.4	2.589	4.999	319.9	2.059	8.995	331.4	1.888
1.002	300	3.101	4.999	308.5	2.574	8.995	320.3	2.041
2.002	343.1	1.455	4.999	300.4	3.077	8.995	308.5	2.595
2.002	330.8	1.931	5.998	343.2	1.446	8.995	300.4	3.109
2.002	320	2.044	5.998	331.4	1.884	9.994	343.2	1.455
2.002	308.5	2.579	5.998	319.9	2.045	9.994	331.4	1.896
2.002	300.2	3.089	5.998	308.5	2.579	9.994	320.2	2.057
3.001	343.2	1.451	5.998	300.4	3.078	9.994	308.5	2.607
3.001	331.1	1.896	6.997	343.3	1.446	9.994	300.4	3.122
3.001	319.9	2.052	6.997	331.4	1.885	-------	------	-------
3.001	308.5	2.576	6.997	320.1	2.043	-------	------	-------

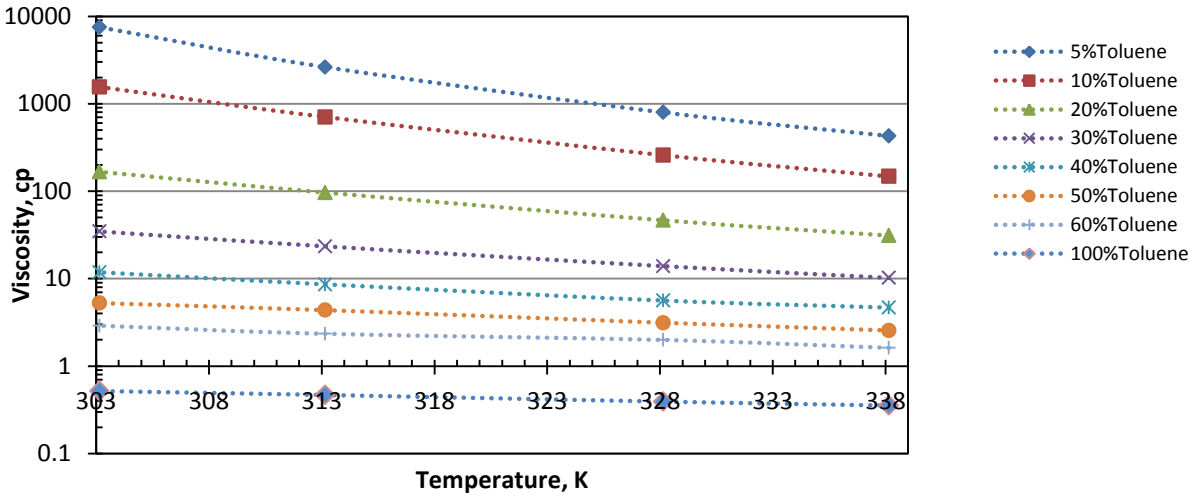

Figure 7 calculated viscosity, μ_m, of bitumen/toluene mixtures through TCC procedure (Eq. 3-3) versus temperature, T as dependence of toluene weight fraction, w_s and at lowest constant pressure of 0.125 MPa;

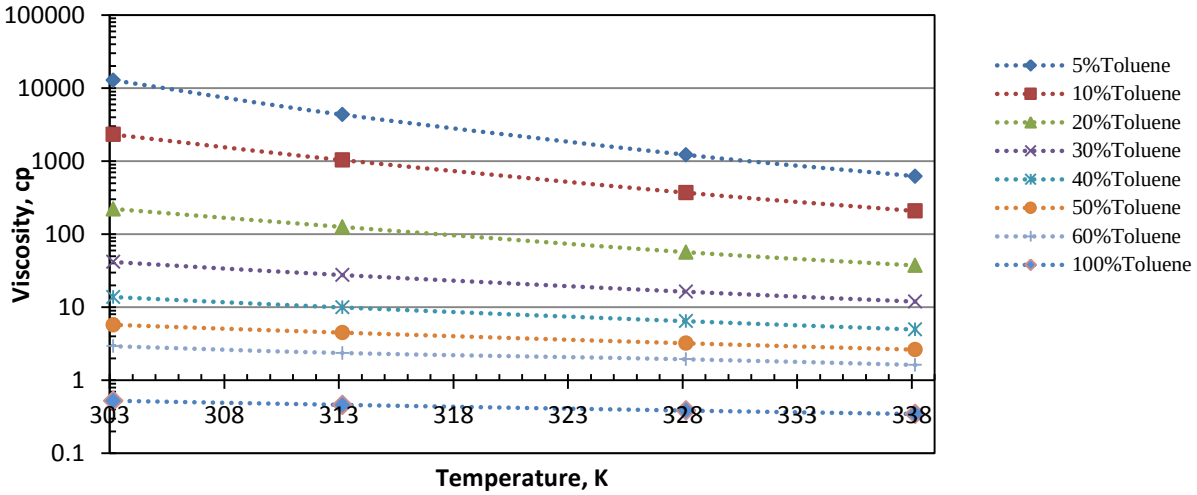

Figure 8 calculated viscosity, μ_m, of bitumen/toluene mixtures through TCC procedure (Eq. 3-3) versus temperature, T as dependence of toluene weight fraction, w_s and at highest constant pressure of 9.994 MPa;

Since the mixture viscosity is sensitive with temperature. To investigate the influence of solvent concentration upon binary mixtures viscosity, it is better to compare the viscosity value at exact same temperature point. To fulfil so, TCC calculation procure [3-3] that mentioned in Chapter 3 has been taken to calculate the viscosity value at temperatures 303K, 313K, 328K, and 338K respectively.

Figure 7 descript the impact of different toluene concentrations on Athabasca bitumen and toluene mixture viscosity at fixed lowest pressure 0.125MPa. Figure 8 shows the effect of toluene concentration on mixtures viscosity at fixed highest pressure 9.994MPa.

In addition, the trend of viscosity at different temperatures and toluene weight fractions are showing in both graphics simultaneously. From Figure 7 and Figure 8, the same trend for each specific toluene concentration can be observed. But the diversity of trend at different toluene weight fraction is obvious.

4.3.2 Measured Density Values of bitumen/toluene Mixtures

To present the density values for Athabasca bitumen and Toluene binary system properly, the similar method as viscosity of Athabasca bitumen and Toluene binary mixture has been adapted. Also, density of binary mixtures is the function of temperature, pressure. In addition, the density of mixtures has certain relationship with solvent concentration.

Through table 24 to 30, a systemic measured density values for Athabasca bitumen and toluene mixtures are summarized at different conditions. From table 24 to 30, the toluene weight fractions are 5%, 10%, 20%, 30%, 40%, 50%, and 60% respectively. For each toluene

concentration, the experiment measuring values were gained under pressure up to ~10MPa, temperature up to ~333.1K

Table 24 experimental measured densities of bitumen/toluene mixtures as function of temperatures, T, and pressures, P for constant weight fraction of toluene (w_s=0.05) in the mixture.

w_s = 0.05

P/MPa	*T*/K	ρ_m(kg/m^3)	*P*/MPa	*T*/K	ρ_m(kg/m^3)	*P*/MPa	*T*/K	ρ_m(kg/m^3)
0.125	296.6	997.4	3.001	333.2	975.5	6.997	323.3	983.9
0.125	303.5	992.5	4.000	296.6	999.5	6.997	333.1	978.0
0.125	312.9	986.4	4.000	303.5	994.7	7.996	296.6	1001.5
0.125	323.3	979.8	4.000	313.3	988.4	7.996	303.5	996.8
0.125	333.1	973.8	4.000	323.3	982.1	7.996	313.2	990.7
1.002	296.6	997.8	4.000	333.1	976.2	7.996	323.3	984.5
1.002	303.5	993.0	4.999	296.6	1000.0	7.996	333.1	978.6
1.002	313.1	986.8	4.999	303.5	995.2	8.994	296.6	1002
1.002	323.3	980.3	4.999	313.3	989.0	8.994	303.5	997.3
1.002	333.1	974.3	4.999	323.3	982.7	8.994	313.2	991.3
2.003	296.6	998.4	4.999	333.1	976.8	8.994	323.2	985.0
2.003	303.5	993.5	5.999	296.6	1000.6	8.994	333.1	979.1
2.003	313.1	987.4	5.999	303.5	995.7	9.994	296.6	1002.5
2.003	323.3	980.9	5.999	313.2	989.6	9.994	303.5	997.8
2.003	333.2	974.9	5.999	323.3	983.3	9.995	313.1	991.8
3.001	296.6	999.0	5.999	333.1	977.4	9.995	323.2	985.5
3.001	303.5	994.1	6.997	296.6	1001.0	9.995	333.1	979.6
3.001	313.2	987.9	6.997	303.5	996.3	-------	--------	-------
3.001	323.3	981.5	6.997	333.2	975.5	-------	--------	-------

Table 25 experimental measured densities of bitumen/toluene mixtures as function of temperatures, T, and pressures, P for constant weight fraction of toluene (w_s=0.1) in the mixture.

w_s = 0.1

P/MPa	*T*/K	ρ_m(kg/m^3)	*P*/MPa	*T*/K	ρ_m(kg/m^3)	*P*/MPa	*T*/K	ρ_m(kg/m^3)
0.125	296.8	988.8	3.001	333.1	967.1	6.997	323.2	975.9
0.125	303.5	984.5	4.000	296.8	991.0	6.997	333.1	969.6
0.125	313.1	978.3	4.000	303.5	986.8	7.996	296.9	993.1
0.125	323.3	971.6	4.000	313.2	980.5	7.996	303.5	989.0
0.125	333.0	965.3	4.000	323.2	974.0	7.996	313.2	982.8
1.002	296.8	989.3	4.000	333.1	967.7	7.996	323.2	976.3
1.002	303.5	985.0	4.999	296.9	991.5	7.996	333.1	970.2
1.002	313.1	978.7	4.999	303.5	987.4	8.994	296.9	993.5
1.002	323.2	972.1	4.999	313.2	981.1	8.994	303.5	989.5
1.002	333.0	965.8	4.999	323.2	974.7	8.994	313.2	983.3
2.003	296.8	989.9	4.999	333.1	968.3	8.994	323.2	976.9
2.003	303.5	985.6	5.999	296.9	992.1	8.994	333.0	970.8
2.003	313.2	979.4	5.999	303.5	988.0	9.994	296.9	994.1
2.003	323.2	972.9	5.999	313.2	981.7	9.994	303.5	990.0
2.003	333.1	966.5	5.999	323.2	975.3	9.995	313.2	983.8
3.001	296.8	990.5	5.999	333.1	969.0	9.995	323.3	977.4
3.001	303.5	986.3	6.997	296.9	992.6	9.995	333.1	971.3
3.001	313.1	980.0	6.997	303.5	988.5	-------	--------	-------
3.001	323.3	973.4	6.997	313.2	982.2	-------	--------	-------

Table 26 experimental measured densities of bitumen/toluene mixtures as function of temperatures, T, and pressures, P for constant weight fraction of toluene (w_s=0.2) in the mixture.

w_s = 0.2

P/MPa	*T*/K	ρ_m(kg/m^3)	*P*/MPa	*T*/K	ρ_m(kg/m^3)	*P*/MPa	*T*/K	ρ_m(kg/m^3)
0.125	296.3	973.5	3.001	333.3	950.0	6.997	323.3	959.3
0.125	303.4	968.8	4.000	296.4	975.7	6.997	333.3	952.6
0.125	313.2	961.9	4.000	303.5	971.1	7.996	296.4	977.9
0.125	323.3	954.9	4.000	313.3	964.3	7.996	303.1	973.6
0.125	333.3	948.1	4.000	323.3	957.5	7.996	313.1	966.7
1.002	296.3	974.0	4.000	333.3	950.7	7.996	323.3	959.9
1.002	303.4	969.3	4.999	296.4	976.3	7.996	333.3	953.3
1.002	313.1	962.6	4.999	303.5	971.6	8.994	296.5	978.4
1.002	323.3	955.4	4.999	313.1	965.1	8.994	303.1	974.1
1.002	333.3	948.6	4.999	323.3	958.0	8.994	313.2	967.2
2.003	296.3	974.6	4.999	333.3	951.4	8.994	323.3	960.5
2.003	303.4	969.9	5.999	296.4	976.8	8.994	333.3	953.9
2.003	313.2	963.0	5.999	303.5	972.2	9.994	296.5	978.9
2.003	323.3	956.1	5.999	313.0	965.7	9.994	303.2	974.5
2.003	333.3	949.3	5.999	323.3	958.7	9.995	313.3	967.7
3.001	296.4	975.1	5.999	333.3	952.0	9.995	323.3	961.1
3.001	303.4	970.6	6.997	296.4	977.4	9.995	333.3	954.5
3.001	313.3	963.6	6.997	303.5	972.8	-------	--------	-------
3.001	323.3	956.8	6.997	313.0	966.3	-------	--------	-------

Table 27 experimental measured densities of bitumen/toluene mixtures as function of temperatures, T, and pressures, P for constant weight fraction of toluene (w_s=0.3) in the mixture.

w_s = 0.3

P/MPa	*T*/K	ρ_m(kg/m^3)	*P*/MPa	*T*/K	ρ_m(kg/m^3)	*P*/MPa	*T*/K	ρ_m(kg/m^3)
0.125	296.5	958.1	3.001	333.2	933.8	6.997	323.3	943.2
0.125	303.2	952.9	4.000	296.6	960.4	6.997	333.1	936.6
0.125	313.1	945.8	4.000	303.4	955.3	7.996	296.8	962.5
0.125	323.3	938.4	4.000	313.1	948.4	7.996	303.3	957.8
0.125	333.2	931.5	4.000	323.4	941.2	7.996	313.1	950.9
1.002	296.5	958.6	4.000	333.2	934.5	7.996	323.3	943.8
1.002	303.3	953.4	4.999	296.6	960.9	7.996	333.1	937.2
1.002	313.1	946.4	4.999	303.4	955.9	8.994	296.8	963.1
1.002	323.3	939.0	4.999	313.1	949.0	8.994	303.3	958.3
1.002	333.1	932.3	4.999	323.4	941.8	8.994	313.1	951.5
2.003	296.5	959.2	4.999	333.2	935.2	8.994	323.3	944.5
2.003	303.3	954.1	5.999	296.7	961.5	8.994	333.2	937.8
2.003	313.1	947.1	5.999	303.5	956.5	9.994	296.8	963.7
2.003	323.3	939.8	5.999	313.1	949.7	9.994	303.4	958.8
2.003	333.1	933.1	5.999	323.4	942.5	9.995	313.1	952.0
3.001	296.5	959.9	5.999	333.1	935.9	9.995	323.3	945.0
3.001	303.4	954.7	6.997	296.7	962.0	9.995	333.2	938.4
3.001	313.1	947.7	6.997	303.2	957.2	-------	--------	-------
3.001	323.4	940.5	6.997	313.1	950.3	-------	--------	-------

Table 28 experimental measured densities of bitumen/toluene mixtures as function of temperatures, T, and pressures, P for constant weight fraction of toluene (w_s=0.4) in the mixture.

w_s = 0.4

P/MPa	*T*/K	ρ_m(kg/m^3)	*P*/MPa	*T*/K	ρ_m(kg/m^3)	*P*/MPa	*T*/K	ρ_m(kg/m^3)
0.125	297.0	942.9	3.001	333.2	918.3	6.997	323.1	928.2
0.125	303.4	938.0	4.000	297.0	945.4	6.997	333.3	921.0
0.125	313.3	930.5	4.000	303.4	940.5	7.996	296.9	947.9
0.125	323.2	923.3	4.000	313.3	933.2	7.996	303.2	943.2
0.125	333.2	915.9	4.000	323.2	926.0	7.996	313.3	935.8
1.002	297.0	943.5	4.000	333.2	918.9	7.996	323.2	928.8
1.002	303.5	938.5	4.999	296.9	946.1	7.996	333.3	921.7
1.002	313.3	931.1	4.999	303.3	941.3	8.994	296.9	948.5
1.002	323.2	923.9	4.999	313.3	933.9	8.994	303.2	943.7
1.002	333.2	916.6	4.999	323.2	926.7	8.994	313.3	936.5
2.003	297.0	944.1	4.999	333.2	919.6	8.994	323.2	929.5
2.003	303.5	939.1	5.999	296.9	946.7	8.994	333.3	922.4
2.003	313.3	931.8	5.999	303.2	941.9	9.994	296.9	949.1
2.003	323.2	924.6	5.999	313.3	934.5	9.994	303.2	944.3
2.003	333.3	917.3	5.999	323.2	927.5	9.995	313.3	937.1
3.001	297.0	944.8	5.999	333.3	920.3	9.995	323.2	930.1
3.001	303.4	939.8	6.997	296.9	947.3	9.995	333.3	923.1
3.001	313.3	932.5	6.997	303.2	942.5	-------	--------	-------
3.001	323.2	925.3	6.997	313.3	935.2	-------	--------	-------

Table 29 experimental measured densities of bitumen/toluene mixtures as function of temperatures, T, and pressures, P for constant weight fraction of toluene (w_s=0.5) in the mixture.

w_s = 0.5

P/MPa	*T*/K	ρ_m(kg/m^3)	*P*/MPa	*T*/K	ρ_m(kg/m^3)	*P*/MPa	*T*/K	ρ_m(kg/m^3)
0.125	296.0	929.1	3.001	333.3	902.7	6.997	323.2	913.1
0.125	303.0	923.6	4.000	296.2	931.6	6.997	333.2	905.7
0.125	313.0	915.7	4.000	303.0	926.3	7.996	296.2	934.1
0.125	323.2	907.9	4.000	313.1	918.4	7.996	303.0	928.9
0.125	333.4	900.1	4.000	323.2	910.9	7.996	313.2	921.1
1.002	296.1	929.7	4.000	333.3	903.5	7.996	323.2	913.8
1.002	303.0	924.3	4.999	296.2	932.3	7.996	333.2	906.5
1.002	313.1	916.3	4.999	303.0	926.9	8.994	296.3	934.7
1.002	323.2	908.6	4.999	313.1	919.1	8.994	303.0	929.5
1.002	333.4	900.8	4.999	323.2	911.7	8.994	313.2	921.8
2.003	296.1	930.3	4.999	333.2	904.2	8.994	323.2	914.5
2.003	303.0	925.0	5.999	296.2	932.9	8.994	333.3	907.1
2.003	313.1	917.0	5.999	303.0	927.6	9.994	296.3	935.3
2.003	323.2	909.4	5.999	313.1	919.8	9.994	303.0	930.1
2.003	333.4	901.7	5.999	323.2	912.4	9.995	313.2	922.4
3.001	296.1	931.0	5.999	333.2	905.0	9.995	323.2	915.2
3.001	303.0	925.6	6.997	296.2	933.5	9.995	333.3	907.9
3.001	313.1	917.7	6.997	303.0	928.2	-------	--------	-------
3.001	323.2	910.2	6.997	313.2	920.4	-------	--------	-------

Table 30 experimental measured densities of bitumen/toluene mixtures as function of temperatures, T, and pressures, P for constant weight fraction of toluene (w_s=0.6) in the mixture.

w_s = 0.6

P/MPa	*T*/K	ρ_m(kg/m^3)	*P*/MPa	*T*/K	ρ_m(kg/m^3)	*P*/MPa	*T*/K	ρ_m(kg/m^3)
0.125	296	915.1	3.001	333.2	887.4	6.997	323.2	898.5
0.125	302.9	909.5	4.000	296	917.8	6.997	333.3	890.6
0.125	313.1	901.2	4.000	302.9	912.2	7.996	296.1	920.4
0.125	323.2	893.0	4.000	313.1	904.2	7.996	302.9	914.9
0.125	333.2	885.2	4.000	323.1	896.2	7.996	313.2	907.0
1.002	296	915.8	4.000	333.2	888.2	7.996	323.2	899.2
1.002	302.9	910.1	4.999	296	918.4	7.996	333.4	891.4
1.002	313.1	901.9	4.999	302.9	912.9	8.994	296.1	921.0
1.002	323.2	893.8	4.999	313.1	904.9	8.994	302.9	915.6
1.002	333.1	885.8	4.999	323.1	897.0	8.994	313.2	907.6
2.003	296	916.5	4.999	333.3	889.0	8.994	323.2	899.9
2.003	302.9	910.8	5.999	296	919.1	8.994	333.3	892.2
2.003	313.1	902.7	5.999	302.9	913.6	9.994	296.1	921.6
2.003	323.2	894.7	5.999	313.1	905.6	9.994	302.9	916.2
2.003	333.2	886.5	5.999	323.2	897.7	9.995	313.2	908.3
3.001	296	917.1	5.999	333.3	889.7	9.995	323.2	900.6
3.001	302.9	911.5	6.997	296.1	919.8	9.995	333.3	893.0
3.001	313.1	903.4	6.997	302.9	914.3	-------	--------	-------
3.001	323.1	895.4	6.997	313.1	906.3	-------	--------	-------

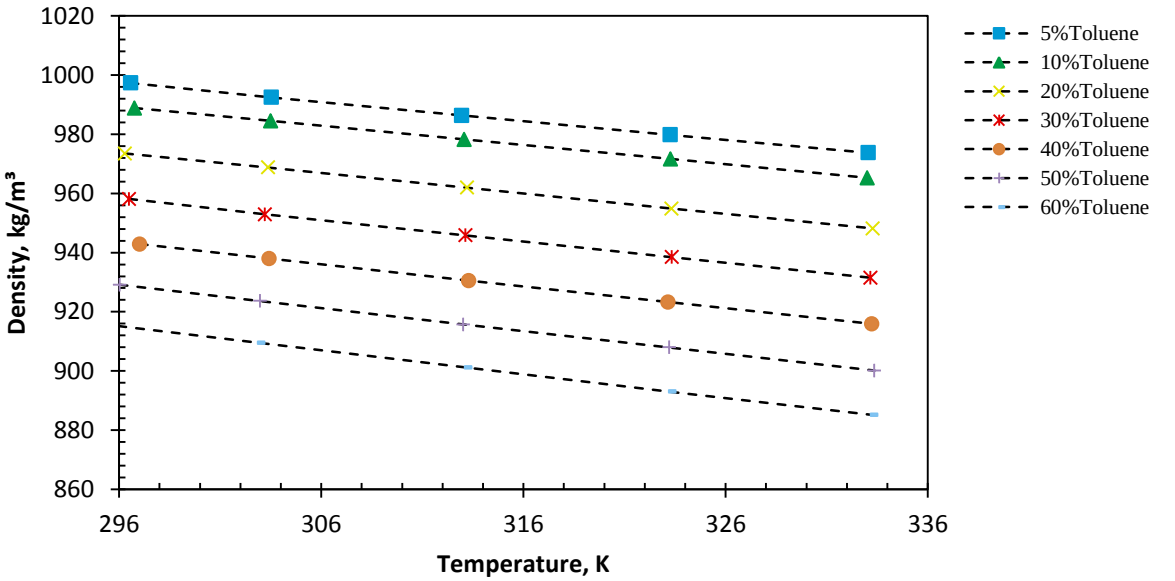

Figure 9 Effect of temperature, T, on the density, ρ_m, of bitumen/toluene mixtures as dependence of weight fraction, w_s, and at lowest constant pressure P=0.125MPa

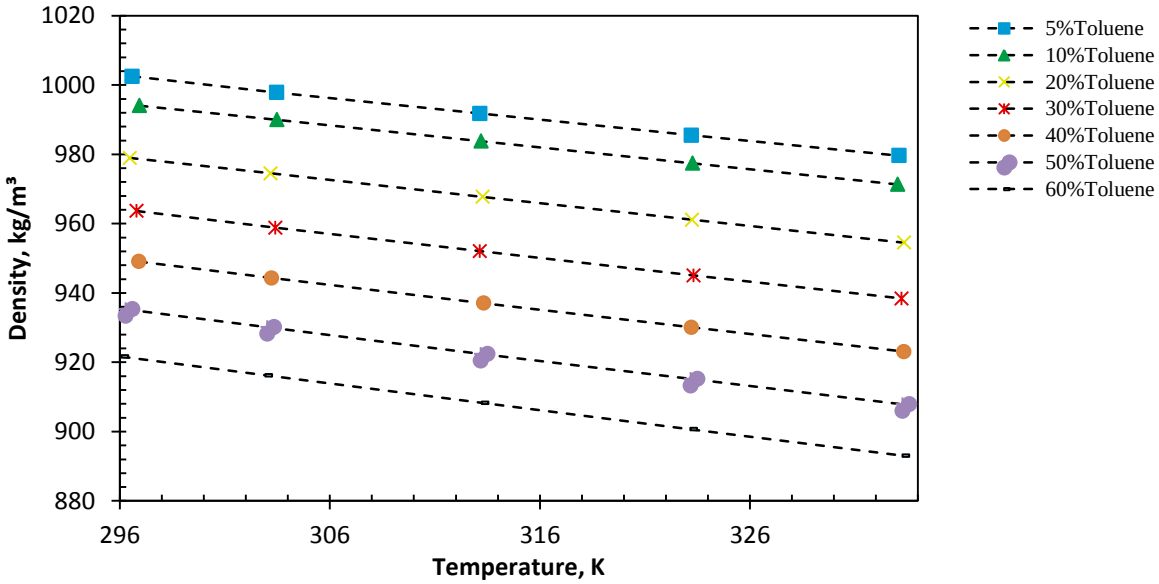

Figure 10 Effect of temperature, T, on the density, ρ_m, of bitumen/toluene mixtures as dependence of weight fraction, w_s, and at highest constant pressure P=9.995MPa

To investigate the relationship of density with respective of temperature and solvent concentration, two extreme pressure situations have been taken to consider. The measured data points are taken from highest pressure that is 9.995MPa and lowest pressure that is 0.125MPa to form Figure 9 and Figure 10 respectively.

Figure 9 descript the impact of different toluene concentrations on Athabasca bitumen and toluene mixture density at fixed lowest pressure 0.125MPa. Figure 9 shows the effect of toluene concentration on mixtures viscosity at fixed highest pressure 9.995MPa.

In addition, the trend of density at different temperatures and toluene weight fractions are showing in both graphics simultaneously. From Figure 9 and Figure 10, the linear relationship between density and temperature for each specific toluene concentration can be observed. Moreover, the inverse ratio trend between bitumen and toluene mixture density and toluene weight fraction can be well known.

4.4. Physical Properties of bitumen/xylene Binary System

4.4.1Measured Viscosity Values of bitumen/xylene Mixtures

From table 31 to 37, a systemic measured viscosity values for Athabasca bitumen and xylene mixtures are summarized at different conditions. The viscosity data from table 31 to 37 were taken for different xylene weight fractions that are 5%, 10%, 20%, 30%, 40%, 50%, and 60% respectively. For each xylene concentration, the experiment measuring values were gained under pressure up to ~10MPa, temperature up to ~333.1K.

Similarly as viscosity of bitumen/toluene binary mixture, viscosity of bitumen/xylene binary mixtures is the function of temperature, pressure too. In addition, the viscosity of mixtures has certain relationship with xylene concentration.

Table 31 experimental measured viscosities of bitumen/xylene mixtures as function of temperatures, T, and pressures, P; for constant weight fraction of xyelen (w_s=0.05) in the mixture

w_s = 0.05

P/MPa	*T*/K	μ_m/(mPa.s)	*P*/MPa	*T*/K	μ_m/(mPa.s)	*P*/MPa	*T*/K	μ_m/(mPa.s)
0.124	301.1	12566	3.001	344.5	362.1	6.997	332.8	911.9
0.124	309.4	5065	4.000	301.2	15986	6.997	344.6	418.4
0.124	319.6	2002	4.000	308.8	6987	7.996	301.5	18865
0.124	332.2	710.9	4.000	319.5	2613	7.996	308.9	8418
0.124	344.8	320.1	4.000	332.6	803.3	7.996	320.0	2881
1.002	301.1	14215	4.000	344.5	375.5	7.996	332.8	945.3
1.002	309.2	5793	4.999	301.2	17115	7.996	344.6	433.1
1.002	319.3	2290	4.999	308.3	7699	8.995	301.6	19495
1.002	332.3	733.7	4.999	319.6	2640	8.995	309.0	8441
1.002	344.6	336.8	4.999	332.7	836.3	8.995	320.1	2957
2.002	301.1	15010	4.999	344.5	388.3	8.995	332.8	997.7
2.002	308.7	6497	5.998	301.3	17652	8.995	344.6	451.6
2.002	319.4	2397	5.998	308.0	8330	9.994	301.6	20338
2.002	332.4	756	5.998	319.9	2696	9.994	309.1	8791
2.002	344.5	349.9	5.998	332.7	876.3	9.994	320.1	3103
3.001	301.1	15770	5.998	344.6	402	9.994	332.8	1043
3.001	309.0	6523	6.997	301.4	18182	9.994	344.6	468.1
3.001	319.4	2486	6.997	308.3	8437	--------	--------	--------
3.001	332.5	778.1	6.997	320.0	2781	--------	--------	--------

Table 32 experimental measured viscosities of bitumen/xylene mixtures as function of temperatures, T, and pressures, P; for constant weight fraction of xyelen (w_s=0.1) in the mixture

w_s = 0.1

P/MPa	*T*/K	μ_m/(mPa.s)	*P*/MPa	*T*/K	μ_m/(mPa.s)	*P*/MPa	*T*/K	μ_m/(mPa.s)
0.124	302.0	2092	3.001	344.5	362.1	6.997	333.2	275.6
0.124	309.4	1119	4.000	301.2	15986	6.997	344.6	153.5
0.124	321.1	470.1	4.000	308.8	6987	7.996	302.2	2772
0.124	333.2	226.2	4.000	319.5	2613	7.996	310.2	1421
0.124	343.9	128.2	4.000	332.6	803.3	7.996	321.5	594.3
1.002	302.2	2137	4.000	344.5	375.5	7.996	333.2	286.6
1.002	309.7	1126	4.999	301.2	17115	7.996	344.6	159.3
1.002	321.4	473.3	4.999	308.3	7699	8.995	302.2	2906
1.002	333.2	232.4	4.999	319.6	2640	8.995	310.2	1483
1.002	344.4	129.3	4.999	332.7	836.3	8.995	321.5	617.9
2.002	302.2	2203	4.999	344.5	388.3	8.995	333.2	296.5
2.002	309.9	1145	5.998	301.3	17652	8.995	344.6	166.7
2.002	321.5	486.1	5.998	308.0	8330	9.994	302.2	3021
2.002	333.3	233.6	5.998	319.9	2696	9.994	310.2	1549
2.002	344.5	132.8	5.998	332.7	876.3	9.994	321.5	642.5
3.001	302.1	2290	5.998	344.6	402	9.994	333.2	309.5
3.001	309.9	1176	6.997	301.4	18182	9.994	344.6	172.8
3.001	321.5	499.4	6.997	308.3	8437	-------	--------	-------
3.001	333.3	240.2	6.997	320.0	2781	-------	--------	-------

Table 33 experimental measured viscosities of bitumen/xylene mixtures as function of temperatures, T, and pressures, P; for constant weight fraction of xyelen (w_s=0.2) in the mixture

w_s = 0.2

P/MPa	*T*/K	μ_m/(mPa.s)	*P*/MPa	*T*/K	μ_m/(mPa.s)	*P*/MPa	*T*/K	μ_m/(mPa.s)
0.124	301.9	225.7	3.001	343.9	28.28	6.997	332.3	49.35
0.124	308.1	145.3	4.000	302.5	245.6	6.997	343.9	30.49
0.124	320.5	76.62	4.000	310.4	141.3	7.996	302.5	281.3
0.124	332.2	44.01	4.000	320.7	80.01	7.996	310.1	163.5
0.124	344.0	27.56	4.000	332.3	46.38	7.996	320.7	87.3
1.002	302.2	228.4	4.000	343.9	28.74	7.996	332.3	50.39
1.002	309.4	137	4.999	302.4	254.3	7.996	343.9	31.05
1.002	320.5	76.69	4.999	310.4	145.5	8.995	302.5	292.7
1.002	332.2	44.24	4.999	320.7	81.73	8.995	310.0	170.9
1.002	343.9	27.54	4.999	332.3	47.3	8.995	320.7	89.54
2.002	302.3	233.7	4.999	343.9	29.29	8.995	332.3	51.62
2.002	309.8	137.5	5.998	302.5	263.4	8.995	343.9	31.77
2.002	320.6	77.53	5.998	310.3	151	9.994	302.5	304.5
2.002	332.3	44.78	5.998	320.8	83.52	9.994	309.9	178.1
2.002	343.9	27.86	5.998	332.3	48.42	9.994	320.8	91.62
3.001	302.4	238	5.998	343.9	29.78	9.994	332.3	52.99
3.001	310.3	137.7	6.997	302.5	272.2	9.994	343.9	32.48
3.001	320.6	78.89	6.997	310.2	157.1	-------	--------	-------
3.001	332.3	45.51	6.997	320.7	85.4	-------	--------	-------

Table 34 experimental measured viscosities of bitumen/xylene mixtures as function of temperatures, T, and pressures, P; for constant weight fraction of xyelen (w_s=0.3) in the mixture

w_s = 0.3

P/MPa	*T*/K	μ_m/(mPa.s)	*P*/MPa	*T*/K	μ_m/(mPa.s)	*P*/MPa	*T*/K	μ_m/(mPa.s)
0.124	301.4	41.83	3.001	343.8	10.39	6.997	332.6	15.19
0.124	309.4	29.87	4.000	302.0	42.76	6.997	343.8	11.09
0.124	318.9	21.33	4.000	309.5	31.61	7.996	302.0	46.98
0.124	330.9	14.51	4.000	320.5	21.26	7.996	309.4	34.22
0.124	343.7	10.08	4.000	332.5	14.47	7.996	320.6	22.71
1.002	301.8	41.33	4.000	343.8	10.54	7.996	332.6	15.47
1.002	309.5	30.26	4.999	302.0	43.89	7.996	343.9	11.28
1.002	319.9	20.77	4.999	309.4	32.24	8.995	302.1	47.85
1.002	332.3	13.99	4.999	320.5	21.57	8.995	309.4	34.89
1.002	343.7	10.14	4.999	332.5	14.71	8.995	320.7	23.19
2.002	301.9	42.02	4.999	343.8	10.69	8.995	332.6	15.79
2.002	309.5	30.71	5.998	302.1	45.67	8.995	343.9	11.47
2.002	320.1	20.89	5.998	309.4	32.88	9.994	302.1	49.1
2.002	332.4	14.13	5.998	320.6	21.91	9.994	309.3	35.86
2.002	343.7	10.23	5.998	332.5	14.96	9.994	320.7	23.66
3.001	301.9	42.57	5.998	343.8	10.91	9.994	332.6	16.01
3.001	309.5	31.09	6.997	302.1	45.78	9.994	343.9	11.71
3.001	320.4	20.99	6.997	309.4	33.47	-------	--------	-------
3.001	332.4	14.31	6.997	320.6	22.32	-------	--------	-------

Table 35 experimental measured viscosities of bitumen/xylene mixtures as function of temperatures, T, and pressures, P; for constant weight fraction of xyelen (w_s=0.4) in the mixture

w_s = 0.4

P/MPa	*T*/K	μ_m/(mPa.s)	*P*/MPa	*T*/K	μ_m/(mPa.s)	*P*/MPa	*T*/K	μ_m/(mPa.s)
0.124	300.3	16.19	3.001	343.5	4.552	6.997	332.0	6.565
0.124	308.9	11.9	4.000	301.5	16.17	6.997	342.8	4.903
0.124	318.6	8.786	4.000	309.3	12.31	7.996	301.5	17.27
0.124	331.1	6.153	4.000	320.5	8.649	7.996	309.3	13.14
0.124	343.8	4.374	4.000	332.1	6.245	7.996	320.6	9.27
1.002	301.3	15.74	4.000	343.4	4.612	7.996	332.0	6.664
1.002	309.1	11.93	4.999	301.5	16.41	7.996	342.9	4.981
1.002	320.0	8.504	4.999	309.3	12.49	8.995	301.5	17.59
1.002	331.8	6.059	4.999	320.5	8.813	8.995	309.3	13.48
1.002	343.4	4.477	4.999	332.1	6.36	8.995	320.6	9.43
2.002	301.3	15.84	4.999	342.7	4.767	8.995	332.1	6.792
2.002	309.2	12.02	5.998	301.5	16.66	8.995	343.0	5.068
2.002	320.3	8.494	5.998	309.3	12.67	9.994	301.5	17.9
2.002	332.1	6.066	5.998	320.5	8.958	9.994	309.3	13.74
2.002	343.4	4.5	5.998	332.0	6.479	9.994	320.6	9.638
3.001	301.4	15.97	5.998	342.7	4.85	9.994	332.0	6.941
3.001	309.3	12.15	6.997	301.5	16.97	9.994	343.1	5.161
3.001	320.4	8.573	6.997	309.3	12.9	-------	--------	-------
3.001	332.1	6.163	6.997	320.6	9.096	-------	--------	-------

Table 36 experimental measured viscosities of bitumen/xylene mixtures as function of temperatures, T, and pressures, P; for constant weight fraction of xyelen (w_s=0.5) in the mixture

w_s = 0.5

P/MPa	*T*/K	μ_m/(mPa.s)	*P*/MPa	*T*/K	μ_m/(mPa.s)	*P*/MPa	*T*/K	μ_m/(mPa.s)
0.124	301.1	6.312	3.001	342.7	2.764	6.997	331.1	3.513
0.124	309.0	5.007	4.000	301.3	6.582	6.997	342.7	2.764
0.124	319.6	4.471	4.000	309.2	5.187	7.996	301.3	6.971
0.124	331.1	3.473	4.000	319.9	4.476	7.996	309.4	5.504
0.124	342.7	2.751	4.000	330.7	3.582	7.996	319.9	4.521
1.002	301.2	6.325	4.000	342.7	2.752	7.996	331.2	3.525
1.002	309.1	5.006	4.999	301.2	6.65	7.996	342.7	2.774
1.002	319.7	4.45	4.999	309.3	5.27	8.995	301.3	7.085
1.002	331.1	3.529	4.999	319.9	4.484	8.995	309.4	5.616
1.002	342.7	2.761	4.999	330.9	3.522	8.995	319.9	4.545
2.002	301.3	6.399	4.999	342.7	2.761	8.995	331.2	3.531
2.002	309.1	5.064	5.998	301.2	6.759	8.995	342.8	2.79
2.002	319.8	4.454	5.998	309.3	5.35	9.994	301.2	7.234
2.002	331.2	3.504	5.998	319.9	4.497	9.994	309.4	5.711
2.002	342.7	2.777	5.998	331.1	3.513	9.994	319.9	4.562
3.001	301.2	6.481	5.998	342.7	2.773	9.994	331.2	3.548
3.001	309.2	5.112	6.997	301.3	6.845	9.994	342.8	2.796
3.001	319.8	4.45	6.997	309.3	5.446	-------	--------	-------
3.001	330.8	3.545	6.997	319.9	4.502	-------	--------	-------

Table 37 experimental measured viscosities of bitumen/xylene mixtures as function of temperatures, T, and pressures, P; for constant weight fraction of xyelen (w_s=0.5) in the mixture

w_s = 0.6

P/MPa	*T*/K	μ_m/(mPa.s)	*P*/MPa	*T*/K	μ_m/(mPa.s)	*P*/MPa	*T*/K	μ_m/(mPa.s)
0.124	300.0	3.373	3.001	342.6	1.504	6.997	331.0	1.824
0.124	307.1	2.885	4.000	300.3	3.375	6.997	342.8	1.512
0.124	318.5	2.423	4.000	308.5	3.002	7.996	300.4	3.424
0.124	331.1	1.8	4.000	319.6	2.353	7.996	308.6	3.017
0.124	341.9	1.515	4.000	331.0	1.812	7.996	319.7	2.385
1.002	300.1	3.364	4.000	342.7	1.504	7.996	331.0	1.828
1.002	308.1	2.91	4.999	300.3	3.396	7.996	342.8	1.514
1.002	319.2	2.362	4.999	308.5	3.004	8.995	300.5	3.445
1.002	331.1	1.8	4.999	319.6	2.362	8.995	308.6	3.024
1.002	342.2	1.505	4.999	331	1.812	8.995	319.7	2.39
2.002	300.2	3.386	4.999	342.8	1.508	8.995	331.0	1.838
2.002	308.3	2.899	5.998	300.4	3.399	8.995	342.8	1.517
2.002	319.4	2.368	5.998	308.5	2.997	9.994	300.5	3.456
2.002	331.1	1.814	5.998	319.7	2.373	9.994	308.6	3.04
2.002	342.4	1.514	5.998	331.0	1.813	9.994	319.7	2.402
3.001	300.3	3.385	5.998	342.8	1.508	9.994	331.0	1.843
3.001	308.3	2.91	6.997	300.4	3.405	9.994	342.8	1.523
3.001	319.5	2.369	6.997	308.5	3.007	-------	--------	-------
3.001	331.1	1.812	6.997	319.7	2.372	-------	--------	-------

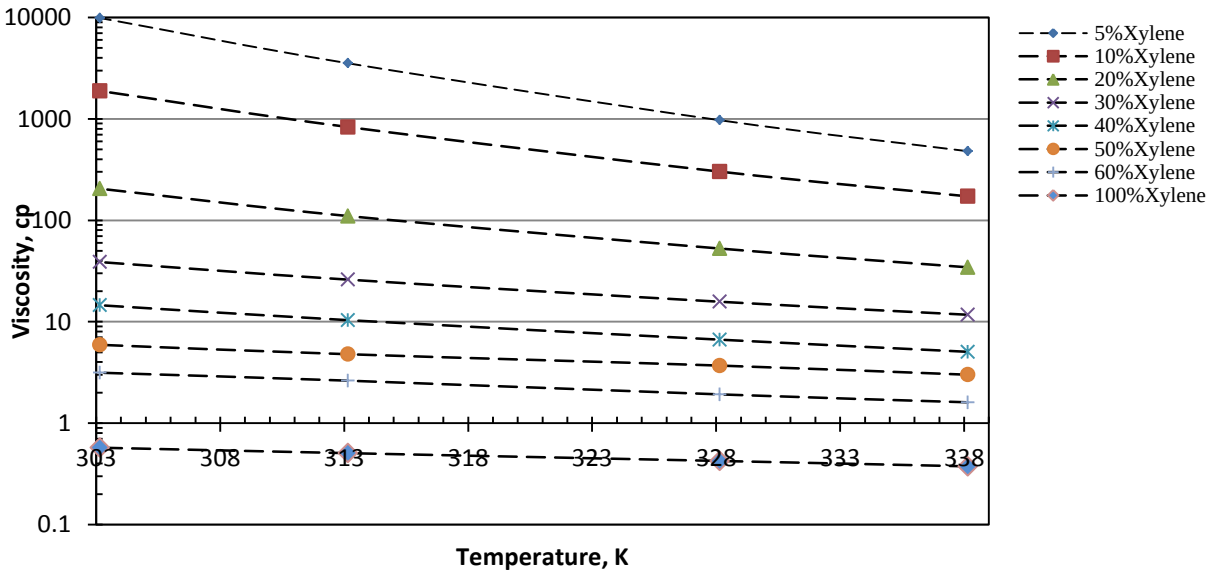

Figure 11 calculated viscosity, μ_m, of bitumen/xylene mixtures through TCC procedure (Eq. 3-3) versus temperatures T as dependence of xylene weight fraction, w_s, and at lowest constant pressure of 0.124 MPa;

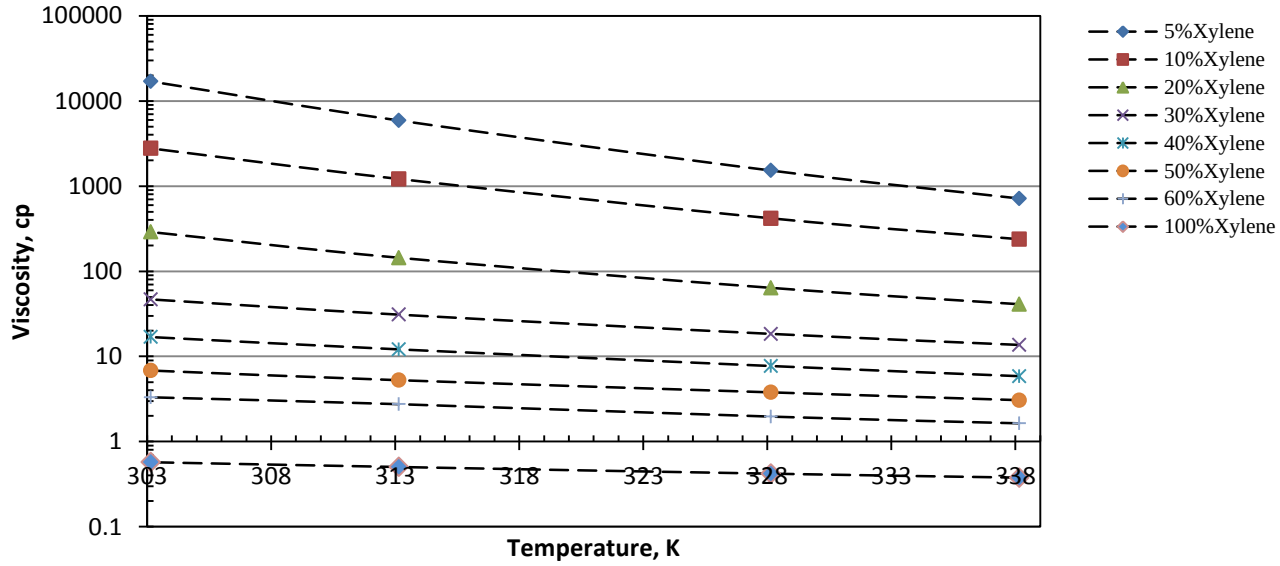

Figure 12 calculated viscosity, μ_m, of bitumen/xylene mixtures through TCC procedure (Eq. 3-3) versus temperatures T as dependence of xylene weight fraction, w_s, and at highest constant pressure of 9.99 MPa;

To investigate the viable of bitumen/xylene binary mixture system with temperature and xylene concentration, two extreme pressure conditions that are highest and lowest point have been considered and formed Figure 11 and Figure 12.

Similar with bitumen/toluene mixture viscosity, the viscosity of bitumen/xylene mixture is sensitive with temperature too. To investigate the influence of xylene concentration upon binary mixtures viscosity, it is better to compare the viscosity value at exact same temperature point. To fulfil so, TCC calculation procure [3-3] that mentioned in Chapter 3 has been taken to calculate the viscosity value at temperatures 303K, 313K, 328K, and 338K respectively.

Figure 11 descript the impact of different toluene concentrations on Athabasca bitumen and toluene mixture viscosity at fixed lowest pressure 0.124MPa. Figure 12 shows the effect of toluene concentration on mixtures viscosity at fixed highest pressure 9.990MPa.

In addition, the trend of viscosity at different temperatures and toluene weight fractions are showing in both graphics simultaneously. From Figure 11 and Figure 12, the same trend for each specific xylene concentration can be observed. But the diversity of trend at different xylene weight fraction is obvious.

4.4.2Measured Density Values of bitumen/xylene Mixtures

To present the density values for Athabasca bitumen and xylene binary system properly, the similar method as viscosity of Athabasca bitumen and xylene binary mixture has been adapted. Also, density of binary mixtures is the function of temperature, pressure. In addition, the density of mixtures has certain relationship with solvent concentration.

Through table 38 to 44, a systemic measured density values for Athabasca bitumen and xylene mixtures are summarized at different conditions. The viscosity data from table 37 to 43

were taken for different xylene weight fractions that are 5%, 10%, 20%, 30%, 40%, 50%, and 60% respectively. For each xylene concentration, the experiment measuring values were gained under pressure from ~0.125MPa up to ~10MPa, temperature from ~296.4K up to ~333.1K.

Table 38 experimental measured densities of bitumen/xylene mixtures as function of temperatures, T, and pressures, P for constant weight fraction of toluene (w_s=0.05) in the mixture.

w_s = 0.05

P/MPa	*T*/K	μ_m/(mPa.s)	*P*/MPa	*T*/K	μ_m/(mPa.s)	*P*/MPa	*T*/K	μ_m/(mPa.s)
0.125	296.4	997.1	3.001	333.2	975.6	6.996	323.0	984
0.125	303.3	992.5	4.001	296.5	999.2	6.996	333.2	978
0.125	313.4	985.9	4.001	303.4	994.6	7.997	296.6	1001.2
0.125	322.9	980.0	4.001	313.1	988.4	7.997	303.1	997
0.125	333.1	973.9	4.001	323.0	982.4	7.997	313.0	990.7
1.003	296.5	997.6	4.001	333.2	976.2	7.997	323.0	984.6
1.003	303.4	993.0	4.998	296.5	999.7	7.997	333.3	978.6
1.003	313.2	986.4	4.998	303.3	995.2	8.996	296.7	1001.6
1.003	322.9	980.6	4.998	313.0	989.0	8.996	303.1	997.4
1.003	333.2	974.4	4.998	323.0	982.9	8.996	313.0	991.2
2.000	296.5	998.1	4.998	333.2	976.8	8.996	323.0	985.1
2.000	303.4	993.6	5.997	296.6	1000.2	8.996	333.3	979.1
2.000	313.2	987.0	5.997	303.1	995.9	9.995	296.7	1002.1
2.000	322.9	981.2	5.997	313.0	989.6	9.995	303.2	997.9
2.000	333.2	975.0	5.997	323.0	983.5	9.995	313.0	991.7
3.001	296.5	998.6	5.997	333.2	977.4	9.995	323.0	985.7
3.001	303.4	994.1	6.996	296.6	1000.7	9.995	333.3	979.7
3.001	313.1	987.7	6.996	303.1	996.5	-------	--------	-------
3.001	323.0	981.8	6.996	313.0	990.1	-------	--------	-------

Table 39 experimental measured densities of bitumen/xylene mixtures as function of temperatures, T, and pressures, P for constant weight fraction of toluene (w_s=0.1) in the mixture.

w_s = 0.1

P/MPa	*T*/K	μ_m/(mPa.s)	*P*/MPa	*T*/K	μ_m/(mPa.s)	*P*/MPa	*T*/K	μ_m/(mPa.s)
0.125	296.5	988.8	3.001	333.0	967.2	6.996	323.4	975.4
0.125	302.9	984.4	4.001	296.5	991.0	6.996	333.1	969.6
0.125	313.3	977.7	4.001	303.0	986.6	7.997	296.5	993.0
0.125	323.5	971.2	4.001	313.2	980.1	7.997	303.1	988.6
0.125	332.8	965.4	4.001	323.5	973.6	7.997	313.2	982.3
1.003	296.5	989.3	4.001	333.1	967.8	7.997	323.4	976.0
1.003	303.0	984.9	4.998	296.5	991.5	7.997	333.2	970.1
1.003	313.2	978.3	4.998	303.0	987.1	8.996	296.5	993.5
1.003	323.5	971.7	4.998	313.2	980.6	8.996	303.1	989.1
1.003	332.9	966.0	4.998	323.5	974.2	8.996	313.2	982.8
2.000	296.5	989.9	4.998	333.1	968.4	8.996	323.4	976.5
2.000	303.0	985.5	5.997	296.5	992.0	8.996	333.2	970.7
2.000	313.2	978.9	5.997	303.0	987.6	9.995	296.5	994.0
2.000	323.5	972.4	5.997	313.2	981.2	9.995	303.2	989.6
2.000	333.0	966.6	5.997	323.4	974.8	9.995	313.2	983.4
3.001	296.5	990.4	5.997	333.1	969.0	9.995	323.4	977.1
3.001	303.0	986.0	6.996	296.5	992.5	9.995	333.2	971.2
3.001	313.2	979.5	6.996	303.1	988.2	-------	--------	-------
3.001	323.5	973.0	6.996	313.2	981.7	-------	--------	-------

Table 40 experimental measured densities of bitumen/xylene mixtures as function of temperatures, T, and pressures, P for constant weight fraction of toluene (w_s=0.2) in the mixture.

w_s = 0.2

P/MPa	*T*/K	μ_m/(mPa.s)	*P*/MPa	*T*/K	μ_m/(mPa.s)	*P*/MPa	*T*/K	μ_m/(mPa.s)
0.125	296.8	972.5	3.001	333.3	948.9	6.996	323.3	958.1
0.125	303.4	967.9	4.001	296.9	974.7	6.996	333.3	951.5
0.125	313.0	961	4.001	303.5	970.1	7.997	296.9	976.9
0.125	323.3	953.9	4.001	313.0	963.4	7.997	303.5	972.4
0.125	333.2	947.1	4.001	323.3	956.2	7.997	313.0	965.7
1.003	296.8	973.0	4.001	333.3	949.6	7.997	323.3	958.7
1.003	303.4	968.3	4.998	296.9	975.3	7.997	333.3	952.1
1.003	313.0	961.6	4.998	303.5	970.6	8.996	296.9	977.4
1.003	323.3	954.3	4.998	313.0	964.0	8.996	303.5	972.9
1.003	333.3	947.5	4.998	323.3	956.9	8.996	313.0	966.3
2.000	296.8	973.6	4.998	333.3	950.2	8.996	323.3	959.3
2.000	303.4	969.0	5.997	296.9	975.8	8.996	333.3	952.7
2.000	313.0	962.2	5.997	303.5	971.2	9.995	296.9	978.0
2.000	323.3	955.0	5.997	313.0	964.6	9.995	----	----
2.000	333.3	948.3	5.997	323.3	957.5	9.995	313.1	966.8
3.001	296.9	974.2	5.997	333.3	950.9	9.995	323.3	959.9
3.001	303.5	969.6	6.996	296.9	976.4	9.995	333.3	953.3
3.001	313.0	962.8	6.996	303.5	971.8	-------	--------	-------
3.001	323.3	955.6	6.996	313.0	965.2	-------	--------	-------

Table 41 experimental measured densities of bitumen/xylene mixtures as function of temperatures, T, and pressures, P for constant weight fraction of toluene (w_s=0.3) in the mixture.

w_s = 0.3

P/MPa	*T*/K	μ_m/(mPa.s)	*P*/MPa	*T*/K	μ_m/(mPa.s)	*P*/MPa	*T*/K	μ_m/(mPa.s)
0.125	296.9	955.4	3.001	333.2	933.5	6.996	323.5	942.0
0.125	303.3	951.1	4.001	296.9	957.7	6.996	333.3	936.1
0.125	313.0	944.5	4.001	303.3	953.7	7.997	297.0	960.0
0.125	323.4	937.5	4.001	313.0	946.9	7.997	303.3	956.0
0.125	333.2	931.4	4.001	323.4	940.2	7.997	313.1	949.4
1.003	296.9	955.9	4.001	333.2	934.1	7.997	323.5	942.7
1.003	303.3	951.7	4.998	296.9	958.3	7.997	333.3	936.8
1.003	313.0	945.0	4.998	303.3	954.3	8.996	297.0	960.5
1.003	323.4	938.1	4.998	313.0	947.6	8.996	303.3	956.6
1.003	333.2	932.1	4.998	323.4	940.8	8.996	313.1	949.9
2.000	296.9	956.5	4.998	333.2	934.8	8.996	323.5	943.3
2.000	303.3	952.5	5.997	297.0	958.8	8.996	333.3	937.4
2.000	313.0	945.7	5.997	303.3	954.9	9.995	297.0	961.1
2.000	323.4	938.8	5.997	313.0	948.2	9.995	303.3	957.1
2.000	333.2	932.8	5.997	323.4	941.4	9.995	313.1	950.5
3.001	296.9	957.1	5.997	333.3	935.5	9.995	323.5	943.9
3.001	303.3	953.1	6.996	297.0	959.4	9.995	333.3	938.0
3.001	313.0	946.3	6.996	303.3	955.5	-------	--------	-------
3.001	323.4	939.5	6.996	313.0	948.8	-------	--------	-------

Table 42 experimental measured densities of bitumen/xylene mixtures as function of temperatures, T, and pressures, P for constant weight fraction of toluene (w_s=0.4) in the mixture.

w_s = 0.4

P/MPa	*T*/K	μ_m/(mPa.s)	*P*/MPa	*T*/K	μ_m/(mPa.s)	*P*/MPa	*T*/K	μ_m/(mPa.s)
0.125	296.5	942.6	3.001	333.2	918.2	6.996	323.2	927.7
0.125	303.2	937.7	4.001	296.5	945.1	6.996	333.1	921.0
0.125	312.8	930.6	4.001	303.2	940.2	7.997	296.5	947.4
0.125	323.2	923.0	4.001	312.9	933.1	7.997	303.2	942.7
0.125	333.2	916.2	4.001	323.3	925.7	7.997	313.0	935.6
1.003	296.5	943.2	4.001	333.2	918.8	7.997	323.2	928.4
1.003	303.2	938.3	4.998	296.5	945.7	7.997	333.1	921.7
1.003	312.9	931.1	4.998	303.2	940.8	8.996	296.5	948.0
1.003	323.3	923.6	4.998	312.9	933.8	8.996	303.2	943.3
1.003	333.2	916.8	4.998	323.3	926.4	8.996	313.0	936.2
2.000	296.5	943.8	4.998	333.2	919.5	8.996	323.3	928.9
2.000	303.2	938.9	5.997	296.5	946.2	8.996	333.1	922.4
2.000	312.9	931.8	5.997	303.2	941.5	9.995	296.5	948.5
2.000	323.3	924.4	5.997	312.9	934.4	9.995	303.2	943.8
2.000	333.1	917.6	5.997	323.2	927.0	9.995	313.0	936.8
3.001	296.5	944.4	5.997	333.1	920.3	9.995	323.3	929.5
3.001	303.2	939.6	6.996	296.5	946.8	9.995	333.1	923.0
3.001	312.9	932.5	6.996	303.2	942.1	-------	--------	-------
3.001	323.3	925.0	6.996	312.9	935.0	-------	--------	-------

Table 43 experimental measured densities of bitumen/xylene mixtures as function of temperatures, T, and pressures, P for constant weight fraction of toluene (w_s=0.5) in the mixture.

w_s = 0.5

P/MPa	*T*/K	μ_m/(mPa.s)	*P*/MPa	*T*/K	μ_m/(mPa.s)	*P*/MPa	*T*/K	μ_m/(mPa.s)
0.125	296.4	928.2	3.001	333.1	903.1	6.996	323.2	912.8
0.125	303.0	923.0	4.001	296.4	930.7	6.996	333.1	906.0
0.125	313.1	915.6	4.001	303.0	925.6	7.997	296.4	933.2
0.125	323.2	907.9	4.001	313.1	918.3	7.997	303.2	928.0
0.125	333.1	900.8	4.001	323.2	910.7	7.997	313.1	920.9
1.003	296.4	928.8	4.001	333.1	903.8	7.997	323.2	913.5
1.003	303.0	923.7	4.998	296.4	931.4	7.997	333.1	906.7
1.003	313.1	916.2	4.998	303.1	926.2	8.996	296.4	933.8
1.003	323.2	908.6	4.998	313.1	919	8.996	303.2	928.6
1.003	333.1	901.5	4.998	323.2	911.4	8.996	313.1	921.6
2.000	296.4	929.4	4.998	333.1	904.6	8.996	323.2	914.1
2.000	303.0	924.3	5.997	296.4	932.0	8.996	333.2	907.4
2.000	313.1	916.9	5.997	303.1	926.8	9.995	296.4	934.4
2.000	323.2	909.2	5.997	313.1	919.7	9.995	303.2	929.2
2.000	333.1	902.3	5.997	323.2	912.1	9.995	313.1	922.2
3.001	296.4	930.1	5.997	333.1	905.3	9.995	323.2	914.7
3.001	303.0	924.9	6.996	296.4	932.6	9.995	333.2	908.1
3.001	313.1	917.6	6.996	303.1	927.4	-------	--------	-------
3.001	323.2	909.9	6.996	313.1	920.3	-------	--------	-------

Table 44 experimental measured densities of bitumen/xylene mixtures as function of temperatures, T, and pressures, P for constant weight fraction of toluene (w_s=0.6) in the mixture.

w_s = 0.6

P/MPa	*T*/K	μ_m/(mPa.s)	*P*/MPa	*T*/K	μ_m/(mPa.s)	*P*/MPa	*T*/K	μ_m/(mPa.s)
0.125	296.4	914.2	3.001	333.2	887.9	6.996	323.3	898.1
0.125	303.0	908.7	4.001	296.2	917.0	6.996	333.2	890.9
0.125	312.8	901.1	4.001	303.0	911.4	7.997	296.2	919.5
0.125	323.3	893.0	4.001	312.8	904.0	7.997	303.0	914.0
0.125	333.1	885.5	4.001	323.3	896.0	7.997	312.8	906.7
1.003	296.4	914.8	4.001	333.2	888.6	7.997	323.3	898.8
1.003	303.0	909.4	4.998	296.2	917.7	7.997	333.2	891.7
1.003	312.8	901.8	4.998	303.0	912.1	8.996	296.2	920.1
1.003	323.3	893.7	4.998	312.8	904.6	8.996	303.0	914.6
1.003	333.1	886.3	4.998	323.3	896.7	8.996	312.8	907.3
2.000	296.4	915.5	4.998	333.2	889.4	8.996	323.3	899.5
2.000	303.0	910.1	5.997	296.2	918.3	8.996	333.2	892.4
2.000	312.8	902.5	5.997	303.0	912.7	9.995	296.2	920.7
2.000	323.3	894.5	5.997	312.8	905.3	9.995	303.1	915.3
2.000	333.1	887.1	5.997	323.3	897.4	9.995	312.8	908.0
3.001	296.2	916.3	5.997	333.2	890.2	9.995	323.3	900.2
3.001	303.0	910.8	6.996	296.2	918.9	9.995	333.2	893.1
3.001	312.8	903.3	6.996	303.0	913.4	-------	--------	-------
3.001	323.3	895.2	6.996	312.8	906.0	-------	--------	-------

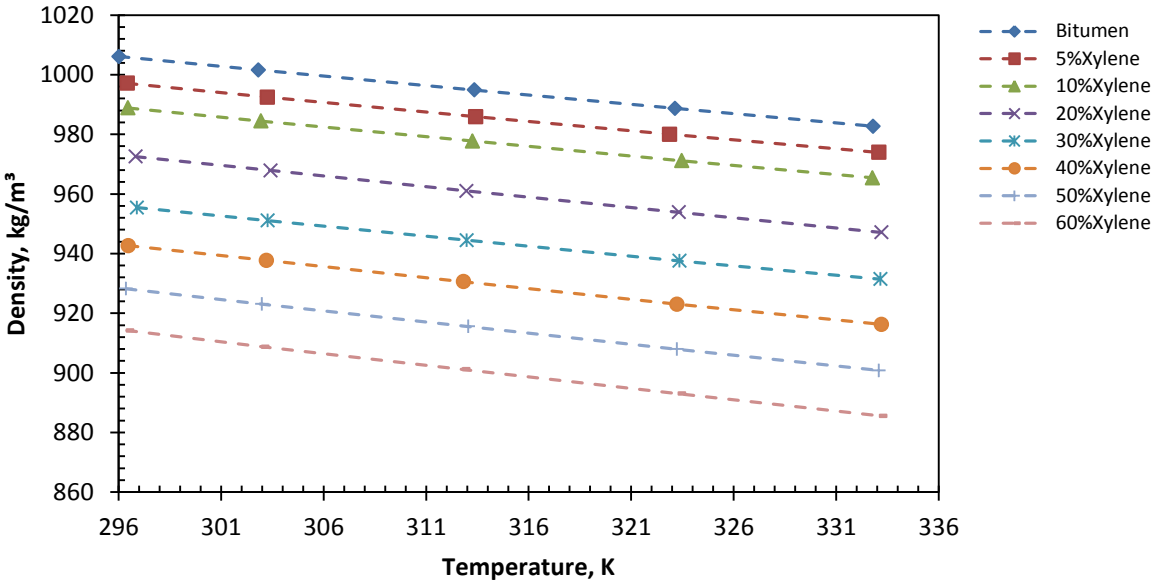

Figure 13 Effect of temperature, T, on the density, ρ_m, of bitumen/xylene mixtures as dependence of xylene weight fraction, $w_{s,}$ and at lowest constant pressure P=0.125MPa;

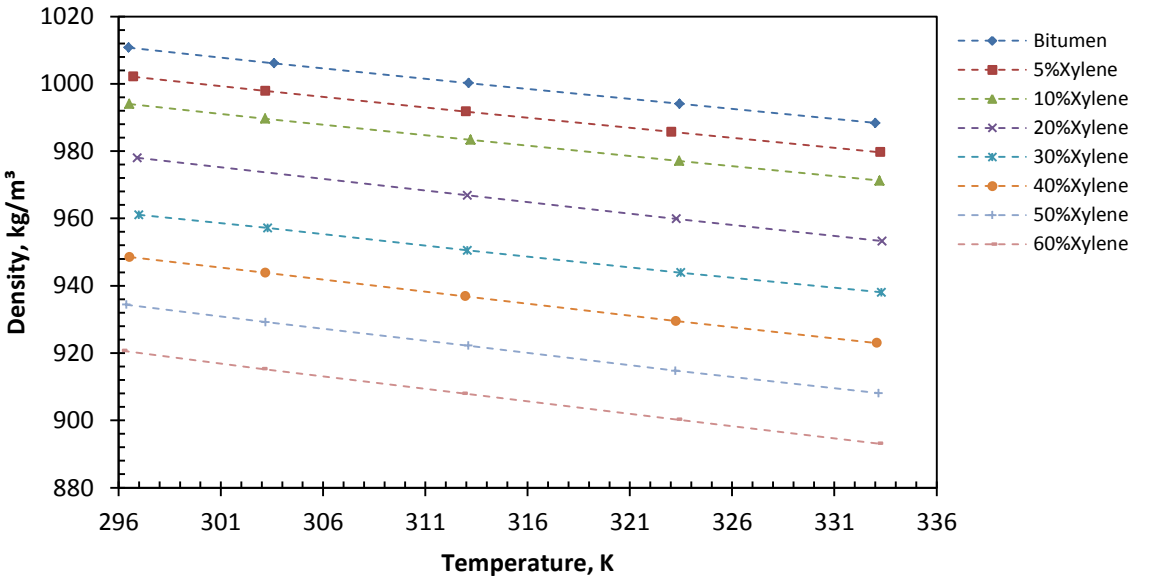

Figure 14 Effect of temperature, T, on the density, ρ_m, of bitumen/xylene mixtures as dependence of xylene weight fraction, $w_{s,}$ and at highest constant pressure P=9.994MPa;

Similar with the way to tread for bitumen/toluene mixture, to investigate the relationship of bitumen/xylene binary mixture density with respective of temperature and solvent concentration, two extreme pressure situations have been taken to consider. The measured data points are taken from highest pressure that is 9.994MPa and lowest pressure that is 0.125MPa to form Figure 13 and Figure 14 respectively.

Figure 13 descript the impact of different xylene concentrations on Athabasca bitumen and xylene mixture density at fixed lowest pressure 0.125MPa. Figure 14 shows the effect of xylene concentration on mixtures viscosity at fixed highest pressure 9.994MPa.

In addition, the trend of density at different temperatures and xylene weight fractions are showing in both graphics simultaneously. From Figure 13 and Figure 14, the linear relationship between density and temperature for each specific xylene concentration can be observed. Moreover, the inverse ratio trend between bitumen and xylene mixture density and xylene weight fraction can be well known.

Chapter 5 Modeling Investigation and Discussion

Numerous different modelling techniques of based on different theories and concepts are available in the literature. Mehrotra, Monnery and Svrcek (1996) [67] reviewed and summarized the most widely known viscosity models for hydrocarbon liquids and mixtures proposed in recent years.

I. Semi-Theoretical Methods

In general, semi-theoretical modelling is derived from applied statistical mechanics and obeys the law of corresponding states theory, reaction rate theory and hard sphere theory. In these methods, the viscosity is dependent on the substance's temperature and density. A summary of semi-theoretical methods is listed below:

1. Corresponding states theory,
2. Reaction rate theory,
3. Hard sphere (Enskog) models,
4. Square well models,
5. Lennard-Jones models, and
6. Modified Chapman-Enskog theory.

II. Empirical Methods

In application to viscosity modelling, empirical methods generally mean approaches using a collection of data to derive a correlation. These methods may be categorized as follows:

1. Andrade equation and its modifications,
2. ASTM or Walther equation,
3. Viscosity equations of state, and
4. Liquid mixture viscosity equations.

5.1. Physical Properties Model for Pure Solvent

5.1.1. Viscosity Modeling

In 1934, Andrade proposed a correlation to express the variation of liquid viscosity with temperature, and can be employed to predict the viscosities of the pure aromatic solvents that were fitted with a semi-logarithm correlation:

$$\ln(\mu_{solv}) = a + \frac{b}{T} \qquad 5\text{-}1$$

Where

Aromatic solvent viscosity $\mu_{sol\,\mathrm{in}}$ mPa.s; temperature T in K

In this equation, the impact of pressure has been ignored reasonable based on the analysed experimental data that present in table 14.

5.1.2. Density Modeling

In 2009, Badamchi-Zadeh et al. conducted a study on physical properties of Athabasca bitumen and propane mixture. The measured density values were correlated with the following equation [34]:

$$\rho = (a_1 + a_2[T - 273.15])\exp\{(a_3[T - 273.15] + a_4)\} \quad 5\text{-}2$$

Where

T is temperature in K, P is the pressure in kPa, and ρ is the density in kg/m^3; α_1, α_2, α_3, and α_4 are adjustable characteristic parameters, Badamchi-Zadeh et al. obtained the values by regression 15 experimental data points. The average deviation was within ±0.4kg/m^3.

5.2. Physical Properties Model for Raw Bitumen

5.2.1. Viscosity Modeling

In 1986, Mehrotra and Svrcek [32] modified Khan's model, took the pressure effect into account, and presented the following two empirical correlations for the viscosity of solvent-free bitumen:

$$\ln(\mu_{bit}) = \exp[b_1 + b_2 \ln(T)] + b_3 P_g \quad 5\text{-}3$$

$$\ln(\ln(\mu_{bit})) = [b_1 + b_2 \ln(T)] + b_3 P_g \quad 5\text{-}4$$

in which μ_{bit} is the bitumen viscosity in mPa.s, T is the temperature in K, and P_g is the gauge pressure in MPa; b_1 ,b_2 ,b_3 are adjustable parameter. Mehrotra and Svrcek generalized the value for b_1 ,b_2 ,b_3 based on 30 experimental data point. The prediction for Athabasca bitumen fitted measured data quite well, and the average absolute deviation for equation [5-3] was 2.8% and 1.8% for equation [5-4] respectively.

5.2.2. Density Modeling

The density model of raw bitumen has the same form with pure solvent model, which can be descript as the following Badamchi-Zadeh equation [34]:

$$\rho = (a_1 + a_2[T - 273.15])\exp\{(a_3[T - 273.15] + a_4) \quad 5\text{-}5$$

In which, the adjustable parameter α1, α2, α3, and α4 have different values with pure solvent's.

5.3. Physical Properties Model for Binary Mixture

5.3.1. Viscosity Modeling (Mixing Rules)

In 1887, Arrhenius [63] proposed a logarithm type mixing rule and commonly was descripted as following form:

$$\mu_m = \mu_s^{x_s} \times \mu_B^{(1-x_s)} \quad 5\text{-}6$$

Or in log form:

$$\ln \mu_m = x_s \ln \mu_s + (1 - x_s) \ln \mu_B \quad 5\text{-}7$$

Where

x_s is the mole fraction of the solvent and μ_s and μ_B are the viscosities of the solvent and bitumen, respectively.

The Arrhenius mixing rule was designed for "ideal" solutions and was generally not very accurate for use in predicting viscosities of petroleum oil blends.

In 1917, Kendall and Monroe [64] proposed a mixing rule in which cube root of viscosity was taken to be additive function. The power law correlation is based on the Kendall model [64], in which the viscosity of mixture is directly dependent on the concentration:

$$\mu_m = \left[x_s \mu_s^n + (1 - x_s)\mu_B^n\right]^{\frac{1}{n}} \quad 5\text{-}8$$

Where

x_s is the mole fraction of the solvent; and, μ_s and μ_B are the viscosities of the solvent and bitumen, respectively. The exponent term, n, is the adjustable parameter in this correlation, and can be provided by a least-square regression.

The power law lacks generality for all solvent proportions. In low solvent concentration, this mixing rule can provide acceptable results. However, at higher solvent proportions, the power law rule cannot express the mixture viscosity behavior properly.

In 1933, Lederer [65] proposed a modified version of classic Arrhenius viscosity mixing rule as:

$$\ln \mu_m = \left(1 - \frac{\alpha v_B}{\alpha v_B + v_s}\right) \ln \mu_s + \left(\frac{\alpha v_B}{\alpha v_B + v_s}\right) \ln \mu_B \quad 5\text{-}9$$

Where

α is an adjustable parameter with values between 0 and unity.

Rahmes and Nelson in 1948 conducted an experiment to investigate several mixing rules including Ledered's model. In which, total 30 binary petroleum oil systems using 17 different oils had been evaluated. The study results showed the Ledered's rule matched experimental data very well and gave an average error of 0.9%. In addition, the study reflected the volume fraction and weight fraction had slight different in results.

In 1984, Shu [66] investigated the Lederer's model critically. The study exhibited the reliability of this mixing rule to predict the mixture viscosity in wide range conditions. Furthermore, Shu developed a method to generalize the empirical constant, α by transforming Einstein Equation and using standard linear multiple regression routine. The parameter α can be expressed as function of viscosity ratio and component densites. The equation can be descripted as following:

$$\alpha = \frac{17.04(\rho_B - \rho_s)^{0.5237}\rho_B^{3.2745}\rho_s^{1.6316}}{\ln\left(\frac{\mu_B}{\mu_s}\right)} \qquad 5\text{-}10$$

Where

v_s and v_B are the volume fractions of the solvent and bitumen, respectively; and, ρ_s and ρ_B are the densities of the solvent and bitumen, respectively. Shu [66] validated this prediction correlation in the high-viscosity region (>10^4). Simultaneously, Shu point out this method didn't consider the temperature effect.

5.3.2. Density Modeling

The generated density data of bitumen/toluene mixtures were correlated with the following equation:

$$\rho_{mix} = \frac{1}{\frac{w_s}{\rho_s} + \frac{1-w_s}{\rho_{Bit}}} \qquad 5\text{-}11$$

Where

w_s is the weight fraction of solvent, ρ_s and ρ_{Bit} are the densities of the solvent and bitumen, respectively. This equation was developed on the basis of one assumption: binary mixture is "ideal fluid", which means no excess volume due to mixing.

5.4. Results and Discussion

5.4.1. Pure Solvents Viscosity and Density

Prior to measurements of the binary bitumen/solvent mixtures, the density and viscosity of the pure solvents were measured over wide ranges of temperature and pressure, in order to predict the mixture properties. The impact of pressure on the viscosity of the pure solvent was insignificant. Thus, the viscosity data were measured only with respect to temperature and are listed in Table 45. As expected, the solvent viscosity decreased with increased temperature. From Figures 7, 8 and Figures 11, 12, the relationship of logarithm value of pure solvents viscosity with temperatures can be perceived directly into the inverse linear ratio. The results of the fitted correlations [5-1] for toluene and xylene are also presented in Table 45. The coefficients of the correlations are mentioned in the footnotes of Table 45.

The average absolute relative deviations (AARDs) were calculated as:

$$AARD(\%) = \left(\frac{100}{N}\right)\sum\left|\frac{\mu_{corr} - \mu_{\exp}}{\mu_{\exp}}\right| \qquad 5\text{-}12$$

The AARDs for the toluene and xylene correlations were 0.9% and 0.6%, respectively.

Table 45 measured viscosities, μexp, of toluene and xylene at different temperatures, T, and a pressure of 0.124 MPa.

Toluene				***Xylene***			
***T*/K**	**μ_{exp}/(kg/m^3)**	**μ_{corr}/(kg/m^3)**	**ARD (%)**	***T*/K**	**μ_{exp}/(kg/m^3)**	**μ_{corr}/(kg/m^3)**	**ARD (%)**
341.6	0.343	0.344	0.3	342.7	0.356	0.359	0.8
330.2	0.384	0.385	0.3	330.9	0.412	0.409	0.7
319.8	0.433	0.430	0.7	317.5	0.482	0.478	0.8
308.3	0.498	0.490	1.6	306.2	0.551	0.552	0.2
300.5	0.530	0.538	1.5	299.1	0.605	0.608	0.5

ARD (%) = $100\times|\mu_{corr} - \mu_{exp}|/\mu_{exp}$

$\ln(\mu_{toluene}) = -4.3305+1115.1/T$

$\ln(\mu_{xylene}) = -4.6304+1236/T$

The densities of pure toluene and xylene were also measured, and the data is presented in Table 13. As one can see, the densities of the solvents increased with pressure and decreased with temperature. The fitted correlations predicted the densities of toluene within ± 0.2 kg/m^3 and xylene within ± 0.6 kg/m^3. The best fitted coefficients for the two solvents are summarized in Table 46.

Table 46 Calculated coefficients for toluene and xylenes density correlations (Eq. 5-5)

Coefficients in Eq. (1-127)	a_1	a_2	a_3	a_4
Toluene	884.86	-0.9399	7.1697×10^{-09}	7.1437×10^{-07}
Xylene	881.46	-0.8834	6.8014×10^{-09}	7.063×10^{-07}

5.4.2. Physical Properties of Raw Bitumen

5.4.2.1 Raw Bitumen Density

The densities and viscosities of the bitumen were measured over a wide range of temperature by an Anton Paar density measuring cell and a Cambridge viscometer, respectively. The temperature was varied within ±0.1 K, and the pressure was controlled with the ISCO pump. The uncertainty of the pressure and density measurements was 7 kPa and 0.1 kg/m^3, respectively.

The measured density data at temperatures of 296, 303, 313, 323 and 333 K over the pressure range of atmospheric pressure to 10 MPa are listed in Table 15, and compared with predictions obtained using the Eq. [5-5] listing within table 47. The regression of the coefficients was performed using a MATLAB subroutine. Table 48 summarizes the best fitted coefficients. The correlated values show a maximum deviation of ± 0.3 kg/m^3 with the measured ones. Badamchi-Zadeh et al. [34] also measured the density of Athabasca bitumen at three different pressures (90, 1470 and 3540 kPa) over the temperature range of 283 to 323 K. The measurements attempted to fit with Eq. [5-5]. The coefficients obtained by Badamchi-Zadeh et al. [34] are also mentioned in Table 47 for comparison.

Table 47 correlated, ρcorr, density of Athabasca bitumen at different temperatures, T, and pressures, P.

***T*/K**	***P*/MPa**	**ρ_{corr}/(kg/m^3)**	**$\Delta\rho$/(kg/m^3)***	***T*/K**	***P*/MPa**	**ρ_{corr}/(kg/m^3)**	**$\Delta\rho$/(kg/m^3)***
296.0	0.127	1006.0	-0.2	313.2	5.002	997.7	0.0
296.1	1.003	1006.3	-0.2	313.2	5.997	998.3	0.1
296.2	2.001	1006.8	0.0	313.1	6.998	998.9	0.2
296.3	3.003	1007.2	-0.1	313.1	7.998	999.4	0.2
296.3	4.004	1007.7	-0.1	313.1	8.996	999.9	0.1
296.4	4.996	1008.2	-0.2	313.1	9.997	1000.5	0.3

296.4	5.997	1008.7	-0.2	323.2	0.123	988.8	0.1
296.4	6.998	1009.2	-0.2	323.2	1.001	989.3	0.1
296.4	7.995	1009.7	-0.2	323.3	2.000	989.8	0.0
296.5	8.995	1010.1	-0.2	323.3	2.998	990.3	0.0
296.5	9.992	1010.6	-0.1	323.3	4.003	990.9	0.0
302.8	0.123	1001.7	0.2	323.3	4.999	991.5	0.0
303.2	1.005	1001.9	0.2	323.3	6.000	992.0	0.0
303.3	2.003	1002.3	0.1	323.4	6.996	992.5	0.0
303.4	2.998	1002.8	0.1	323.4	7.995	993.1	0.1
303.4	4.002	1003.3	0.1	323.4	8.993	993.6	0.1
303.6	5.000	1003.7	0.0	323.4	9.997	994.2	0.1
303.6	5.999	1004.2	0.0	332.8	0.121	982.7	0.0
303.6	6.999	1004.7	0.0	333.0	1.004	983.1	-0.1
303.6	7.996	1005.3	0.0	333.0	3.002	984.3	-0.1
303.6	8.999	1005.8	0.1	333.0	4.003	984.8	-0.2
303.6	9.995	1006.3	0.2	333.0	4.995	985.4	-0.2
313.4	0.129	995.0	0.1	333.0	6.001	986.0	-0.2
313.3	1.003	995.5	0.1	333.0	6.994	986.6	-0.1
313.2	2.000	996.1	0.1	333.0	8.001	987.2	-0.1
313.2	3.000	996.7	0.0	333.0	8.995	987.7	-0.1
313.2	4.000	997.2	0.0	333.0	9.996	988.3	-0.1

*$\Delta\rho = (\rho_{corr} - \rho_{exp})$

Table 48 Calculated coefficients of bitumen density correlation (Eq. 5-5)

Coefficients in Eq. (5-5)	a_1	a_2	a_3	a_4
This study	1020.30	-0.63096	2.27016×10^{-09}	4.49743×10^{-07}
Badamchi-Zadeh et al. [34]	1020.0	-0.6317	2.521×10^{-09}	6.8072×10^{-07}

The measured and correlated densities are plotted in Figure 15 with respect to pressure at different temperatures. As expected, the density of the bitumen increased with increasing pressure at a constant temperature. This behavior was observed for all temperatures, and linear trends for the variation of density with pressure were seen. The impact of temperature on the bitumen density is also demonstrated in Figure 15. At a constant pressure, the bitumen density decreased with increasing temperature.

The variation of bitumen density with temperature can be further investigated by plotting the density with respect to temperature. Similar to the density/pressure plot, linear trends were obtained. Thus, the bitumen density showed linear variations with pressure and temperature.

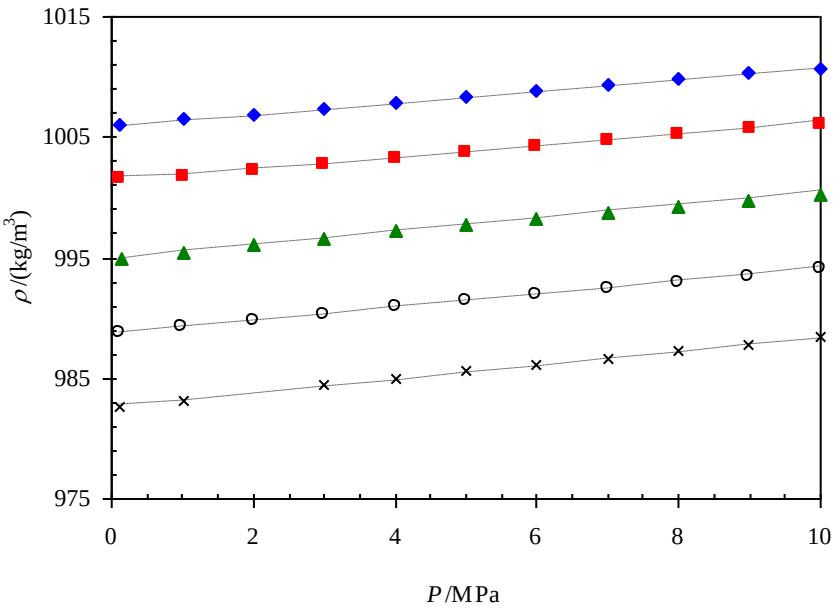

Figure 15 Density of bitumen, ρ, versus pressure, P, at different temperature, T; ♦,■,▲,○,×, measured densities; ♦, T = 296 K; ■, T = 303 K; ▲, T = 313 K; ○, T = 323 K; ×, T = 333 K; ----, calculated densities using Eq 1-123.

5.4.2.2. Raw Bitumen Viscosity

The viscosity of the bitumen was also measured at four temperatures (342, 331, 320, and 309 K) over the pressure range of atmospheric to 10 MPa. The measured data are summarized in Table 49. The viscosity data were fitted with two correlations developed by Mehrotra and Svrcek [32]. The correlations take into account the impact of both of pressure and temperature on bitumen viscosity, and the developed correlations have been examined by the presented viscosity measurements over temperature and pressure ranges of 313 to 393 K and 0.124MPa–10 MPa, respectively. The constants of Equations [5-3] and [5-4] are summarized in Table 50 along with coefficients fitted by other authors for Athabasca bitumen.

The correlated data with two viscosity correlations using the coefficients mentioned in Table 50 are also listed in Table 49. The last column of Table 49 shows the AARDs between the measured data and correlated values, which were 2.1% and 1.7% for Eq. 1-125 and Eq. 1-126, respectively.

Table 49 Measured, μexp, and correlated, μcorr, viscosity of Athabasca bitumen at different temperatures, T, and pressures, P.

***P*/MPa**	***T*/K**	μ_{exp}**/(mPa.s)**	μ_{corr}**/(mPa.s)**		**ARD (%)**	
			Eq. 5-3	Eq. 5-4	Eq. 5-3	Eq. 5-4
0.124	342.2	1236	1291	1324	4.5	7.1
1.002	341.1	1465	1471	1497	0.4	2.2
2.002	342.0	1499	1438	1454	4.0	3.0
4.000	342.2	1561	1562	1557	0.1	0.3
4.999	341.8	1708	1693	1677	0.9	1.8
5.998	342.6	1643	1670	1642	1.6	0.1

6.997	342.3	1765	1795	1756	1.7	0.5
7.996	342.6	1789	1842	1789	3.0	0.0
8.995	342.7	1859	1919	1853	3.2	0.3
9.994	342.8	1944	2000	1920	2.9	1.3
0.124	330.0	3619	3688	3718	1.9	2.7
1.002	331.3	3519	3413	3440	3.0	2.2
2.002	330.3	3945	3933	3954	0.3	0.2
3.001	331.5	3728	3696	3712	0.8	0.4
4.000	331.6	3876	3847	3857	0.7	0.5
4.999	331.6	4053	4040	4046	0.3	0.2
5.998	331.6	4246	4244	4244	0.1	0.0
6.997	331.6	4433	4457	4454	0.5	0.5
7.996	331.7	4621	4639	4632	0.4	0.2
8.995	331.7	4848	4872	4863	0.5	0.3
9.994	331.7	5061	5117	5108	1.1	0.9
0.124	319.5	10499	10686	10564	1.8	0.6
1.002	319.8	11135	10798	10722	3.0	3.7
2.002	319.9	11882	11219	11191	5.6	5.8
3.001	319.9	12446	11783	11810	5.3	5.1
4.000	319.9	12869	12376	12468	3.8	3.1
4.999	319.9	13342	12998	13166	2.6	1.3
5.998	319.9	13843	13652	13908	1.4	0.5
6.997	319.8	14590	14495	14860	0.7	1.8
7.996	319.9	15184	15059	15533	0.8	2.3
8.995	319.9	16119	15817	16424	1.9	1.9
9.994	319.9	17048	16612	17371	2.6	1.9
0.124	308.7	36164	38547	37116	6.6	2.6
1.002	308.8	38371	39730	38659	3.5	0.8

2.002	308.9	40237	41198	40575	2.4	0.8
3.001	309.0	41420	42718	42592	3.1	2.8

ARD (%) = $100\times|\mu_{corr} - \mu_{exp}|/\mu_{exp}$

Table 50 Calculated coefficients of bitumen viscosity correlation (Eqs. 5-3 and 5-4)

Coefficients		a_1	a_2	a_3
This study	Eq. 1-125	23.95318	-3.76743	0.049118
	Eq. 1-126	23.55379	-3.69839	0.005766
Mehrotra and Svrcek [32]	Eq. 1-125	23.42920	-3.67720	0.0345755
	Eq. 1-126	22.85150	-3.57840	0.00511938

Figure 16 shows the measured and correlated viscosity data versus pressure at different temperatures for Athabasca bitumen. In this plot, the dashed lines denote the calculation results by Eqs. [5-3] and [5-4], and the dots show the experimental data. As one can see, the viscosity of bitumen increased with increasing pressure and decreased with increasing temperature. The impact of temperature on bitumen viscosity was more pronounced than that of pressure. As depicted in Figure 16, the viscosity data was well fitted with the two empirical correlations. The results of the two models at low pressures were close. However, as the pressure increased, the deviation of the two models from each other became more pronounced.

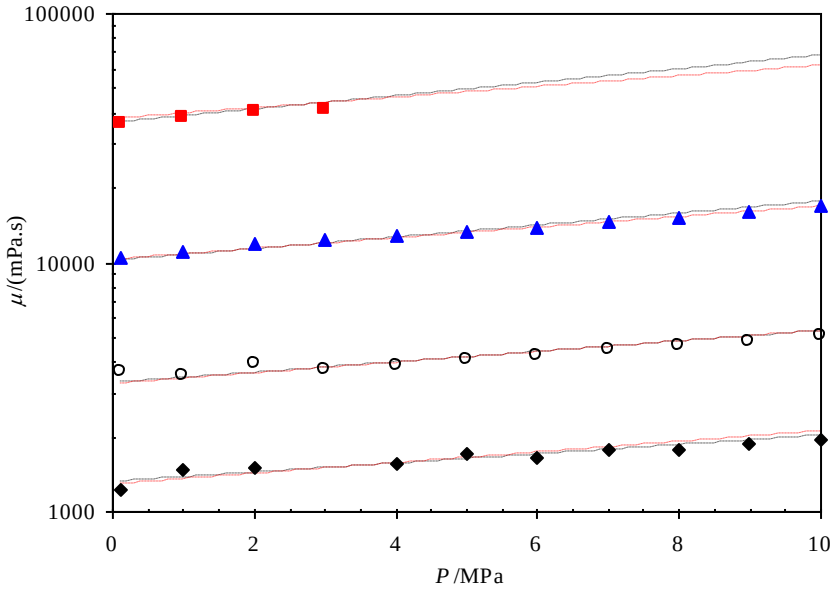

Figure 16 Viscosity of bitumen, μ, versus pressure, P, at different temperature, T; ♦,■,▲,○, measured viscosity data; ♦, T = 308.9 K; ○, T = 319.8 K; ▲, T = 331.3 K; ■, T = 342.2 K; -----, calculated viscosities using Eq 2; -----, calculated viscosities using Eq 3.

Overall, the two models predicted the viscosity data well over the studied pressure and temperature ranges. Nevertheless, on the basis of AARDs, Eq. [5-4] resulted in lower deviations.

5.4.3. Physical Properties of bitumen/solvents Binary Mixtures System

The density and viscosity of bitumen diluted with toluene and xylene were measured at different temperatures, pressures and solvent weight fractions. The aim was evaluation of the impact of variations in pressure, temperature and solvent concentration on the viscosity and density of the bitumen/solvent mixtures.

5.4.3.1. Bitumen/Toluene Binary Mixtures

5.4.3.1.1 Density of Bitumen/Toluene Mixtures

The data for the density and viscosity of the mixtures prepared from toluene and bitumen are summarized through Tables 17 to 29, respectively. Generally, the density and viscosity of bitumen/toluene mixtures decreased with increases in temperature and solvent weight fraction, while increased pressure increased the density and viscosity of the mixtures.

The impact of pressure on the mixture viscosity was more pronounced at lower toluene weight fractions. This behavior was expected, because the behavior of the mixtures would be more similar to pure toluene as the toluene concentration increased. The data on the viscosity of pure toluene presented in Chapter 4.1 indicated that the viscosity of toluene was not significantly affected by pressure. On the other hand, the bitumen showed more viscosity changes under pressure variations. Thus, any mixture prepared from the species of bitumen and toluene showed a behavior similar to bitumen at low toluene concentrations.

The impact of pressure on the mixture viscosity was also dependent on the temperature, i.e., at lower temperatures, the pressure resulted in higher viscosity variations. This trend was also observed for solvent-free bitumen data presented in Chapter 4.2. The bitumen viscosity demonstrated higher variations with pressure at lower temperatures.

As previously mentioned, the density of bitumen/solvent mixtures increased with increased pressure and decreased with increased solvent concentration and temperature. The impacts of pressure and solvent concentration on the mixture density followed linear trends. The generated density data of bitumen/toluene mixtures were correlated with the equation [5-6]. The data were fitted using the above equation with a 0.04% AARD, and the predicted results were in good agreement with the measured data. The densities of pure toluene and raw bitumen at each

temperature and pressure were calculated using Eq. [5-5] with the coefficients summarized in Tables 45 and 47. Figures 17 and 18 displayed the measured density data for bitumen/toluene mixtures along with the correlated values. In these figures, the density was plotted versus toluene concentration at different temperatures. The dots are the measured experimental data, and the lines are the predictions using Eq. [5-11]. As one can see, the data were well matched with the predictions. Figure 17 shows the variation of density with toluene weight fraction at the lowest pressure (i.e., 0.125 MPa), and Figure 18 shows variations at the highest pressure (i.e., 10 MPa).

As depicted in Figure 17, the mixture density linearly decreased with increased toluene concentration. This trend was observed for all temperatures considered in this study (the symbols with the same color indicate a constant temperature). The data also showed a linear decrease in the density of mixture with respect to increased solvent concentration at other pressures. Figure 18 illustrates the density measurements over concentration variations at the highest pressure.

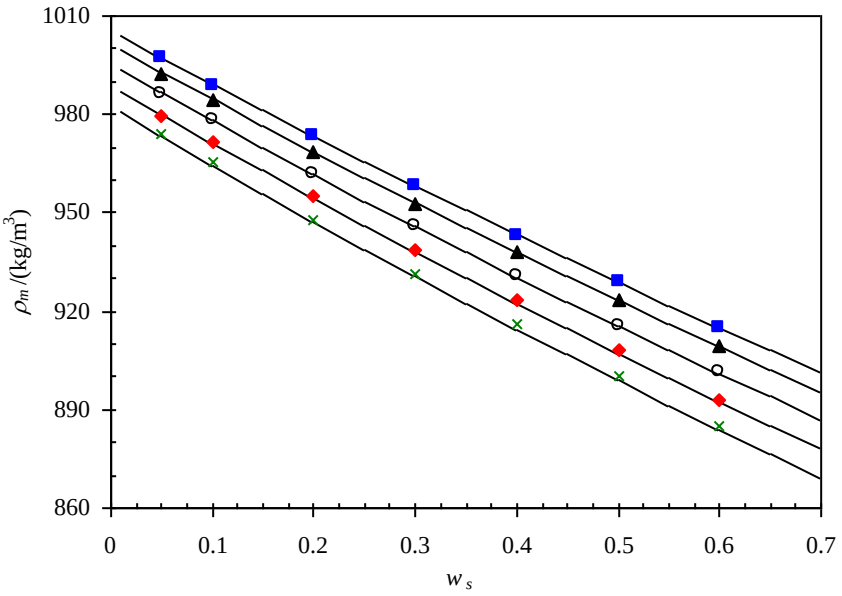

Figure 17 Density, ρ_m, of bitumen/toluene mixtures versus toluene weight fraction, w_s, at different temperatures and a pressure of 0.125 MPa; ■,▲,○,♦,×, experimental data; ─, correlation; ■, 296.5 K; ▲, 303.3 K; ○, 313.1 K; ♦, 323.3 K; ×, 333.2 K.

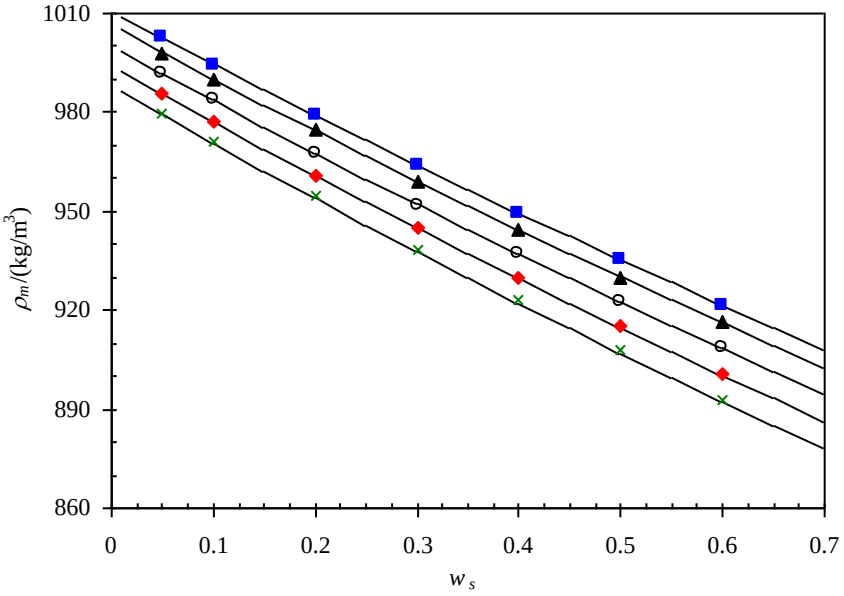

Figure 18 Density, ρ_m, of bitumen/toluene mixtures versus toluene weight fraction, w_s, at different temperatures and a pressure of 10 MPa; ■,▲,○,♦,×, experimental data; ─, correlation; ■, 296.6 K; ▲, 303.2 K; ○, 313.2 K; ♦, 323.2 K; ×, 333.2 K.

To evaluate the impact of pressure on the mixture density, the density data were plotted versus pressure at different temperatures and are shown in Figures 19 and 20. For these plots, the solvent concentrations were fixed at two extreme values (lowest and highest) – 0.05 and 0.6 weight fractions of toluene. The dots are the measured density data, and the predictions using Eq. [5-11] are shown by solid lines. As presented in these figures, the density data obey linear increasing trends with increased pressure. Although the increase in temperature decreased the mixture density, the linear trends were also satisfied at higher temperatures.

As can also be seen from the comparison of Figures 19 and 20, a large increase in toluene concentration did not impact the linear behavior of the density data with pressure. The only

remarkable point was that the predicted results at the highest temperature (333 K) and highest toluene concentration (0.6 toluene weight fraction) showed slight deviations from the measured values. This may be due to deviation from the assumption of no volume change on mixing at higher toluene concentrations. It can be concluded that, at higher temperatures, the assumption of ideal mixing for toluene and bitumen mixtures is not appropriate.

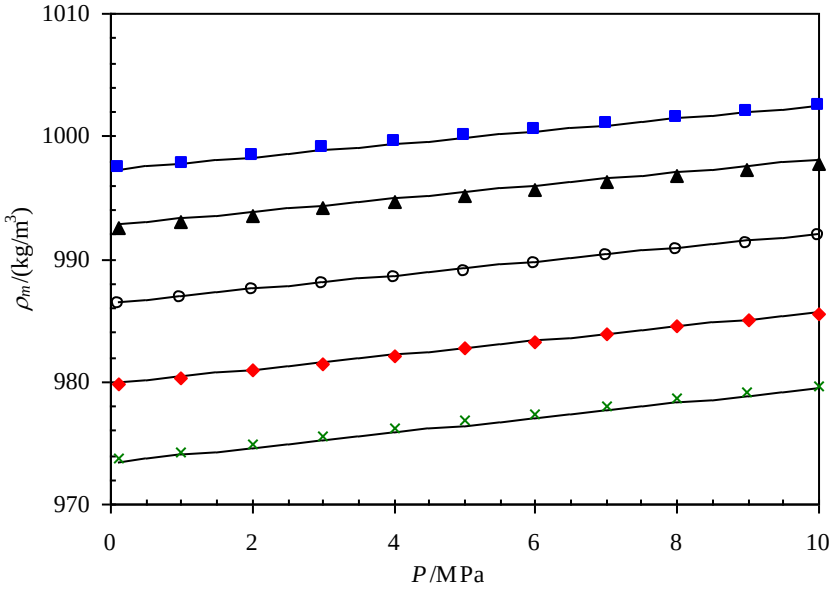

Figure 19 Effect of pressure, P, on the density, ρ_m, of bitumen/toluene mixtures at different temperatures and a constant toluene weight fraction of 0.05; ■,▲,○,♦,×, experimental data; ─, correlation; ■, 296.6 K; ▲, 303.5 K; ○, 313.2 K; ♦, 323.3 K; ×, 333.1 K.

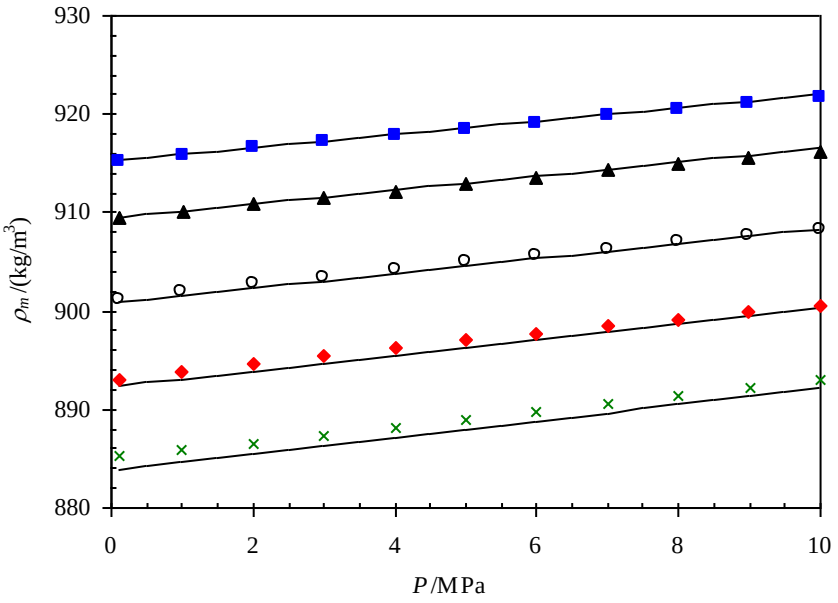

Figure 20 Effect of pressure, P, on the density, ρ_m, of bitumen/toluene mixtures at different temperatures and a constant toluene weight fraction of 0.6; ■,▲,○,♦,×, experimental data; ─, correlation; ■, 296.0 K; ▲, 302.9 K; ○, 313.1 K; ♦, 323.2 K; ×, 333.3 K.

5.4.3.1.2 Viscosity of Bitumen/Toluene Mixtures

The measured viscosity data of the bitumen/toluene mixtures were also evaluated with correlations developed for mixtures. These correlations were mostly developed for light and medium oils diluted with solvents. Centeno et al. [62] summarized a total of 26 mixing rules and classified them according to the number and type of parameters, as well as the information required for each correlation.

In this study, we evaluated four correlations – Arrhenius, power law, Lederer and Shu models. These correlations are commonly used for bitumen/solvent mixtures and resulted in acceptable results in this study.

The results of the four aforementioned correlations for the viscosity of bitumen/toluene mixtures are presented in Figure 21. The viscosity of the pure solvent was calculated using the correlation presented in Table 13, and the viscosity of the raw bitumen at different temperatures and pressures was calculated using Eq. [5-4] (coefficients listed in Table 49).

Figure 21 illustrates the calculated results using the different mixing rules compared to experimental viscosity data. The results indicated that Lederer's model and the power law model fit the data better than the Shu correlation and Arrhenius's model. The viscosity results using the Lederer and power law models led to almost the same predictions. However, an AARD comparison showed that the AARD for Lederer's model was 14.8%, while this value was found to be 19.2% for the power law model. The adjustable parameters for these two models were obtained by regression of all data as n = 0.0503 (exponential term in power law model) and α = 0.2858 (adjustable coefficient in Lederer's model).

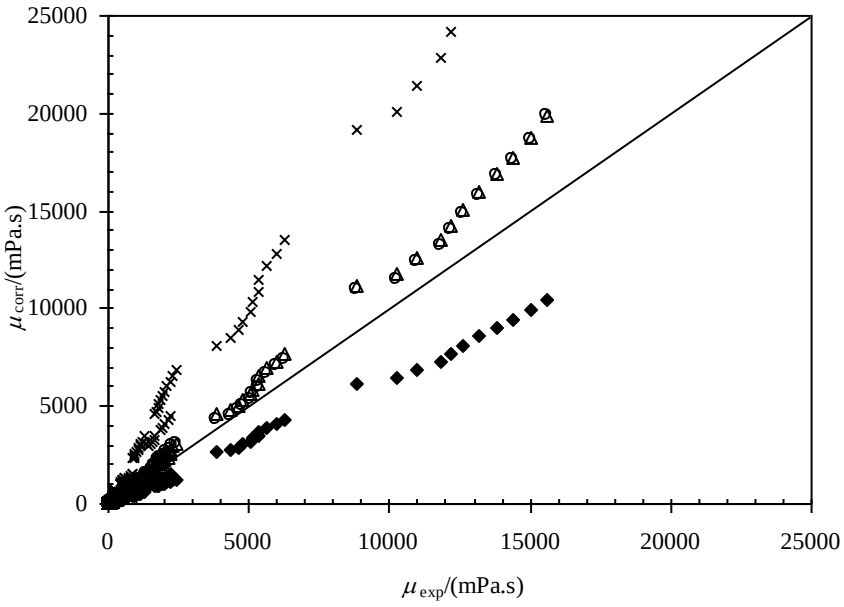

Figure 21 Experimental mixture viscosities, μ_{exp}, versus calculated values, μ_{corr}, for bitumen/toluene mixtures using different mixing rules; Δ, Lederer's model; ○, power law model; ×, Shu correlation; ♦, Arrhenius's model.

Due to better predictions of the results of the Lederer and power law models, these two models were compared with the experimental data to analyze the data and find trends, as shown in Figures 22, 23, 24, 25, 26, and 27. The results obtained by Lederer's model are indicated by solid lines in these figures, and the dashed lines represent the results of the power law model.

Figures 22 and 23 illustrate the effect of increased toluene concentration on the mixture viscosity at different temperatures. Figure 22 shows the results at the lowest pressure (0.125 MPa), and Figure 23 displays the data at the highest pressure (10 MPa). The viscosity results are shown in semi-log plots.

As presented in these figures, the viscosity of the mixtures showed a curvilinear trend with respect to the toluene concentration at two different pressures. The impact of temperature on the viscosity of mixture was less pronounced at higher toluene concentrations. The experimental

data were well correlated with the Lederer and power law models. Although there were no significant differences in the results of two models, Lederer's model predicted the experimental data better than the power law model at higher temperatures.

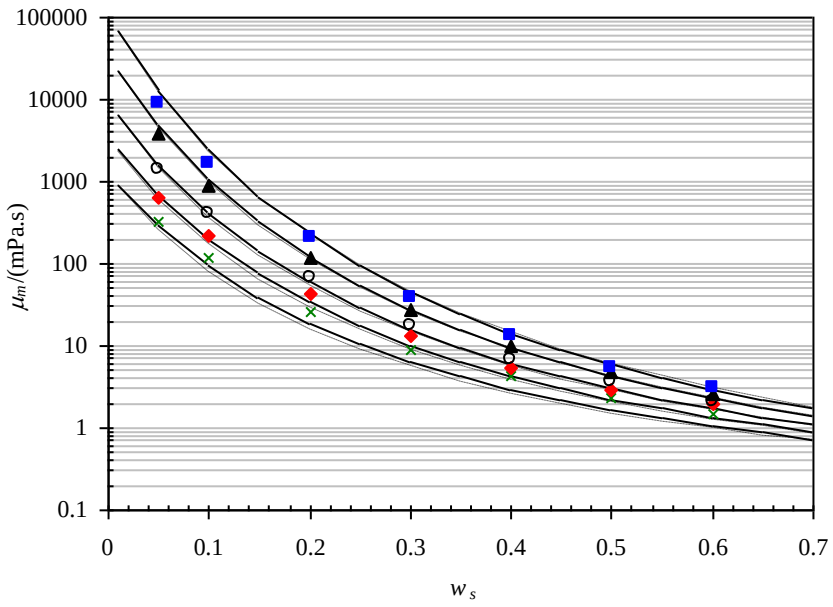

Figure 22 Viscosity, μ_m, of bitumen/toluene mixtures versus toluene weight fraction, w_s, at different temperatures and a constant pressure of 0.125 MPa; ■,▲,○,♦,×, experimental data; ─, Lereder's model; ---, power law model; ■, 300.6 K; ▲, 309.2 K; ○, 320.4 K; ♦, 330.8 K; ×, 342.9 K.

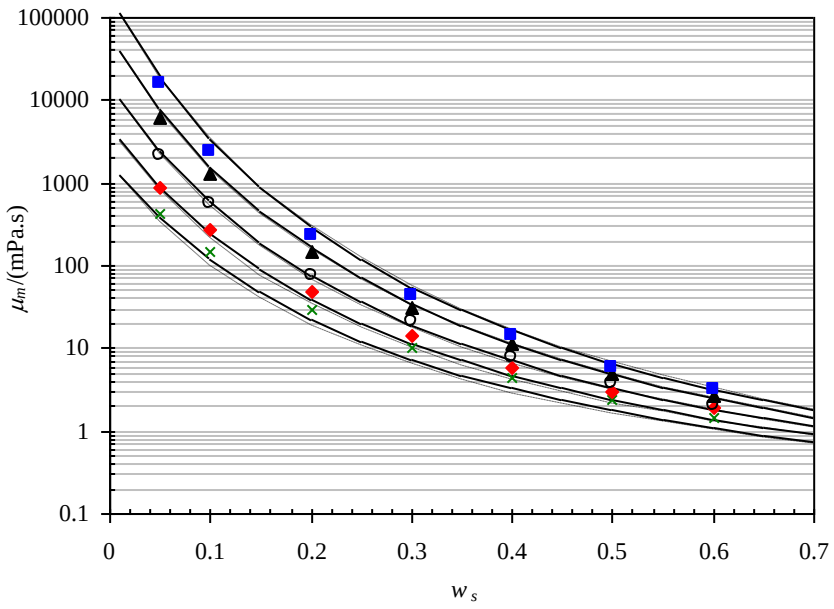

Figure 23 Viscosity, μ_m, of bitumen/toluene mixtures versus toluene weight fraction, w_s, at different temperatures and a constant pressure of 10 MPa; ■,▲,○,♦,×, experimental data; ─, Lereder's model; ---, power law model; ■, 301.8 K; ▲, 309.6 K; ○, 320.8 K; ♦, 332.3 K; ×, 343.8 K.

The impact of pressure on the viscosity of bitumen/toluene was also evaluated and is presented in Figures 24 and 25. To determine the effect of pressure along with the dilution of mixture with toluene on viscosity, the viscosity data at 0.05 and 0.6 weight fractions of toluene are plotted versus pressure in Figures 24 and 25, respectively. The dots with the same color indicate a constant temperature in these plots. Comparing Figures 24 and 25, one can see that the effect of pressure on the mixture viscosity showed a linear increase at each temperature and that this effect was greater at the lower toluene concentration (i.e., 0.05 weight fraction of toluene). A closer examination of Figure 25 reveals that the predictions from the two models at the highest temperature and highest toluene concentration deviated from the experimental data.

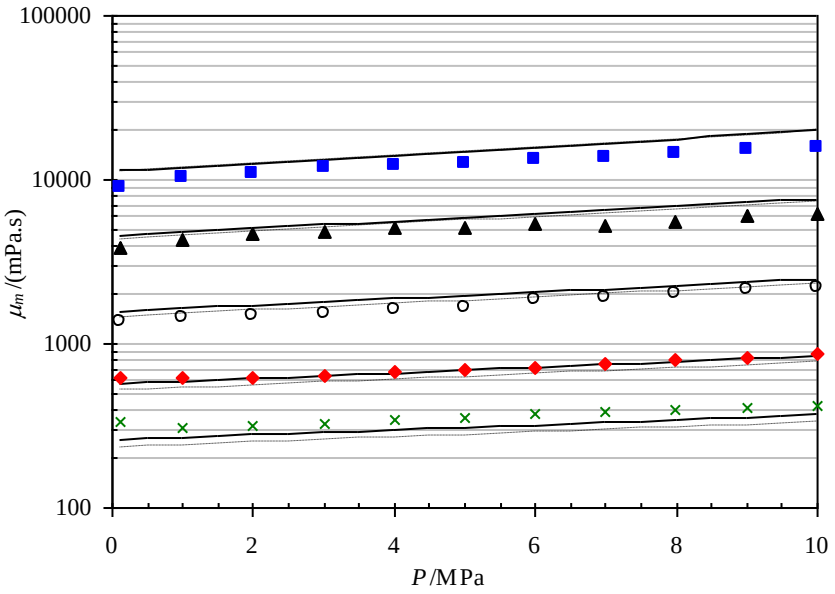

Figure 24 Effect of pressure, P, on the viscosity, μ_m, of bitumen/toluene mixtures at different temperatures and a constant toluene weight fraction of 0.05; ■,▲,○,♦,×, experimental data; ─, Lereder's model; ---, power law model; ■, 301.5 K; ▲, 309.6 K; ○, 320.6 K; ♦, 333 K; ×, 344.3 K.

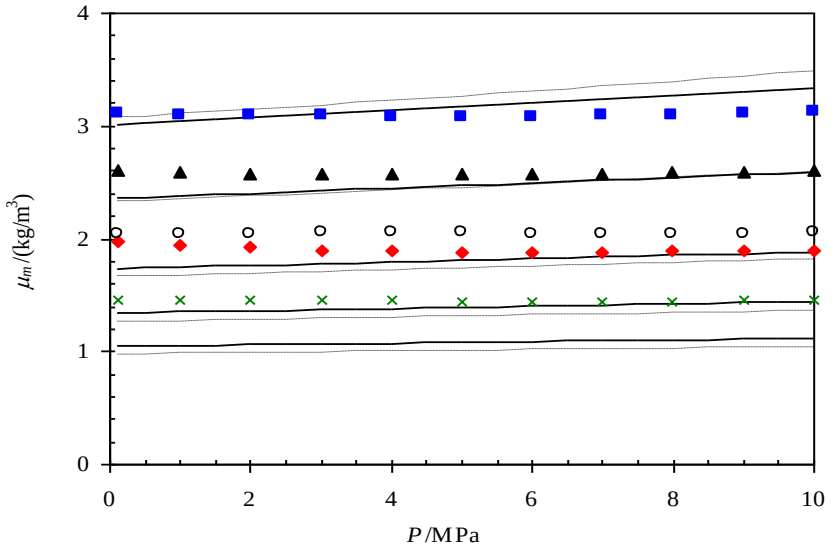

Figure 25 Effect of pressure, P, on the viscosity, μ_m, of bitumen/toluene mixtures at different temperatures and a constant toluene weight fraction of 0.6; ■,▲,○,♦,×, experimental data; ─, Lereder's model; ---, power law model; ■, 300.3 K; ▲, 308.5 K; ○, 320.0 K; ♦, 331.1 K; ×, 343.1 K.

To have a better representation of the data and a comparison with the models, the viscosity data at different toluene concentrations were plotted versus pressure in Figures 26 and 27. Figure 26 shows the results at the highest temperature, while the viscosity data at the lowest temperature are shown in Figure 27. The calculated values of the two models were slightly larger than the experimental data at the lowest temperature (301.5 K). However, at the highest temperature (343.6 K), the deviations between the correlated data and experimental results were more pronounced, which would be even more significant at higher toluene concentrations. Thus, from Figures 24-27, one can conclude that the predictions obtained by the two models showed more deviations from the experimental data at the higher temperature and higher toluene concentration.

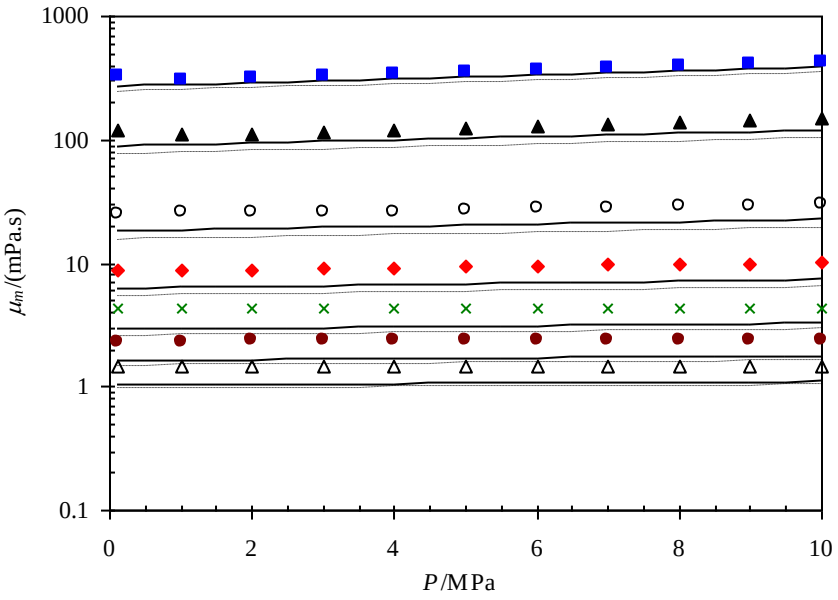

Figure 26 Effect of toluene concentration, w_s, (in weight fraction) and pressure, P, on the viscosity, μ_m, of bitumen/toluene mixtures at the highest temperature (343.6 K); ■,▲,○,♦,×,●,Δ, experimental data; ─, Lereder's model; ---, power law model; ■, w_s = 0.05; ▲, w_s = 0.1; ○, w_s = 0.2; ♦, w_s = 0.3; ×, w_s = 0.4; ●, w_s = 0.5; Δ, w_s = 0.6.

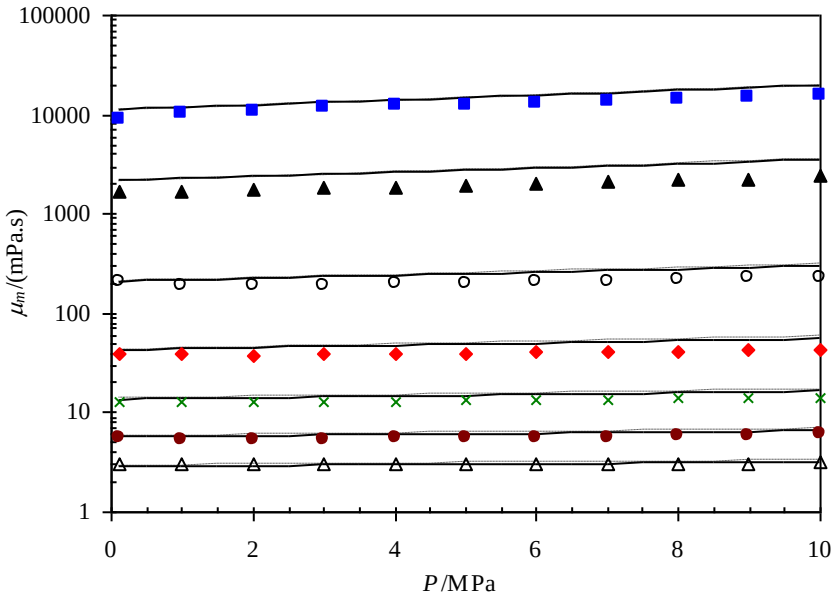

Figure 27 Effect of toluene concentration, w_s, (in weight fraction) and pressure, P, on the viscosity, μ_m, of bitumen/toluene mixtures at the lowest temperature (301.5 K); ■,▲,○,♦,×,●,Δ, experimental data; ─, Lereder's model; ---, power law model; ■, w_s = 0.05; ▲, w_s = 0.1; ○, w_s = 0.2; ♦, w_s = 0.3; ×, w_s = 0.4; ●, w_s = 0.5; Δ, w_s = 0.6.

5.4.3.2. Bitumen/Xylene Binary Mixtures

5.4.3.2.1 Density of Bitumen/Xylene Binary System

The density and viscosity of bitumen/xylene mixtures were measured at different xylene concentrations and different temperatures over a pressure range of atmospheric pressure to 10 MPa. The aim was evaluation of the viscosity and density reduction with increased temperatures and solvent concentrations. Through tables 24 to 43 summary the measured mixture viscosity and density data, respectively. As expected, the larger the concentration of xylene, the lower the viscosity and density of the mixture. Increased pressure increased the viscosity and density

considering a constant xylene concentration and isotherm condition. The impact of pressure on the mixture viscosity was more pronounced at lower xylene concentrations. This behavior was expected, because the larger, the xylene concentration, and the more similar the behavior of the mixture would be to pure xylene, i.e., no significant viscosity-pressure variations.

On the other hand, the data of bitumen viscosity revealed more changes under pressure variations. Thus, any mixture prepared from the species of bitumen and xylenes showed a behavior similar to bitumen at low xylene concentrations.

The impact of pressure on the viscosity of bitumen/xylene mixtures was also dependent on the temperature, i.e., at lower temperatures, the pressure resulted in higher viscosity variations. This trend was also observed for solvent-free bitumen data presented in Section 4.4. The bitumen viscosity demonstrated higher variations with pressure at lower temperatures.

Similar to the bitumen/toluene mixtures, the measured density data of the bitumen/xylene mixtures were correlated with Eq. [5-11]. The data were fitted using this equation with a 0.06% AARD, and the experimental data were quite well matched with this equation. The densities of pure xylene and raw bitumen at each temperature and pressure were calculated using Eq. [5-5] with the coefficients summarized in Tables 45 and 47.

Figures 28 and 29 illustrate the mixture density data versus xylene weight fraction along with the modeling results. Figures 30 and 31 present the impact of pressure on the mixture density, with the density data plotted versus pressure at different temperatures. In these figures, the dots show the experimental data and lines are the predictions using Eq. [5-11]. As presented in these figures, the predictions were in good agreement with the experimental data.

Figure 28 shows the variation of the mixture density with xylene weight fraction at the lowest pressure (0.125 MPa), and Figure 29 shows the variation at the highest pressure (10

MPa). In Figures 30 and 31, the solvent proportions were fixed at two extreme values – 0.05 and 0.6 weight fractions of xylene – and the impact of pressure at different temperatures was evaluated.

As depicted in Figures 28, the mixture density linearly decreased with increased xylene concentration at a pressure of 0.125 MPa. This trend was observed for all temperatures considered in this study. The data also showed a linear decrease in the density of mixture with respect to the solvent concentration at other pressures (Figure 29 shows the results at 10 MPa).

As presented in Figures 30 and 31, the density data revealed linear trends with pressure. Although the increase in temperature decreased the mixture density, linear trends were also observed at higher temperatures. It can also be seen from the comparison of Figures 30 and 31 that a large increase in the xylene concentration did not impact the linear behavior of density data with pressure. The only remarkable point was that the predicted results at the highest temperature (333 K) and highest xylene concentration (0.6 xylene weight fraction) showed slight deviations from the measured values. As previously mentioned, this may have been due to deviation from the assumption of no volume change on mixing at higher solvent concentrations.

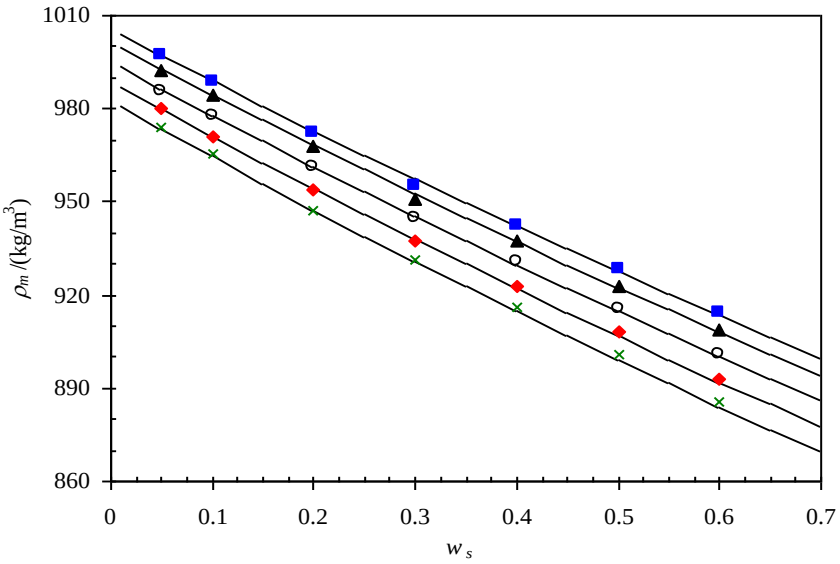

Figure 28 Density, ρ_m, of bitumen/xylene mixtures versus xylene weight fraction, w_s, at different temperatures and a pressure of 0.125 MPa; ■,▲,○,♦,×, experimental data; ─, correlation; ■, 296.6 K; ▲, 303.2 K; ○, 313.1 K; ♦, 323.3 K; ×, 333.1 K.

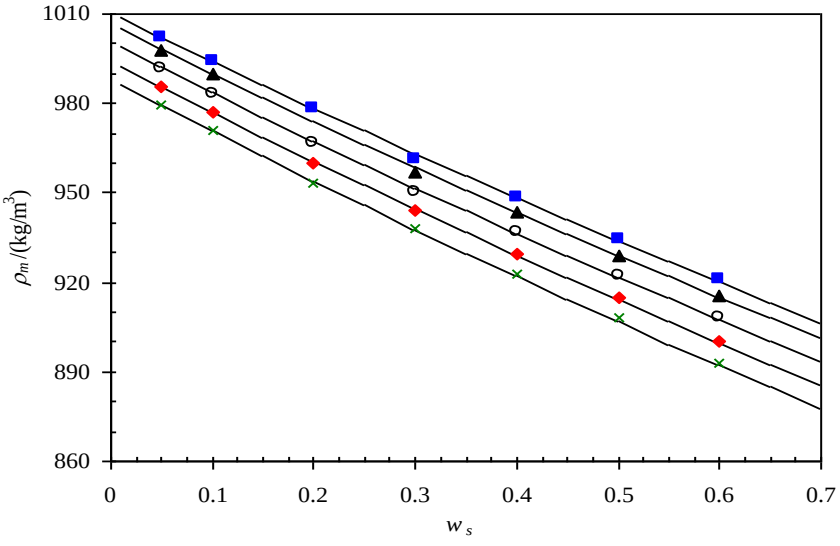

Figure 29 Density, ρ_m, of bitumen/xylene mixtures versus xylene weight fraction, w_s, at different temperatures and a pressure of 10 MPa; ■,▲,○,♦,×, experimental data; ─, correlation; ■, 296.6 K; ▲, 303.2 K; ○, 313.0 K; ♦, 323.3 K; ×, 333.2 K.

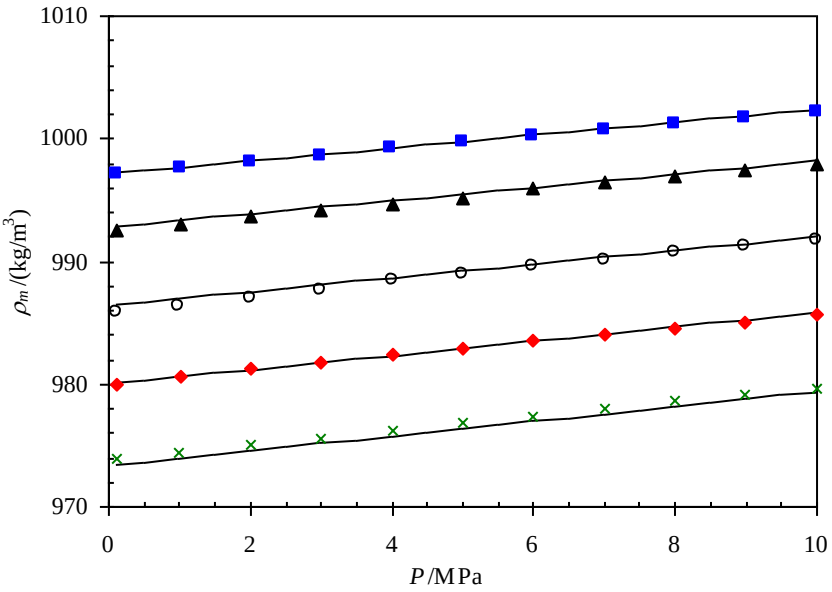

Figure 30 Effect of pressure, P, on the density, ρ_m, of bitumen/xylene mixtures at different temperatures and a constant xylene weight fraction of 0.05; ■,▲,○,♦,×, experimental data; ─, correlation; ■, 296.6 K; ▲, 303.3 K; ○, 313.2 K; ♦, 323.0 K; ×, 333.2 K.

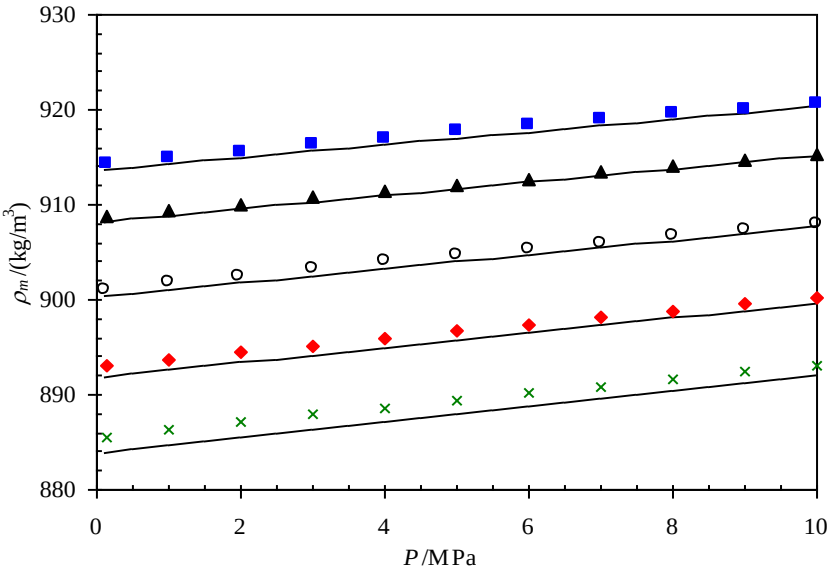

Figure 31 Effect of pressure, P, on the density, ρ_m, of bitumen/xylene mixtures at different temperatures and a constant xylene weight fraction of 0.6; ■,▲,○,♦,×, experimental data; ─, correlation; ■, 296.3 K; ▲, 303.0 K; ○, 312.8 K; ♦, 323.2 K; ×, 333.2 K.

5.4.3.2.2 Viscosity of Bitumen/Xylene Binary System

The measured viscosity data of the bitumen/xylene mixtures were also correlated with the four correlations mentioned through Eq. [7] to Eq. [11]. Again, the capability of these correlations for the viscosity predictions of bitumen/xylene mixtures was tested and presented in Figure 32. The viscosity of pure xylene was calculated with the correlation mentioned in Table 44, and the raw bitumen viscosity was estimated from Eq. [5-4] and coefficients presented in Table 49. It was again found that the Lederer and power law models fit the data better than the Shu correlation and Arrhenius's model. The viscosity results using Lederer's model and the power law model led to almost the same predictions. A comparison on the basis of AARDs showed that the AARD for Lederer's model was 13.8%, while this value was found to be 17.1% for the power law model. The adjustable parameters for these two models were obtained by regression of all data as n = 0.0350 (exponential term in power law model) and α = 0.3034 (adjustable coefficient in Lederer's model).

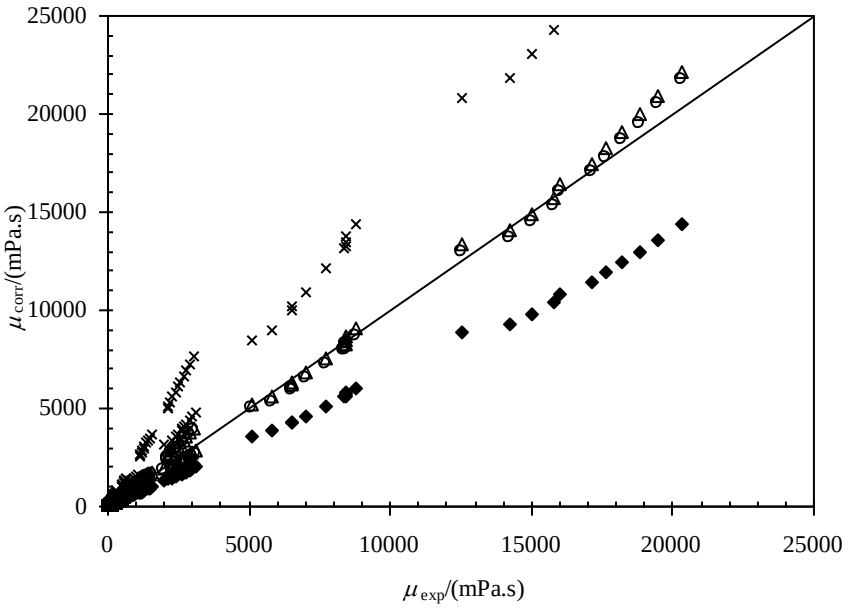

Figure 32 Experimental mixture viscosities, μ_{exp}, versus calculated values, μ_{corr}, for bitumen/xylene mixtures using different mixing rules; Δ, Lederer's model; ○, power law model; ×, Shu correlation; ♦, Arrhenius's model.

Figures 33 and 34 illustrate the effect of the xylene concentration on the mixture viscosity at different temperatures. Figure 33 shows the results at the lowest pressure (0.125 MPa), and Figure 34 displays the data at the highest pressure (10 MPa). As shown in these figures, the viscosity of mixtures showed a curvilinear trend with respect to the xylene concentration at two different pressures. The impact of temperature on the viscosity of mixture was less pronounced at larger xylene concentrations. The experimental data were well correlated using the Lederer and power law models. Although no significant differences in the results of two models were observed, Lederer's model predicted the experimental data better than the power law model at higher temperatures.

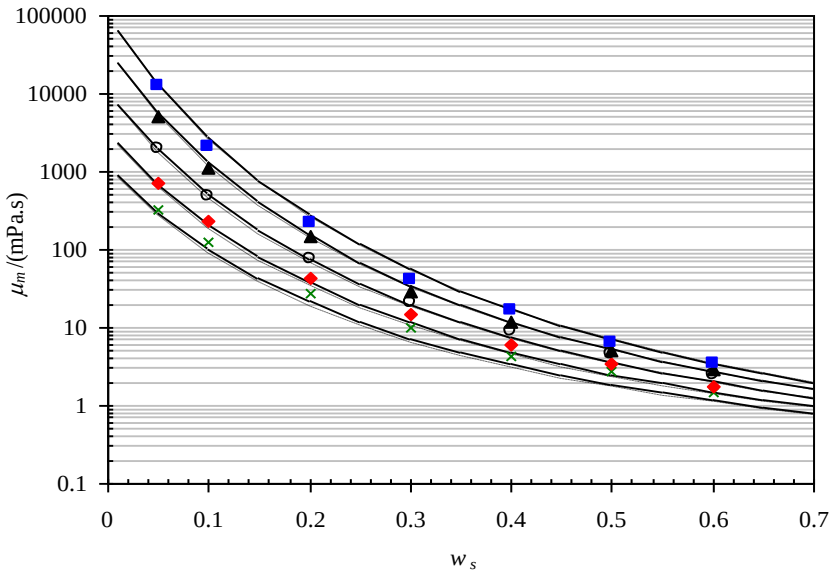

Figure 33 Viscosity, μ_m, of bitumen/xylene mixtures versus xylene weight fraction, w_s, at different temperatures and a constant pressure of 0.125 MPa; ■,▲,○,♦,×, experimental data; ─, Lederer's model; ---, power law model; ■, 301.1 K; ▲, 308.8 K; ○, 319.5 K; ♦, 331.7 K; ×, 343.5 K.

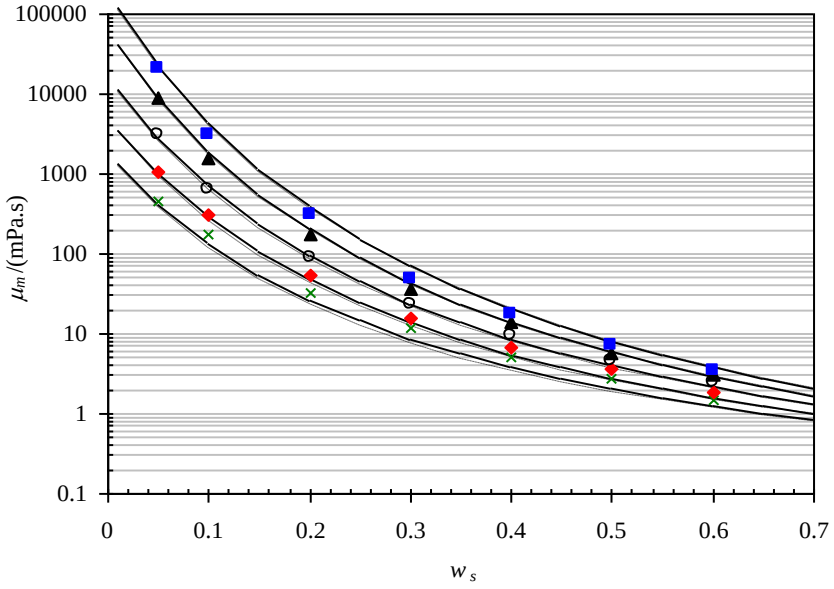

Figure 34 Viscosity, μ_m, of bitumen/xylene mixtures versus xylene weight fraction, w_s, at different temperatures and a constant pressure of 10 MPa; ■,▲,○,♦,×, experimental data; ─, Lederer's model; ---, power law model; ■, 301.7 K; ▲, 309.4 K; ○, 320.5 K; ♦, 332.2 K; ×, 343.7 K.

Figures 35 - 38 show the effect of pressure on the viscosity of the bitumen/xylene mixtures. Figures 35 and 36 illustrate the effect of pressure on the mixture viscosity at different temperatures. Thus, the viscosity data at fixed weight fractions of xylene (0.05 and 0.6) were plotted versus pressure in these figures. To have a better representation of the data and a comparison with the models, the viscosity data at different concentrations were plotted versus pressure in Figures 37 and 38. Figure 37 shows the results at the highest temperature, while the viscosity data at the lowest temperature is shown in Figure 38.

Comparing Figures 35 and 36, one can see that the effect of pressure on the mixture viscosity showed a linear increase at each temperature and that this effect was greater at the lower toluene concentration (0.05 xylene weight fraction). A closer examination of Figure 36 reveals that the predictions from the two models at the highest temperature and highest toluene concentration deviated from the experimental data.

From Figures 37 and 38, the calculated values of the two models were slightly larger than the experimental data at the lowest temperature (301.5 K). However, at the highest temperature (343.6 K), the deviations between the correlated data and experimental results were more significant, which would be even more pronounced at higher toluene concentrations.

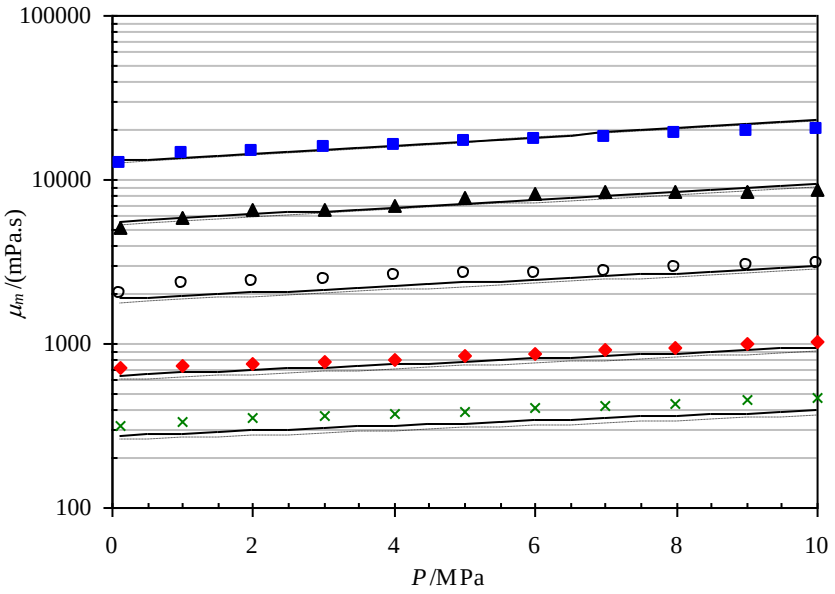

Figure 35 Effect of pressure, *P*, on the viscosity, μ_m, of bitumen/xylene mixtures at different temperatures and a constant xylene weight fraction of 0.05; ■,▲,○,♦,×, experimental data; ─, Shu correlation; ---, power law model; ■, 301.3 K; ▲, 308.8 K; ○, 319.7 K; ♦, 332.6 K; ×, 344.6 K.

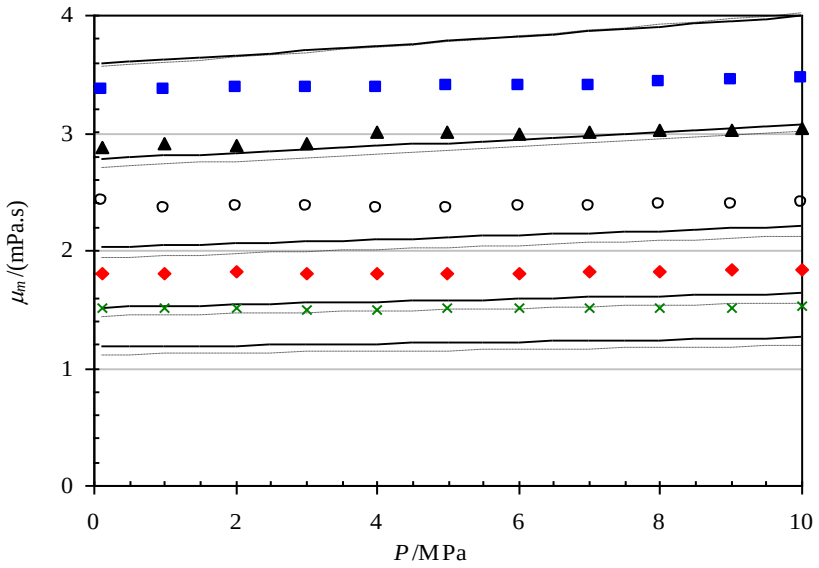

Figure 36 Effect of pressure, *P*, on the viscosity, μ_m, of bitumen/xylene mixtures at different temperatures and a constant xylene weight fraction of 0.6; ■,▲,○,♦,×, experimental data; ─, Shu correlation; ---, power law model; ■, 300.3 K; ▲, 308.3 K; ○, 319.5 K; ♦, 331.0 K; ×, 342.6 K.

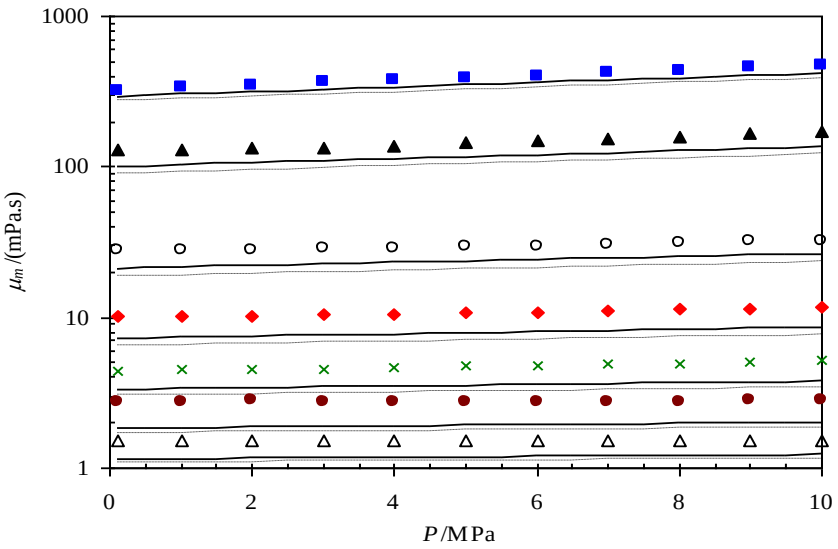

Figure 37 Effect of xylene concentration (in weight fractions), w_s, and pressure, P, on the viscosity, μ_m, of bitumen/xylene mixtures at the highest temperature (343.6 K); ■,▲,○,♦,×,●,Δ, experimental data; ─, Shu correlation; ---, power law model; ■, w_s = 0.05; ▲, w_s = 0.1; ○, w_s = 0.2; ♦, w_s = 0.3; ×, w_s = 0.4; ●, w_s = 0.5; Δ, w_s = 0.6.

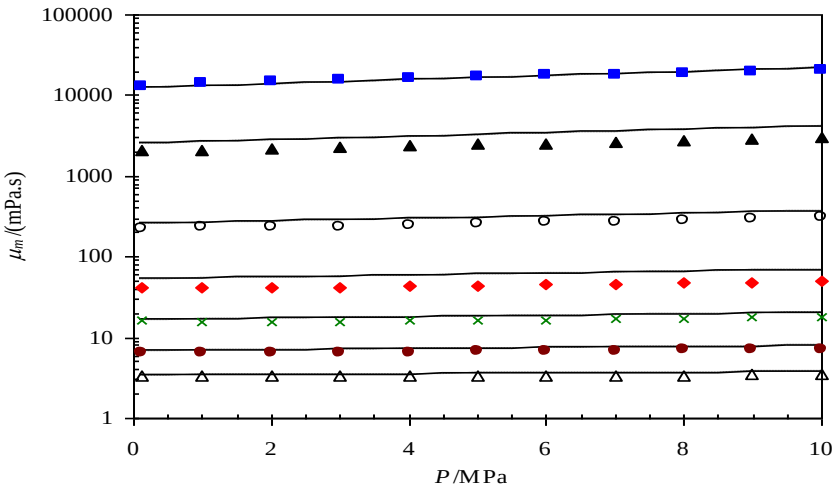

Figure 38 Effect of xylene concentration (in weight fractions), w_s, and pressure, P, on the viscosity, μ_m, of bitumen/xylene mixtures at the lowest temperature (301.5 K); ■,▲,○,♦,×,●,Δ, experimental data; ─, Shu correlation; ---, power law model; ■, w_s = 0.05; ▲, w_s = 0.1; ○, w_s = 0.2; ♦, w_s = 0.3; ×, w_s = 0.4; ●, w_s = 0.5; Δ, w_s = 0.6.

Chapter 6 Conclusion

In this study, the aim was an in-depth investigation of an integrated relationship for physical properties of Athabasca bitumen, pure solvents of toluene and xylene, and bitumen/toluene and bitumen/xylene binary mixtures, with respective to pressures, temperatures and constitutions. A unique experiment was designed, set up and conducted to accurately measure the variations of the viscosity and density values at temperatures from ambient up to 333.15 K at intervals of 10 K and pressures from atmospheric up to 10 MPa at intervals of 1 MPa. The mixtures were prepared in concentrations from 0.05 to 0.6 weight fractions of the aromatic solvents. Based on these systematic and precise measurements, some suitable correlations for raw bitumen, pure solvents and mixtures were correlated to find the ones that best fit each type of material.

6.1 Case Study for Raw Athabasca Bitumen

Raw Athabasca bitumen is highly viscous at ambient temperature and atmospheric pressure. The experimental measurement for viscosity could not be obtained for pressures lower than 3.0 MPa and temperatures lower than 309.0 K, due to the capability limitation of the Viscopro2000 unit.

According to Table 16, the influence of temperature on bitumen viscosity was significant. From the data analysis, a 10 times magnitude order of viscosity change could be observed for the same pressure conditions, but with only a difference of 23 K between two extreme temperature points. In contrast, the impact of pressure on bitumen viscosity was less pronounced. The same magnitude influence could be observed for the same temperature conditions, but with a difference of 9.87 MPa between the highest and lowest pressure sets.

To correlate the relationships of Eq. [5-3] and [5-4] proposed by Mehrotra and Svrcek [32], the adjustable characterized parameters of b_1, b_2, and b_3 were obtained by regression of all of the experimental data points, which are presented in Table 16. The generated values are summarized in Table 50. In comparison with experimental measurements, the predictions by Eq. [5-3] and Eq. [5-4] gave high agreement values, with average absolute relative deviations (AARDs) of 2.1% and 1.7% for Eqs. [5-3] and [5-4], respectively. The viscosity data satisfactorily fit the correlations over the studied temperature and pressure ranges.

The bitumen density data could be measured within the whole temperature and pressure ranges. The data analysis is presented in Table 15. The variation of density along with pressure was a linear proportional ratio. An inverse ratio relationship could be observed between density and temperature.

Based on the experimental data, the adjustable parameters of a_1, a_2, a_3 and a_4 for Eq. [5-5] were obtained by regression. Density data for the raw bitumen was fitted with a correlation considering the impacts of pressure and temperature, with a maximum deviation of ± 0.3 kg/m^3.

6.2 Case Study for Pure Solvents: Toluene and Xylene

Compared to the effect of pressure and temperature on bitumen density and viscosity, the relationship between physical properties of pure solvents with respective to pressures and temperatures was different. The data analysis from Table 14 demonstrates that the influence of pressure on the variation of pure solvents' viscosity was very insignificant and could reasonably be ignored. The inverse ratio relationship between the viscosity natural logarithm value and the temperature was observed.

To correlate the experimental data for pure solvents' viscosity, the Andrade equation [5-1] was the suitable correlation after linear regression of parameters *a* and *b*. The AARDs were less than 1.6% for toluene and less than 0.8% for xylene. As with raw bitumen, the density variation of pure solvents was a function of pressure and temperature. Through analysis of the impact of pressure on toluene density variations (Table 13), a proportional relationship could be observed between density and pressure.

The correlation for pure solvents' density could take the same form as raw bitumen, which is described in Eq. [5-5]. Based on experimental data, the adjustable parameters of a_1, a_2, a_3 and a_4 for Eq. [5-5] were obtained by regression. Density data for the pure solvents was fitted with a correlation considering the impacts of pressure and temperature, with maximum deviations of ± 0.2 kg/m^3 for toluene and ± 0.6 kg/m^3 for xylene.

6.3 Case Study for Bitumen/Toluene and Bitumen/Xylene Binary Mixtures

The data analysis shown in Tables 24 to 30 and 38 to 44, the density variation of bitumen/toluene and bitumen/xylene mixtures was quite explicit, with respect to pressure, temperature and solvent concentration. The data for the densities of bitumen/toluene and bitumen/xylene mixtures revealed linear trends with the variables of pressure and solvent concentrations for the whole temperature range. As expected, density linearly decreased with increasing temperatures and decreasing pressures. The mixture became denser with decreasing temperatures and elevating pressures.

The trend of mixture density also can be observed in Figs. 17 to 20 and 28 to 31 for bitumen/toluene and bitumen/xylene mixtures, respectively. Two important results are that the

effect of temperature on density variation was greater at higher solvent concentrations and that the influence of pressure was less pronounced at higher solvent concentration levels.

The data were quite well represented by $\rho_m=1/(w_s/\rho_m+w_B/\rho_B)$ over the entire temperature, pressure and concentration ranges. The AARDs were 0.04% and 0.06% for the bitumen/toluene and bitumen/xylene mixtures, respectively. The results indicated that the predicted density values at the highest temperature (333 K) and the highest solvent concentration (0.6 solvent weight fractions) show slight deviations from the measured values. This may be caused by deviation from the assumption of no volume change on mixing at higher solvent concentrations.

The mixtures' viscosity behaviours were somewhat diverse and followed different trends at different solvent concentration levels. Generally, the data presented in Tables 17 to 23 and 31 to 37 demonstrate that mixture viscosity decreased when the temperature increased and the pressure decreased. However, the influences of pressure and temperature were of different magnitudes, depending on different solvent concentrations.

Figs. 22 to 27 and 33 to 38 depict the effect of pressure, temperature and solvent concentrations on the viscosity of the bitumen/solvent mixtures. A linear trend can be observed between the logarithm value of mixture viscosity and the pressure at lower solvent concentration levels for the whole temperature range. At highest solvent concentration (solvent weight fracture larger than 60%), the viscosity was only a function of temperature. The effect of pressure was more significant at lower solvent concentrations. The mixture viscosities indicated a curvilinear trend with respect to the solvent concentration and temperatures for the whole pressure range. The impact of temperature was greater at lowest solvent concentrations.

Generally, in terms of physical properties of Athabasca bitumen and aromatic solvent binary mixtures, two conclusions can be made as:

1. The impact of pressure and temperature on viscosity and density was strongly associated with solvent concentration or constitution; and,
2. The lower the solvent concentration in the mixtures, the more likely the mixture viscosity behaviours would resemble those of raw bitumen; and, the higher the solvent concentration, the more likely the mixture viscosity behaviours would resemble those of pure solvent.

The mixture viscosity data were correlated with four frequently used models. The results indicated that Lederer's model and the power law fit the data better than the Shu correlation and Arrhenius's model. The viscosity results using the Lederer and power law models led to almost the same predictions. A comparison on the basis of AARDs showed that those of Lederer's model were 14.8% for the bitumen/toluene mixtures and 13.8% for the bitumen/xylene mixtures; whereas, the AARD values were found to be 19.2% for bitumen/toluene mixtures and 17.1% for bitumen/xylenes mixtures using the power law model. The comparison of experimental and modeling results showed that the viscosity predictions of the two models at the highest temperature and highest toluene concentration deviated from the experimental data.

Bibliography

[1] M.A.B.Khan, A.K.Mehrotra, W.Y.Svrcek, "Viscosity models for gas-free Athabasca bitumen", The Journal of Canadian Petroleum Technology, May-June 1984

[2] Anil K.Mehrotra and Wlliam Y.Svrcek, "Viscosity of Compressed Athabasca Bitumen", The Canadian Journal of Chemical Engineering, Vol.64, 1986

[3] Anil K.Mehrotra and Wlliam Y.Svrcek, "Corresponding states method for calculating bitumen viscosity", The Journal of Canadian Petroleum Technology, Sep.-Oct. 1987, Montreal

[4] Anil K.Mehrotra and Wlliam Y.Svrcek, "Viscosity of Compressed Cold Lake Bitumen", The Canadian Journal of Chemical Engineering, Vol. 65, 1987

[5] Susan E. Johnson, William Y. Svrcek and Anil K. Mehrotra, "Viscosity Prediction of Athabasca Bitumen Using the Extended Principle of Corresponding States", Ind. Eng. Chem. Res. 1987, 26, 2290-2298

[6] Anil K.Mehrotra, Robert R. Eastick and Wlliam Y.Svrcek, "Viscosity of Cold Lake Bitumen and Its Fractions", The Canadian Journal of Chemical Engineering, Vol. 67, 1989

[7] Anil K.Mehrotra, "A generalized viscosity equation for liquid hydrocarbons: Application to oil-sand bitumens", Fluid Phase Equilibria, 75 (1992) 257-268

[8] V. R. Puttagunta, B. Singh and A. Miadonye, "Correlation of Bitumen Viscosity with Temperature and Pressure", The Canadian Journal of Chemical Engineering", Vol. 71, 1993

[9] A. Miadonye, B. Singh, and V.R. Puttagunta, "Modelling the Viscosity-Temperature Relationship of Alberta Bitumen", Petroleum Science and Technology, 12:2, 335-350

[10] A. Miadonye, B. Singh and V.R. Puttagunta, "Viscosity Estimation For Bitumen-Dilluent Mixtures", Fuel Science and Technology International, 13(6), 681-698 (1995)

[11] C. Zhang, H. Zhao, M. Hu, Q. Xiao, J. Li, C. Cai, " A Simple Correlation for the Viscosity of Heavy Oils From Liaohe Basin, NE China", Journal of Canadian Petroleum Technology, Vol. 46, No.4, 2007

[12] Juliet McClatchey Allen and Amyn S. Teja, “Correlation and Prediction of the Viscosity of Defined and undefined Hydrocarbon Liquids”, The Canadian Journal of Chemical Engineering, Vol. 69, 1991

[13] Anil K. Mehrotra, “A Generalized Viscosity Equation for Pure Heavy Hydrocarbon”, Ind. Eng. Chem. Res. 1991, 30, 420-427

[14] Maria A. Barrufet and Agustinus Setiadarma, “Reliable heavy oil-solvent viscosity mixing rules for viscosity up to 450K, oil-solvent viscosity ratios up to 4×10^5, and any solvent proportion”, Fluid Phase Equilibria 213 (2003) 65-79

[15] A. Badamchi-Zadeh, H. W. Yarranton, W. Y. Svrcek, B. B. Maini, “Phase Behaviour and Physical Property Measurements for VAPEX Solvents: Part I. Propane and Athabasca Bitumen”, Journal of Canadian Petroleum Technology, Vol. 48, No.1, 2009

[16] F.A. Jacobs, J.K. Donnelly, J. Stanislav, W.Y.J. Svrcek, “Viscosity of Gas-Saturated bitumen”, The Journal of Canadian Petroleum Technology, 1980, Montreal

[17] W. R. Shu, “A Viscosity Correlation for Mixtures of Heavy Oil, Bitumen, and Petroleum Fractions”, Society of Petroleum Engineers of AIME, 0197-7520/84/0061-1280

[18] Robert R. Eastick and Anil K. Mehrotra, “Viscosity Data and Correlation for Mixtures of Bitumen Fractions”, Fuel Processing Technology, 26 (1990) 25-37

[19] Anil K. Mehrotra, “A mixing rule approach for predicting the viscosity of CO_2-saturated Cold Lake bitumen and bitumen fractions”, Journal of Petroleum Science and Engineering, 6 (1992) 289-299

[20] A. Miadonye, N.Latour and V.R. Puttagunta, “A Correlation for Viscosity and Solvent Mass Fraction of Bitumen-Diluent Mixtures”, Petroleum Science and Technology, 18 (1&2), 1-14 (2000)

[21] N. Lindeloff, K.S. Pedersen, H.P. Ronningsen, and J. Milter, “The Corresponding States Viscosity Model Applied to Heavy Oil Systems”, The Journal of Canadian Petroleum Technology, Vol. 43, No.9, 2004

[22] M.S. Hossain, C. Sarica, H.-Q. Zhang, L. Rhyne and K. L. Greenhill, “Assessment and Development of Heavy-Oil Viscosity Corrlations”, SPE/PS-CIM/CHOA 97907 PS2005-407

[23] Wang, L.-S., Lv, H.-C., "A Unified Model for Representing Densities and Viscosities of Hydrocarbon Liquids and Gases Based on Peng-Robinson Equation of State", The Open Thermodynamics Journal, vol. 3, pp. 24-33, 1874-396X/09

[24] Mohammad Kariznovi, Hossein Nourozieh, and Jalal Abedi, "Phase Behavior and Viscosity Measurements of Heavy Crude Oil with Methane and Ethane at High-Temperature Conditions", SPE 152321

[25] F.A. Jacobs, J.K. Donnelly, J. Stanislav, W.Y.J. Svrcek, "Viscosity of Gas-Saturated bitumen", Can. Pet. Tech. 19 (1980) 46-50.

[26] A.K. Mehrotra, W.Y. Svrcek, "Measurement and Correlation Viscosity, Density and Gas Solubility for Marguerite Lake Bitumen Saturated with Carbon Dioxide", AOSTRA J. Res. 1 (1984) 51–62.

[27] A.K. Mehrotra, W.Y. Svrcek, "Viscosity, Density, and Gas Solubility Data for Oil Sand Bitumens. Part I: Athabasca Bitumen Saturated with CO and C_2H_6." AOSTRA J. Res. 1 (1985) 263–268.

[28] A.K. Mehrotra, W.Y. Svrcek, "Viscosity, Density, and Gas Solubility Data for Oil Sand Bitumens. Part II: Peace River Bitumen Saturated with N_2, CO, CH_4 and CO_2, C_2H_6." AOSTRA J. Res. 1 (1985) 269–279.

[29] A.K. Mehrotra, W.Y. Svrcek, "Viscosity, Density, and Gas Solubility Data for Oil Sand Bitumens. Part III: Wabasca Bitumen Saturated with N_2, CO, CH_4 and CO_2, C_2H_6." AOSTRA J. Res. 2 (1985) 83–93.

[30] A.K. Mehrotra, W.Y. Svrcek, "Property of Cold Lake Bitumen Saturated Pure Gas and Gas Mixtures", Can. J. Chem. Eng. 66 (1988) 656–665.

[31] W.Y. Svrcek, A.K. Mehrotra, "Property of Peace River Bitumen Saturated field Gas Mixtures"J. Can. Pet. Tech. 28 (1989) 50–56.

[32] A.K. Mehrotra, W.Y. Svrcek, "Viscosity of Compressed Athabasca Bitumen", Can. J. Chem. Eng. 64 (1986) 844-847.

[33] A.K. Mehrotra, W.Y. Svrcek, "Viscosity of Compressed Cold Lake Bitumen", Can. J. Chem. Eng. 65 (1987) 672-675.

[34] A. Badamchi-Zadeh, H.W. Yarranton, W.Y. Svrcek, B.B. Maini, "Phase Behaviour and Physical Property Measurements for VAPEX Solvents: Part I. Propane and Athabasca Bitumen", J. Can. Pet. Technol. 48 (2009) 54–61.

[35] A. Badamchi-Zadeh, H.W. Yarranton, B.B. Maini, M.A. Satyro, J. Can. Pet. Technol. 48 (2009) 57–65.

[36] M.A.B. Khan, A.K. Mehrotra, W.Y. Svrcek, "Viscosity models for gas-free Athabasca bitumen", J. Can. Pet. Tech., 23 (1984) 47-53.

[37] W.Y. Svrcek, A.K. Mehrotra, "Gas solubility, viscosity and density measurements for Athabasca bitumen", J. Can. Pet. Tech. 21 (1982) 31–38.

[38] A.K. Mehrotra, J.A. Nighswander, N. Kalogerakis, "Data and Correlation for CO_2-Peace River Bitumen Phase Behaviour at 22-200^{0}C", AOSTRA J. Res. 5 (1989) 351–358.

[39] A.K. Mehrotra, "Development of Mixing Rules for Predicting the Viscosity of Bitumen and Its Fractions Blended with Toluene", Can. J. Chem. Eng. 68 (1990) 839-848.

[40] D. Lal, Solubility of Gases in Heavy Oils. MSc Thesis, The University of Alberta, Edmonton, Alberta, Canada, 1983.

[41] C.T. Fu, V.R. Puttagunta, G. Vilcsak, "Vapour-Liquid Equilibrium Properties for Pseudo-Binary Mixtures of CO_2-Athabasca Bitumen and N_2-Athabasca Bitumen", AOSTRA J. Res. 2 (1985) 73–81.

[42] C.T. Fu, V.R. Puttagunta, G. Vilcsak, "Gas solubility of methane and ethane in Cold Lake bitumen at in situ conditions", J. Can. Pet. Tech. 27 (1988) 79–85.

[43] S.G. Sayegh, D.N. Rao, S. Kokal, J. Najman, "Phase behavior and physical properties of Lindbergh heavy oil/CO_2 Mixtures", J. Can. Pet. Tech. 29 (1990) 31–39.

[44] K.N. Jha. "A lab study of heavy oil recovery with carbon dioxide", J. Can. Pet. Tech. 25 (1986) 54–63.

[45] J.M. Yu, S.H. Huang, M. Radosz, "Phase Behavior of Resevoir Fluids: Supercritical Carbon Dioxide and Cold Lake Bitumen", Fluid Phase Equilib. 53 (1989) 429–438.

[46] S.H. Huang, M. Radosz. "Phase Behavior of Resevoir Fluids II: Supercritical Carbon Dioxide and Bitumen Fractions", Fluid Phase Equilib. 60 (1990) 81–98.

[47] M.D. Deo, J. Hwang, F.V. Hanson, Ind. Eng. Chem. Res. 30 (1991) 532–536.

[48] J.M. Yu, S.H. Huang, M. Radosz, "Phase behavior of reservoir fluids VI. Cosolvent effect on bitumen fractionation with supercritical CO_2", Fluid Phase Equilib. 93 (1994) 353–362.

[49] S.L. Kokal, S.G. Sayegh, “Phase behavior and physical properties of CO_2-saturated heavy oil and its constitutive fractions: Experimental data and correlations”, J. Pet. Sci. Eng. 9 (1993) 289–302.

[50] P. Han, D.Y. Peng, Can. J. Chem. Eng. 70 (1992) 1164–1171.

[51] D. Lal, F.D. Otto, A.E. Mather, “Solubility of hydrogen in Athabasca bitumen”, Fuel 78 (1999) 1437–1441.

[52] T.W.J. Frauenfeld, G. Kissel, S. Zhou, PVT and viscosity measurements for Lloydminster-Aberfeldy and Cold Lake blended oil systems. 2002, SPE International Thermal Operations and Heavy Oil Symposium and International Horizontal Well Technology Conference. Calgary, AB, Canada.

[53] N.P. Freitag, S.G. Sayegh, R. Exelby, A new semiautomatic PVT apparatus for characterizing Vapex systems. 2005, SPE/PS-CIM/CHOA International Thermal Operations and Heavy Oil Symposium. Calgary, AB, Canada.

[54] P. Luo, C. Yang, Y. Gu, “Enhanced Solvent Dissolution in In-situ Upgraded Heavy Oil under Different Pressures”, Fluid Phase Equilib. 252 (2007) 143–151.

[55] P. Luo, C. Yang, A.K. Tharanivasan, Y. Gu, “In-situ Upgrading of Heavy Oil in a Solvent-based Heavy Oil Recovery Process”, J. Can. Pet. Technol. 46 (2007) 37–43.

[56] A. Yazdani, B.B. Maini, “Measurements and Modeling of Phase Behavior and Viscosity of a Heavy Oil/Butane System”, J. Can. Petrol. Tech. 49 (2010) 9-14.

[57] M. Kariznovi, H. Nourozieh, J. Abedi, “Experimental apparatus for phase behavior study of solvent-bitumen systems: A critical review and design of a new apparatus”, Fuel 90 (2010) 536–546.

[58] M. Kariznovi, H. Nourozieh, J. Abedi, 2011, Experimental and Modeling Study of Vapor-Liquid Equilibrium for Propane/Heavy Crude Systems at High Temperature Conditions. Presented at SPE Annual Technical Conference and Exhibition, 30 October-2 November 2011, Denver, Colorado, USA.

[59] H. Nourozieh, M. Kariznovi, J. Abedi, “Physical Properties and Extraction Measurements for Athabasca Bitumen + Light Hydrocarbon System: Evaluation of Pressure Effect, Solvent-to-Bitumen Ratio, and Solvent Type", J. Chem. Eng. Data 56 (2011) 4261–4267.

[60] M. Kariznovi, H. Nourozieh, J. Abedi, Phase Behavior and Viscosity Measurements of Heavy Crude Oil With Methane and Ethane at High-Temperature Conditions. 2012,

Presented at the SPE Western North American Regional Meeting held in Bakersfield, California, USA, 19–23 March 2012.

[61] Thermophysical properties of fluid systems: National Institute of Standards and Technology; http://webbook.nist.gov/chemistry/fluid.

[62] G. Centeno, G. Sánchez-Reyna, J. Ancheyta, J.A.D. Muñoz, N. Cardona, "Testing various mixing rules for calculation of viscosity of petroleum blends", Fuel 90 (2011) 3561-3570.

[63] S.A. Arrhenius, Uber die Dissociation der in Wasser gelosten Stoffe. Z. Phys. Chem. 1 (1887) 631–648.

[64] J. Kendall, K. Monroe, Am. Chem. J. 9 (1917) 1787–1802.

[65] E.L. Lederer, Proc. World. Pet. Cong. Lond. 2 (1933) 526–528.

[66] W.R. Shu, "A Viscosity Correlation for Mixtures of Heavy Oil, Bitumen, and Petroleum Fractions", Soc. Petrol. Eng. J. 24 (1984) 277–282.

[67] Mehrotra, A. K., Monnery, W. D., Svrcek, W. (1996) "A review of practical calculation methods for the viscosity of liquid hydrocarbons and their mixtures", Fluid Phase Equilibria 117 (1996) 344-355